N-1855
February 1993

By John Ferritto

Sponsored By Office of
Naval Technology

NCEL
Technical Note

DEVELOPMENT OF PROCEDURES FOR COMPUTING SITE SEISMICITY

ABSTRACT This report was prepared as part of the Navy's Seismic Hazard Mitigation Program. The Navy has numerous bases located in seismically active regions throughout the world. Safe effective design of waterfront structures requires determining expected earthquake ground motion. The Navy's problem is further complicated by the presence of soft saturated marginal soils that can significantly amplify the levels of seismic shaking as evidenced in the 1989 Loma Prieta earthquake. The Naval Facilities Engineering Command's seismic design manual, NAVFAC P355.1, requires a probabilistic assessment of ground motion for design of essential structures. This report presents the basis for the Navy's Seismic Hazard Analysis procedure that was developed and is intended to be used with the Seismic Hazard Analysis computer program and user's manual. This report also presents data on geology and seismology to establish the background for the seismic hazard model developed. The procedure uses the historical epicenter data base and available geologic data, together with source models, recurrence models, and attenuation relationships to compute the probability distribution of site acceleration and an appropriate spectra. This report discusses the developed stochastic model for seismic hazard evaluation and the associated research.

NAVAL CIVIL ENGINEERING LABORATORY PORT HUENEME, CALIFORNIA 93043-4328

METRIC CONVERSION FACTORS

Approximate Conversions to Metric Measures

Symbol	When You Know	Multiply by	To Find	Symbol
		LENGTH		
in	inches	*2.5	centimeters	cm
ft	feet	30	centimeters	cm
yd	yards	0.9	meters	m
mi	miles	1.6	kilometers	km
		AREA		
in^2	square inches	6.5	square centimeters	cm^2
ft^2	square feet	0.09	square meters	m^2
yd^2	square yards	0.8	square meters	m^2
mi^2	square miles	2.6	square kilometers	km^2
	acres	0.4	hectares	ha
		MASS (weight)		
oz	ounces	28	grams	g
lb	pounds	0.45	kilograms	kg
	short tons (2,000 lb)	0.9	tonnes	t
		VOLUME		
tsp	teaspoons	5	milliliters	ml
Tbsp	tablespoons	15	milliliters	ml
fl oz	fluid ounces	30	milliliters	ml
c	cups	0.24	liters	l
pt	pints	0.47	liters	l
qt	quarts	0.95	liters	l
gal	gallons	3.8	liters	l
ft^3	cubic feet	0.03	cubic meters	m^3
yd^3	cubic yards	0.76	cubic meters	m^3
		TEMPERATURE (exact)		
°F	Fahrenheit temperature	5/9 (after subtracting 32)	Celsius temperature	°C

*1 in = 2.54 (exactly). For other exact conversions and more detailed tables, see NBS Misc. Pub. 286, Units of Weights and Measures, Price $2.25, SD Catalog No. C13.10:286

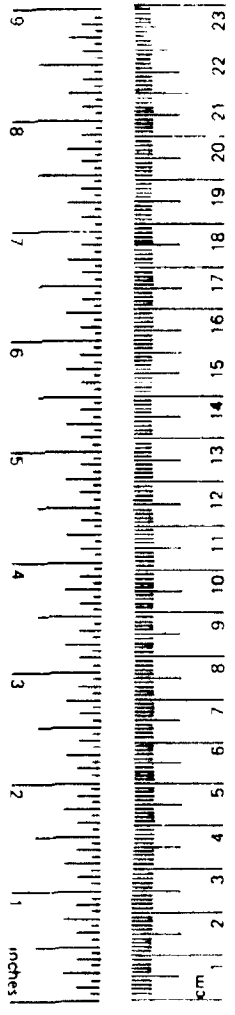

Approximate Conversions from Metric Measures

Symbol	When You Know	Multiply by	To Find	Symbol
		LENGTH		
mm	millimeters	0.04	inches	in
cm	centimeters	0.4	inches	in
m	meters	3.3	feet	ft
m	meters	1.1	yards	yd
km	kilometers	0.6	miles	mi
		AREA		
cm^2	square centimeters	0.16	square inches	in^2
m^2	square meters	1.2	square yards	yd^2
km^2	square kilometers	0.4	square miles	mi^2
ha	hectares (10,000 m^2)	2.5	acres	
		MASS (weight)		
g	grams	0.035	ounces	oz
kg	kilograms	2.2	pounds	lb
t	tonnes (1,000 kg)	1.1	short tons	
		VOLUME		
ml	milliliters	0.03	fluid ounces	fl oz
l	liters	2.1	pints	pt
l	liters	1.06	quarts	qt
l	liters	0.26	gallons	gal
m^3	cubic meters	35	cubic feet	ft^3
m^3	cubic meters	1.3	cubic yards	yd^3
		TEMPERATURE (exact)		
°C	Celsius temperature	9/5 (then add 32)	Fahrenheit temperature	°F

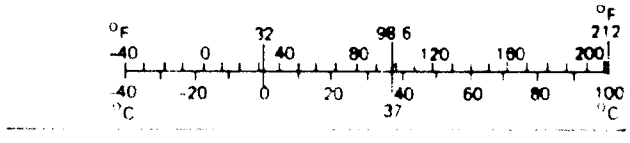

REPORT DOCUMENTATION PAGE

Form Approved
OMB No. 0704-018

1. AGENCY USE ONLY (Leave blank)	2. REPORT DATE	3. REPORT TYPE AND DATES COVERED
	February 1993	Final: Oct 1992 through Oct 1993

4. TITLE AND SUBTITLE

DEVELOPMENT OF PROCEDURES FOR COMPUTING SITE SEISMICITY

5. FUNDING NUMBERS

PR - RM33F60-001-0106
WU - DN387338

6. AUTHOR(S)

John Ferritto

7. PERFORMING ORGANIZATION NAME(S) AND ADDRESS(S)

Naval Civil Engineering Laboratory
Port Hueneme, CA 93043-4328

8. PERFORMING ORGANIZATION REPORT NUMBER

TN-1855

9. SPONSORING/MONITORING AGENCY NAME(S) AND ADDRESS(S)

Office of Naval Technology
Arlington, VA 22217-5000

10. SPONSORING/MONITORING AGENCY REPORT NUMBER

11. SUPPLEMENTARY NOTES

12a. DISTRIBUTION/AVAILABILITY STATEMENT

Approved for public release; distribution unlimited.

12b. DISTRIBUTION CODE

13. ABSTRACT *(Maximum 200 words)*

This report was prepared as part of the Navy's Seismic Hazard Mitigation Program. The Navy has numerous bases located in seismically active regions throughout the world. Safe effective design of waterfront structures requires determining expected earthquake ground motion. The Navy's problem is further complicated by the presence of soft saturated marginal soils that can significantly amplify the levels of seismic shaking as evidenced in the 1989 Loma Prieta earthquake. The Naval Facilities Engineering Command's seismic design manual, NAVFAC P355.1, requires a probabilistic assessment of ground motion for design of essential structures. This report presents the basis for the Navy's Seismic Hazard Analysis procedure that was developed and is intended to be used with the Seismic Hazard Analysis computer program and user's manual. This report also presents data on geology and seismology to establish the background for the seismic hazard model developed. The procedure uses the historical epicenter data base and available geologic data, together with source models, recurrence models, and attenuation relationships to compute the probability distribution of site acceleration and an appropriate spectra. This report discusses the developed stochastic model for seismic hazard evaluation and the associated research.

14. SUBJECT TERMS	15. NUMBER OF PAGES
Earthquake, ground motion, seismic hazard analysis, acceleration	128
	16. PRICE CODE

17. SECURITY CLASSIFICATION OF REPORT	18. SECURITY CLASSIFICATION OF THIS PAGE	19. SECURITY CLASSIFICATION OF ABSTRACT	20. LIMITATION OF ABSTRACT
Unclassified	Unclassified	Unclassified	UL

CONTENTS

CHAPTER 1
WHAT IS A SITE SEISMICITY STUDY?

INTRODUCTION

The objective of a seismicity study is to quantify the level and characteristics of ground motion shaking that pose a risk to a site of interest. The approach taken in this work is to use the historical epicenter data base in conjunction with available geologic data to form a best estimate of the probability distribution of site ground motion.

This report presents techniques that have been automated into a procedure to compute:

- Regional earthquake recurrence parameters
- Regional probability distribution
- Fault earthquake magnitude recurrence parameters
- Probability distribution of site acceleration from each fault
- Total probability distribution of site acceleration
- Causative magnitudes and separation distances associated with acceleration
- Response spectra based on site soil conditions and causative events

OUTLINE OF PROCEDURE

The procedures were developed as computer programs designed to run on standard desktop DOS-based computers. System requirements include 640K of memory, a math coprocessor chip, and a hard disk. A CDROM is required to use the recommended epicenter data base.

The procedure consists of:

- Evaluating tectonics and geologic settings
- Specifying faulting sources
- Determining site soil conditions
- Determining the geologic seismic slip rate data

- Specifying the epicenter search area and search of data base
- Specifying and formulating the site seismicity model
- Developing the recurrence model
- Determining the maximum source events
- Selecting the motion attenuation relationship
- Computing individual fault/source seismic contributions
- Summing the sources
- Determining the site matched spectra for causative events

This report will present a summary and discussion of the technology for each of the elements of the analysis. A separate user's manual is available to assist in program use (Ferritto, 1993).

APPLICATION

The procedures were developed subject to the following limitations:

- The exposure period or life of the structure is 50 years.
- Return times of events of interest are not appreciably longer than about one in a thousand years. This procedure is not intended to predict events such as the 10,000-year event with high accuracy.

REFERENCE

Ferritto, J.M. (1993). Seismic hazard analysis, Naval Civil Engineering Laboratory, User's Guide UG-0027. Port Hueneme, CA, 1993.

CHAPTER 2
EARTHQUAKE ENGINEERING FUNDAMENTALS

PLATE TECTONICS

The United States is located on the North American plate, the western portion of which meets the Pacific plate. The interaction of these two plates is responsible for the high seismic activity that has in the past and continues now to take place in the Western United States. Plate tectonic theory has explained much of the geologic activity. Also explained in terms of plate tectonic theory is the seismic activity experienced in the Central and Eastern United States. This midplate activity can be very destructive.

Figure 2-1 shows a cross section of the earth. The lithosphere, composed largely of basalt, extends to an average depth of about 100 km. Below the lithosphere is the asthenosphere that extends to a depth of 400 km. Because its upper portion is partially molten, seismic velocity in that region is decreased. The lithospheric plates are able to "float" on this plastic layer. Not all of the asthenosphere is molten; however, there is a rigid portion.

Most seismic activity is located at plate boundaries and, therefore, boundaries are of considerable interest. There are three major types of interaction between adjacent plates: (1) spreading boundaries, (2) converging boundaries, and (3) transforming boundaries. Figure 2-2 illustrates the three kinds of boundaries.

GEOLOGIC FAULTS AND EARTHQUAKES

Since the San Francisco earthquake of 1906 and the subsequent work on the elastic rebound theory of earthquakes, general agreement has been reached on the close relationship between earthquakes and geologic faults. Most tectonic earthquakes that cause major structural damage are associated with fracture on a fault. Plate motion causes stress in the earth's rock crust. Earthquakes occur when the strength of the fault can no longer withstand the stress that has built up. Fault plane solutions and earthquake mechanism studies have contributed to a consistent picture of the earthquake generation process that satisfactorily explains most of the observed facts.

A fault is a rupture in the earth along which opposite faces have been displaced. The basic kinds of faults are illustrated in Figure 2-3 and are defined as follows:

1. Strike Slip. Strike is the direction along a fault, and strike slip refers to displacement along this line. Right lateral or left lateral refers to the direction of movement of the opposite side when one faces the fault.

2. Normal. A normal fault refers to movement of one side of the fault away from the other, producing tension.

3. Thrust. A thrust fault refers to movement of one side toward or over the other side producing compression.

Most faults are combinations of strike slip and normal or thrust movement. The fault plane itself can be curved and blocks can be rotated relative to each other. The fault trace is the line of the fault along the ground surface. The strike of a fault is measured from north in degrees. The dip of a fault is used to measure the slope of the fault plane with the surface (Figure 2-4).

Some misunderstandings have occurred, and perhaps some significant differences of opinion, about the direct relationship between geologic faults and the earthquake hazard. There is evidence dating from 1906 to suggest that destructive ground shaking is not necessarily at a maximum in the immediate vicinity of the causative fault (Hudson, 1972). More often than not, the maximum destructive ground shaking is miles from the fault, as explained by a number of the features of the generation and propagation of seismic waves. Classical photographs of the 1906 major movements along the San Andreas fault, for example, show horizontal surface displacements of as much as 5 meters passing close to a small wood-frame house that received no significant damage. Similarly, during the San Fernando earthquake of 9 February 1971, a 2-meter vertical fault scarp passed directly through a wooden barn just a short distance from a single-story residence. The barn was severely damaged, but no significant structural damage to the house was noted (Hudson, 1972). The San Fernando earthquake also furnished numerous examples of surface faulting passing through heavily populated areas. Although severe structural deformation, with a resulting economic loss, occurred in numerous cases, catastrophic collapses leading to loss of life and serious injury were not directly associated with these surface breaks. Hazardous collapses were in all cases the consequence of severe ground shaking, which is pervasive over a large area and is not limited to the vicinity of faults.

The focus or hypocenter is the point within the earth's crust where the initial rupture occurs and from which the first waves are released. The projection of this point to the ground surface is the epicenter. The epicenter and hypocenter do not necessarily indicate the center of the total energy release of the earthquake, but rather the point where the seismic energy waves were first created. For small earthquakes, the center of total energy release and the epicenter are not far apart because the fault break length is short; however, this is not the case for large earthquakes. The majority of earthquakes in the United States have had relatively shallow focal depths (0 to 40 km). In California, earthquakes have occurred in regions where surface fault patterns were clearly visible. In the Puget Sound area, earthquakes are focused at deeper locations within the earth's crust so that a surface rupture is not observable. In the eastern United States, the relationship to surface rupture in general has not been closely identified (Bolt, 1970; Newmark and Rosenblueth, 1971).

A fault undergoing tectonic creep, or one with abrupt displacement, causes changes in the terrain it crosses. Very distinctive patterns are produced where active faults cross streams, such as landslides. The ongoing geologic process causes scarps, trenches, sag ponds, and stream offsets. Figure 2-5 shows a landform with an active fault (Wesson, et al., 1975).

Estimates of the maximum size and frequency of earthquakes on a fault are based on the geologically determined slip rate and the historic record of ground deformation (where available), the seismic history of the fault and surrounding tectonic region, a geological evaluation of the tectonic setting, and empirically derived relationships between earthquake magnitude and fault length.

SURFACE EFFECTS OF FAULT MOVEMENTS

When faults are considered, the assumption is commonly made that the creation of entirely new faults by an earthquake is unlikely (Krinitzsky, 1974). Significant surface faults and their activity can be found by proper geologic investigations. Cluff, Slemmons, and Waggoner (1970) have studied the character of typical surface effects by faults. These are illustrated in Figures 2-6 through 2-8, as reported by Krinitzsky (1974).

EARTHQUAKE MAGNITUDE

Engineers can define a design earthquake for a site in terms of the earthquake magnitude, M, and the strength of ground motion. Factors that influence the selection of a design earthquake are the length of geologic fault structures, the relationship of the fault to the regional tectonic structure, the geologic history of displacement along the structure, and the seismic history of the region.

The design earthquake in engineering terms is a specification of levels of ground motion that the project is required to survive successfully with no loss of life and acceptable damage and loss of service. A design earthquake on a statistical basis considers the probability of the recurrence of a historical event.

Earthquake magnitudes can be specified in terms of a design level earthquake that can reasonably be expected to occur during the life of the structure. As such, this represents a service load that the structure must withstand without significant structural damage or interruption of a required operation. A second level of earthquake magnitude is a maximum credible event for which the structure must not collapse; however, significant structural damage can occur. The inelastic behavior of the structure must be limited to ensure the prevention of collapse and catastrophic loss of life.

The selection of a magnitude level may be based on:

1. Known design-level and maximum-credible earthquake magnitudes associated with a fault whose seismicity has been estimated.

2. Specification of probability of occurrence for a given life of the structure (such as having a 10 percent chance of being exceeded in 25 years).

3. Specification of required level of ground motion as in a code provision.

4. Fault length empirical relationships.

Earthquake magnitude can be related to length of fault for shallow depth earthquakes. Data have been plotted by Seed, et al. (1969), Krinitzsky (1974), Housner (1965), and Tocher (1958) to provide the curves indicated (Figure 2-9). It is important to note that in some regions, correlations of these types are of little value since many of the important geologic features can be deeply buried by weathered materials.

Magnitude as measured on the Richter scale is calculated from a standard earthquake, one which provides a maximum trace amplitude of 1 μm on a standard Wood-Anderson torsion seismograph at a distance of 100 km. Magnitude is the $\log_{10}$ of the ratio of the amplitude of any

earthquake at the standard distance to that of the standard earthquake. Each full numeral step in the scale (two to three, for example) represents an energy increase of about 32 times. Experience with past earthquakes is presently the only useful basis for relating fault length and motion to magnitudes of associated earthquakes.

FAULT LENGTH AND EARTHQUAKE MAGNITUDE

A useful insight into the relationship between earthquake magnitude and length of observed fault slippage is presented by Iida (1965). He groups faults of all types and shows a wide spread of points for which upper and lower boundaries are drawn. Iida's wide spread of values should be kept in mind when one considers the linear relationships that have been suggested by numerous authors.

Fault movements below a magnitude of 5 are usually contained in the subsurface. If active fault movement is found at a site, even short movement, it should be viewed as evidence for an earthquake capability of greater than 5 (Krinitzsky, 1974).

It is important to note the spread in the data. Krinitzsky (1974) concludes, "Any fault break in competent rock, no matter how small, should be taken as indicative of the capability for at least a 5.4 earthquake." It is important that the local seismic history and the behavior of other analogous faults be considered.

Consideration should be given to the possibility of not identifying all the faults in a region that may be active. This is especially true in the Central and Eastern United States. To account for this a "floating earthquake" (one that may be assumed capable of occurring anywhere in the region) should be considered (Krinitzsky, 1974).

Mark and Bonilla (1977) evaluated data to develop relationships between surface fault displacement and earthquake magnitude. More recent data by Coppersmith (1991) are shown in Figures 2-10 and 2-11.

GEOLOGICALLY DETERMINED SLIP RATES

The offset of distinctive rock units establishes the rate of fault movement within fairly wide bounds. Commonly these offsets average the rate of movement over millions of years, and sudden slip cannot be distinguished from creep. Data for the San Andreas fault suggest an average slip rate of 1 to 2 cm/yr over the last 20 million years. But to predict movements in the immediate future, the most recent hundreds to thousands of years are the most important (Wesson, et al., 1975).

The history and rate of fault movement have been obtained within this brief time period in a few special circumstances in southern California, using absolute age dating techniques.

Figure 2-12 is a simplified sketch of a trench wall showing vertical deformation of initially flat-laying sediments and sedimentary contacts associated with predominantly horizontal movement on the Coyote Creek fault of southern California (from Clark, et al., 1972). The trench, dug shortly after the 1968 Borrego Mountain earthquake, crosses a branching break of the fault zone along which about 50 mm of vertical displacement and about the same amount of horizontal displacement took place during the earthquake. Deposits at points A, B, and C were dated radiometrically. The vertical displacement of the sedimentary contacts plotted against the age of the corresponding deposits yields an average rate of vertical deformation of about 0.5

mm/yr for the past 3,000 years. This suggests a recurrence interval for earthquakes the size of the 1968 event of about 200 years, Figure 2-13 (Clark, et al., 1972).

RECURRENCE INTERVALS FROM GEOLOGIC SLIP RATES

Wallace (1970) presented an approach that has been used by Lamar, et al. (1973). The recurrence interval at a point can be estimated by:

$$R_x = \frac{D}{S - C} \qquad (2\text{-}1)$$

where: D = displacement per seismic event
S = long-term slip rate
C = tectonic creep rate
S - C = average seismic slip rate

Lamar, et al. (1973) present the following quoted discussion:

> "The following assumptions are made: (1) Slip on faults occurs incrementally during earthquakes and will continue at the same rate as that determined from geodetic data and offset of geologic units. (2) Elastic strain accumulates between earthquakes; the displacement during an earthquake represents the release of this accumulated elastic strain. (3) Tectonic creep is aseismic slip which reduces the accumulation of elastic strain available for release during earthquakes. ...Recurrence intervals determined by [Equation 2-1] represent a long-term average; there is however, evidence of significant local (Ambraseys, 1970) and worldwide (Davies and Brune, 1971) time variations in the level of seismic activity."

For most faults, creep can be evaluated. Therefore, as an expedient, Equation 2-1 is simplified as:

$$R_x = \frac{D}{S} \qquad (2\text{-}2)$$

Equation 2-2 is appropriate when the rupture length is large compared to the distance of the site to the fault. When this is not the case, Equation 2-2 is multiplied by the ratio of length of rupture to total fault length to account for the spatial distribution.

APPLICATION OF SLIP RATE TO COMPUTE RECURRENCE DATA

Lamar, et al. (1973) have investigated the occurrence data for six faults in the southern California area. Their data are summarized in Table 2-1 and illustrate the concept. The displacement, D, used in Equation 2-2 to calculate recurrence intervals at a given point on a fault were derived from Bonilla and Buchanan (1970), except in the case of the White Wolf and Sierra Madre faults. For these two faults historic displacements were available, and they deviated significantly from the least-squares-fit curve for reverse faults.

Quoting from Lamar, et al. (1973):

> "The determination of long-term slip rates and recurrence intervals provides a new approach to earthquake hazard assessment. The results can be strikingly different from those based on the historic earthquake record. For example, the ... Garlock fault, which has not caused damaging historic movement, may have accumulated sufficient elastic strain for a destructive earthquake. On the other hand, historic ruptures on faults such as the ... San Fernando, have released [some] accumulated elastic strain, so that a destructive earthquake [may be less probable] for the next few hundred years [depending on the amount of strain release and buildup]. The recurrence intervals in [Table 2-1] must be considered tentative and are subject to revision as new information becomes available. For the most part, slip rates are poorly known, and the curves relating magnitude to surface displacement and rupture length are based on meager data with considerable scatter. More accurate age-dates of offset strata on faults are needed, and additional studies following earthquakes throughout the world are required to refine the empirical relations between magnitude, surface displacement and rupture length. This research offers the prospect of more quantitative assessments of earthquake risk."

Since the early work of Wallace (1970), more emphasis has been placed on use of geologic data. The historic seismicity record in the United States and other areas is generally too short to fully define the recurrence of particular individual faults for low probability events. Fault slip rates derived from geologically defined intervals afford the opportunity of spanning several cycles of large earthquakes on a fault. Coppersmith and Youngs (1990) note that the best geologic units for assessing slip rate for recurrence purposes are late-Quarternary or Holocene units. Assessing slip rates over relatively young units will avoid averaging out long-term changes in the slip rate from regional changes in tectonic stress.

SEISMIC MOMENT

Seismic moment has been used in conjunction with slip rate. Seismic moment, M_o, is a means of describing the size of an earthquake in terms of physical parameters:

$$M_o = \mu A_r D \qquad (2\text{-}3)$$

where: μ = rigidity or shear modulus (taken as 3×10^{11} dyne/cm^2)
A_r = rupture area on the fault plane
D = average displacement over slip surface

The total seismic moment rate can be estimated using the above formulation substituting the total fault plane area and the average slip rate along the fault instead of the displacement. Thus, the seismic moment rate provides a link between geologic data and seismicity. Seismic moment rates determined from slip data can be compared with seismic moment rates based on seismicity data (Youngs and Coppersmith, 1985).

Seismic moment, M_o, can be related to magnitude, m, as follows:

$$\log M_o = C\,m + d \qquad (2\text{-}4)$$

Hanks and Kanamori (1979) report that c = 1.5 and d = 16.1 in California. The moment magnitude, m, is considered equivalent to local magnitude when in the range of 3 to 7 and to surface wave magnitude when in the range of 5 to 7.5.

REFERENCES

Ambraseys, N.N. (1970). "Some characteristic features of the Anatolian fault zone," Tectonophysics, vol 9, 1970, pp 143-165.

Bolt, B.A. (1970). "Causes of earthquakes," Earthquake Engineering, R.L. Wiegel, ed. Englewood Cliffs, NJ, Prentice Hall, 1970.

Bonilla, M.G., and J.M. Buchanan (1970). Interim report on worldwide historic surface faulting, U.S. Geological Survey, Open File Series No. 16113. Washington, DC, 1970.

Clark, M.M., A. Grantz, and M. Rubin (1972). "Holocene activity of the Coyote Creek fault as recorded in the sediments of Lake Cahuilla," the Borrego Mountain earthquake of April 9, 1968, U.S. Geological Survey Professional Paper 787, Washington, DC, 1972, pp 1112-1130.

Cluff, R.S., D.B. Slemmons, and E.B. Waggoner (1970). "Active fault zone hazards and related problems of siting works of man," in Proceedings, Fourth Symposium of Earthquake Engineering, 1970, pp 401-410.

Coppersmith, K.J. (1991). "Updated empirical relationships among magnitude, rupture length, rupture area, and surface displacement," Bulletin of the Seismological Society of America, 1991.

Coppersmith, K.J., and R.R. Youngs (1990). "Probabilistic seismic-hazard analysis using expert opinion; An example from the Pacific Northwest," in E.L. Krinitzsky and D.B. Slemmons, Neotectonics in Earthquake Evaluation, Geological Society of America Reviews in Engineering Geology, vol 8, 1990, pp 26-46.

Davies, G.F., and J.H. Brune (1971). "Regional and global fault slip rates from seismicity," Nature, vol 229, 1971, pp 101-107.

Hanks, T.C., and H. Kanamori (1979). "A moment magnitude scale," Journal of Geophysical Research, vol 84, 1979, pp 2348-2350.

Housner, G.W. (1965). "Intensity of earthquake ground shaking near the causative fault," in Proceedings of Third World Conference on Earthquake Engineering, New Zealand, vol 1. Wellington, New Zealand, New Zealand National Committee on Earthquake Engineering, 1965, pp III, 95-115.

Hudson, D.E. (1972). "Strong motion seismology," in Proceedings of the International Conference on Microzonation for Safer Construction Research and Application, Seattle, WA, 30 Oct - 3 Nov 1972. Seattle, WA, National Science Foundation, 1972, pp 39-60.

Iida, K. (1965). "Earthquake magnitude, earthquake fault, and source dimensions," Journal of Earth Sciences, Nagoya University, vol 13, no. 2, 1965, pp 115-132.

Krinitzsky, E. (1974). Fault assessment in earthquake engineering, Army Engineering Waterways Experiment Station, Miscellaneous Paper S-73-1. Vicksburg, MS, May 1974.

Lamar, D.L., P.M. Merifield, and R.J. Proctor (1973). Earthquake recurrence intervals on major faults in southern California, geology seismicity and environmental impact, Association of Engineering Geologists, Special Publication. Los Angeles, CA, University Publishers, 1973.

Mark, R.K., and M.G. Bonilla (1977). Regression analysis of earthquake magnitude and surface fault length using the 1970 data of Bonilla and Buchanan, U.S. Geological Survey, USGS Open File Report 77-164. Menlo Park, CA, 1977.

Newmark, N., and E. Rosenblueth (1971). Fundamentals of earthquake engineering. Englewood Cliffs, NJ, Prentice Hall, 1971.

Seed, H.B., I.M. Idriss, and F.S. Kiefer (1969). "Characteristics of rock motions during earthquakes," Journal of the Soil Mechanics and Foundations Division, ASCE, vol 95, no. SM5, Sep 1960, pp 1199-1218.

Tocher, D. (1958). "Earthquake energy and ground breakage," Bulletin of the Seismological Society of America, vol 48, 1958, pp 147-153.

U.S. Geological Survey (1975). Studies for seismic zonation of the San Francisco Bay legion for reduction of earthquake hazards, R.D. Borcherdt, ed., Professional Paper 941-A. Reston, VA, 1975.

Wallace, R.E. (1970). "Earthquake recurrence intervals on the San Andreas fault," Geological Society of America Bulletin, vol 81, 1970, pp 2875-2890.

Walper, T.L. (1976). State of the art for assessing earthquake hazards in the United States, Army Engineering Waterways Experiment Station. Vicksburg, MS, Mar 1976.

Wesson, R.V., et al. (1975). Faults and future earthquakes studies for seismic zonation of the San Francisco Bay Region, U.S. Geological Survey, Professional Paper 941-A. Reston, VA, 1975.

Youngs, R.R., and K.J. Coppersmith (1985). 'Implication of fault slip rates and earthquake recurrence models to probabilistic seismic hazard estimates," Bulletin of the Seismological Society of America, vol 75, 1985, pp 939-964.

Table 2-1
Recurrence Intervals on Selected Faults in Southern California
(from Lamar, et al., 1973, edited by Southern California Section
of the Association of Engineering Geologists)

Fault	Slip Rate (cm/yr)	Length (km)	Recurrence Intervals (yr) at a Point on Fault (R_x)			Recurrence Intervals (yr) over Length of Fault (R_l)		
			M 6	M 7	M 8	M 6	M 7	M 8
Northwest Trend Right-Slip								
San Andreas (southern segment)	3	500	10	40	200*	0.3-1	3-10	40-100*
San Jacinto Fault System	0.3	440	100*	400*	2000	4-10*	40-100*	400-1000
Whittier-Elsinore-Agua Caliente-Laguna Salada	0.08	260	300	2000	6000	20-90	200-900	3000-6000
Northeast Trend Left-Slip								
Big Pine	0.2	95	100	600*	3000	20-100	300-600*	3000
Garlock	0.8	250	30	200	600	2-10	30-90	300-600
Reverse and Thrust								
White Wolf	0.04	53	1000	2000*	4000	200-900	1000-2000*	4000
Sierra Madre Fault System	0.8	90	100*	300*	800	30-100*	100-300*	800

*Most likely, based on historic record.

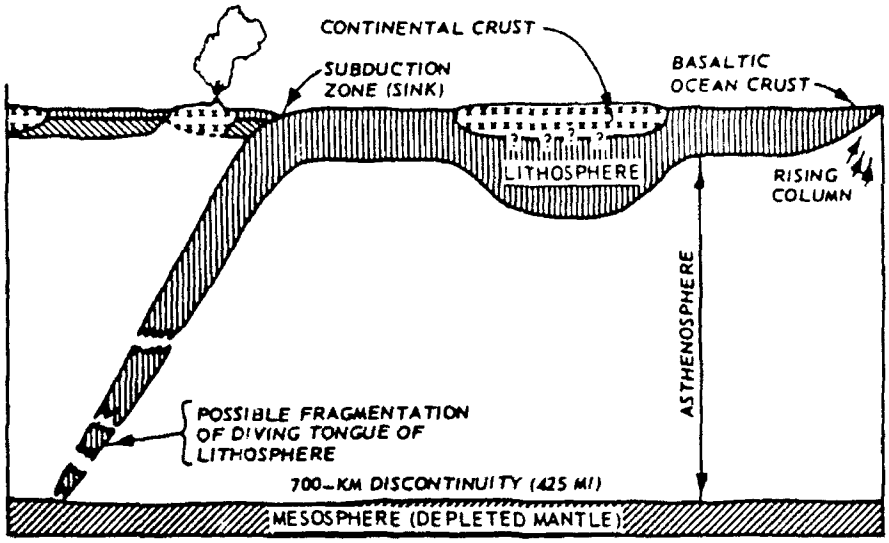

Figure 2-1. Cross section of earth structure (from Walper, 1976).

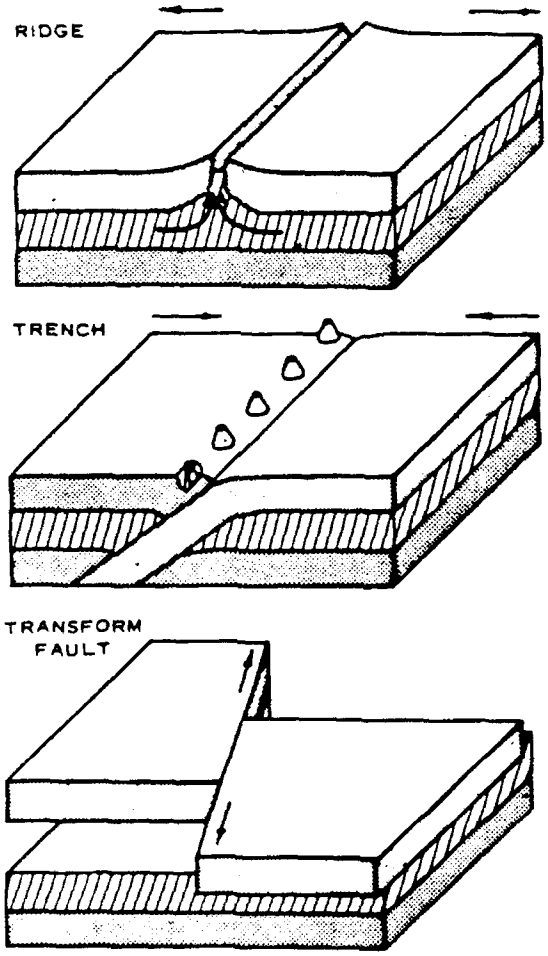

a. Divergent or spreading boundary

b. Convergent or collision boundary

c. Transform or transcursion boundary

Figure 2-2. The three kinds of boundaries between plates (from Walper, 1976).

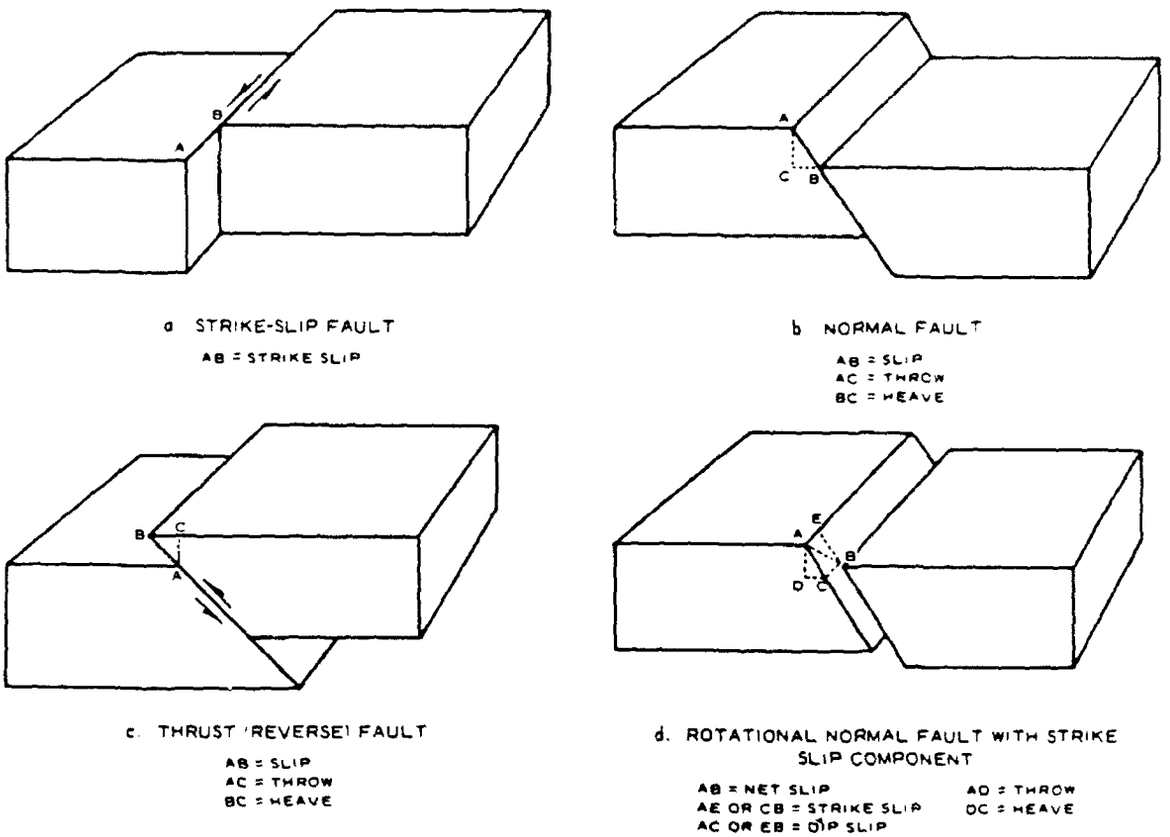

Figure 2-3. Fault terminology (from Krinitzsky, 1974).

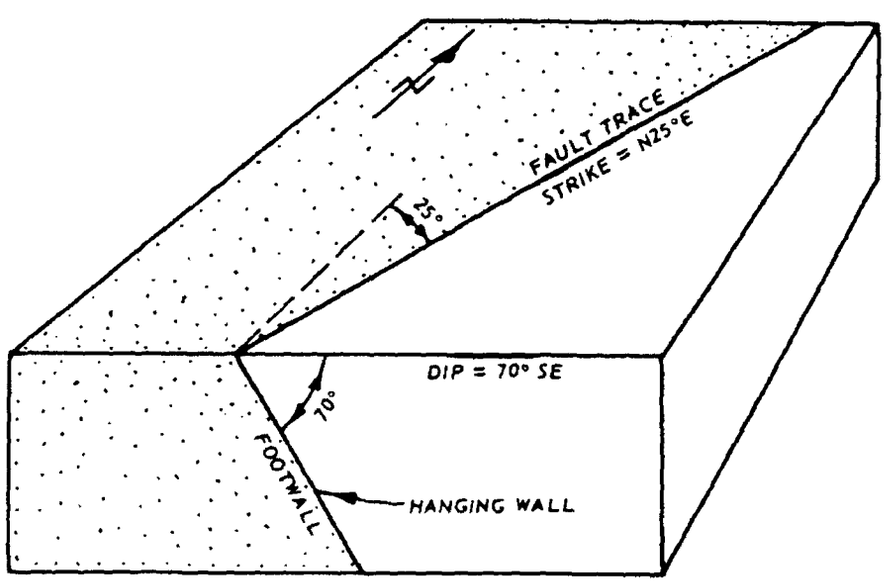

Figure 2-4. Fault measurement (from Krinitzsky, 1974).

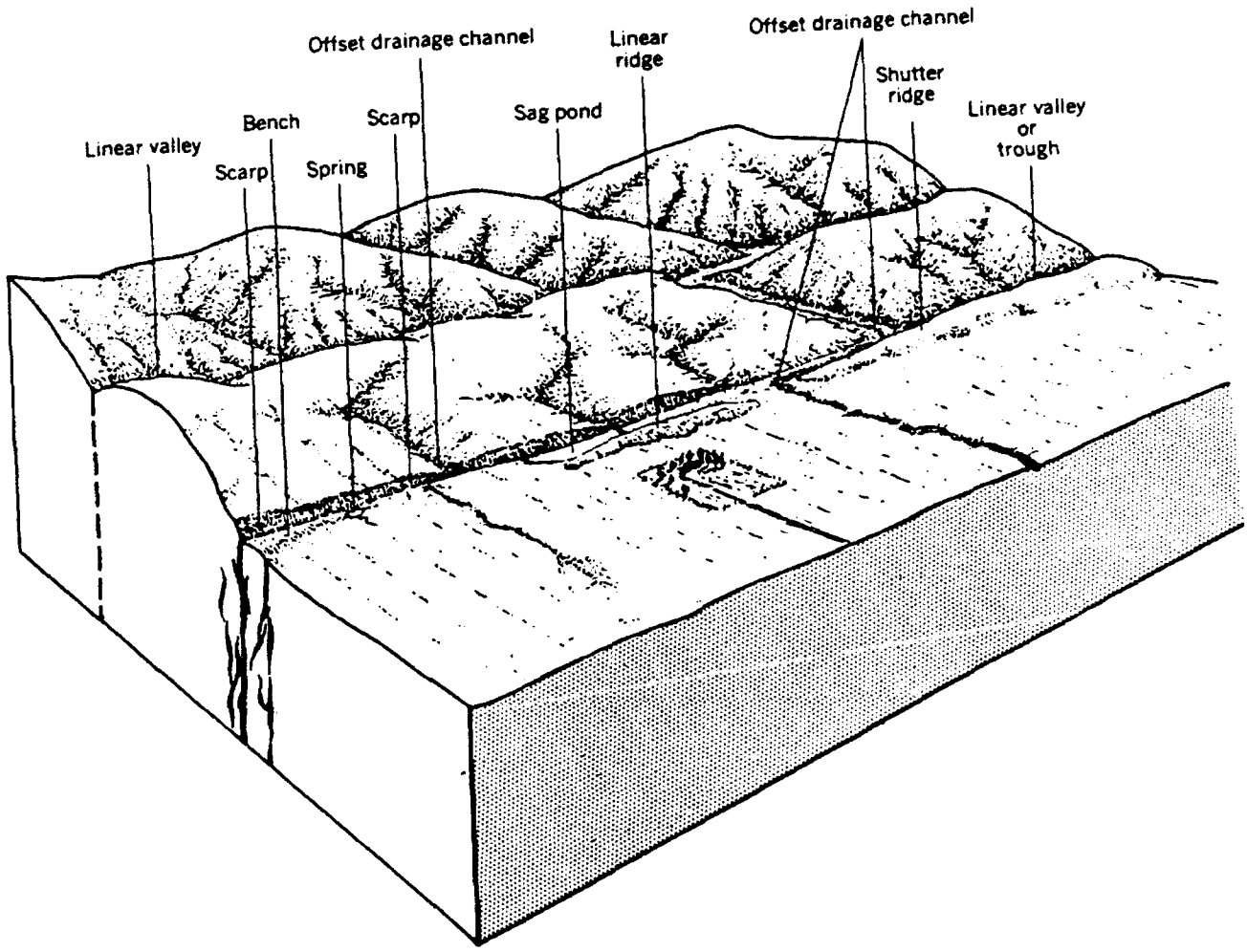

Figure 2-5 Landforms developed along recently active strike-slip faults (after U.S. Geological Survey, 1975).

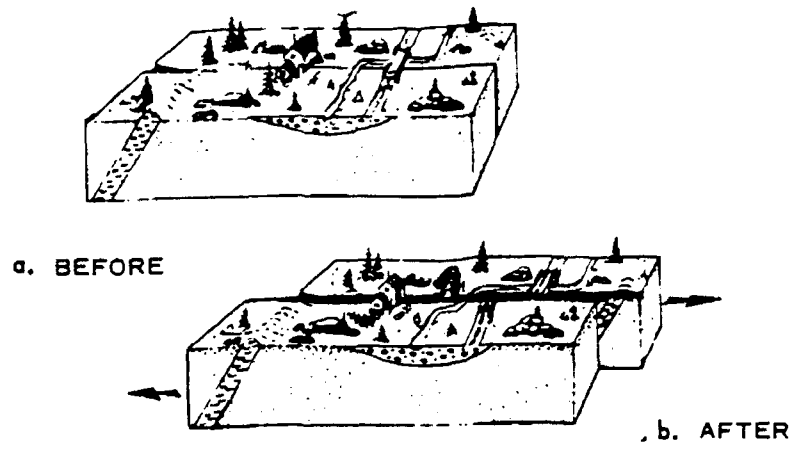

Figure 2-6. Damage associated with movement along strike-slip fault (from Krinitzsky, 1974).

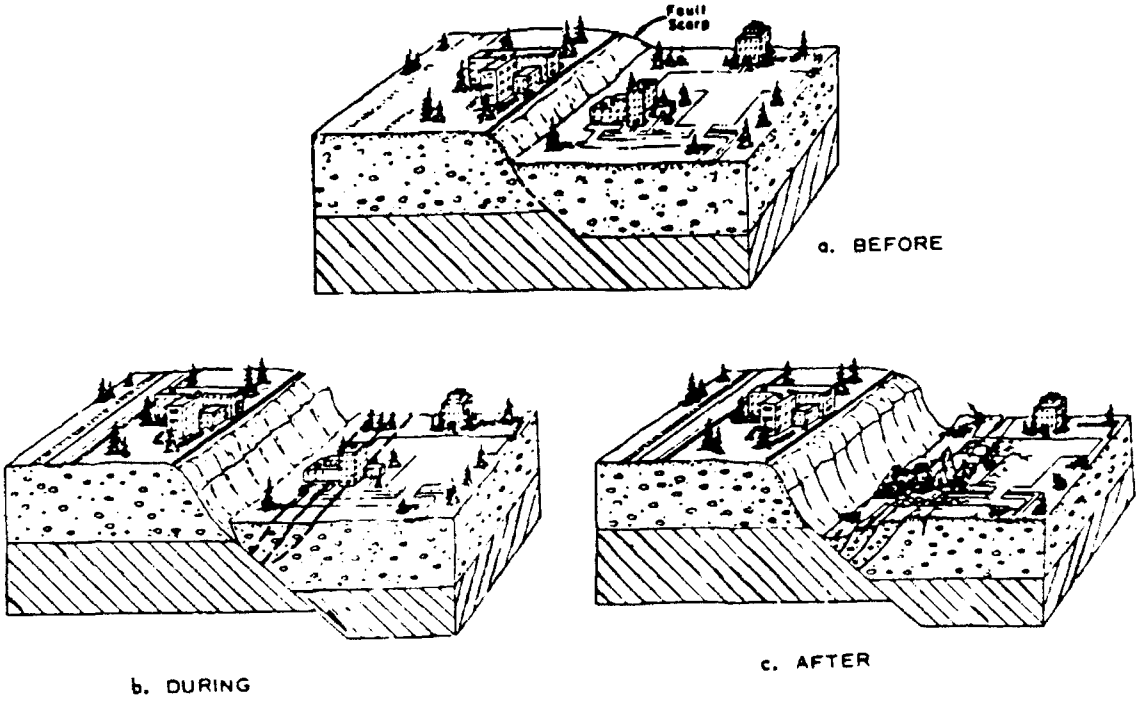

Figure 2-7. Damage from normal fault (from Krinitzsky, 1974).

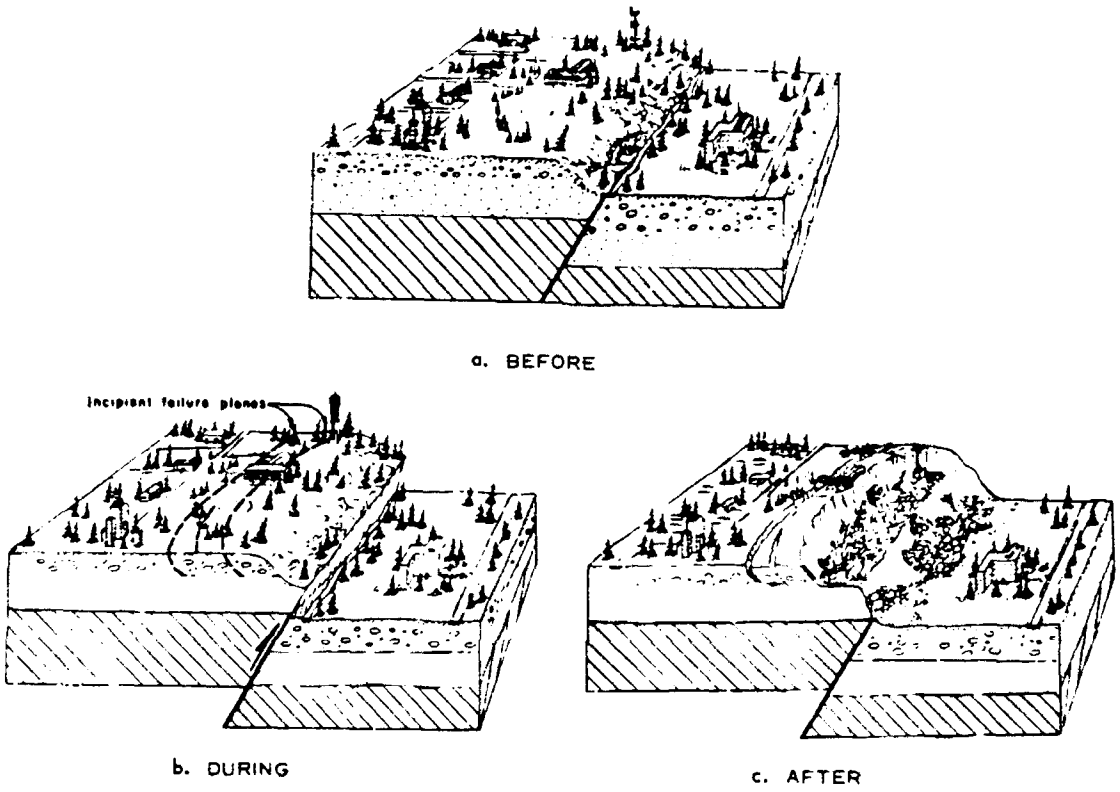

Figure 2-8. Damage from thrust (reverse) fault (from Krinitzsky, 1974).

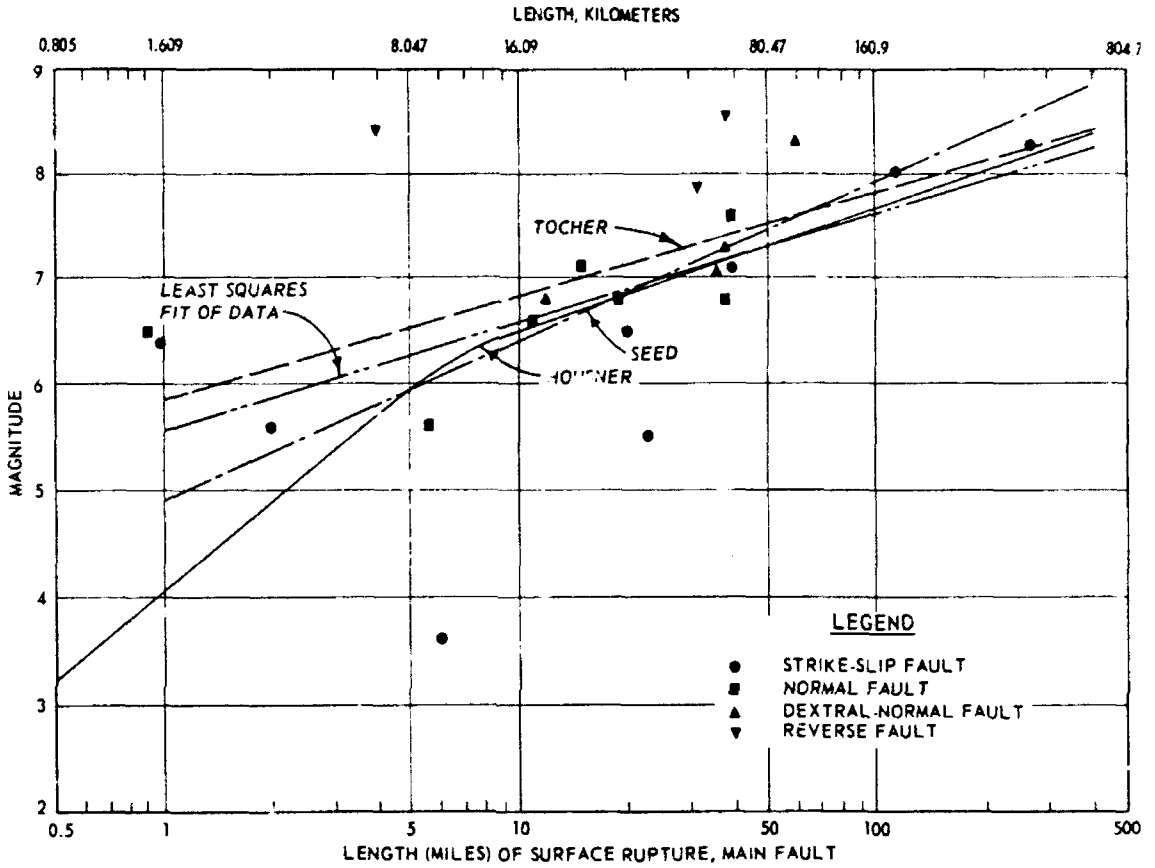

Figure 2-9. Earthquake magnitude versus length of surface rupture (from Krinitzsky, 1974).

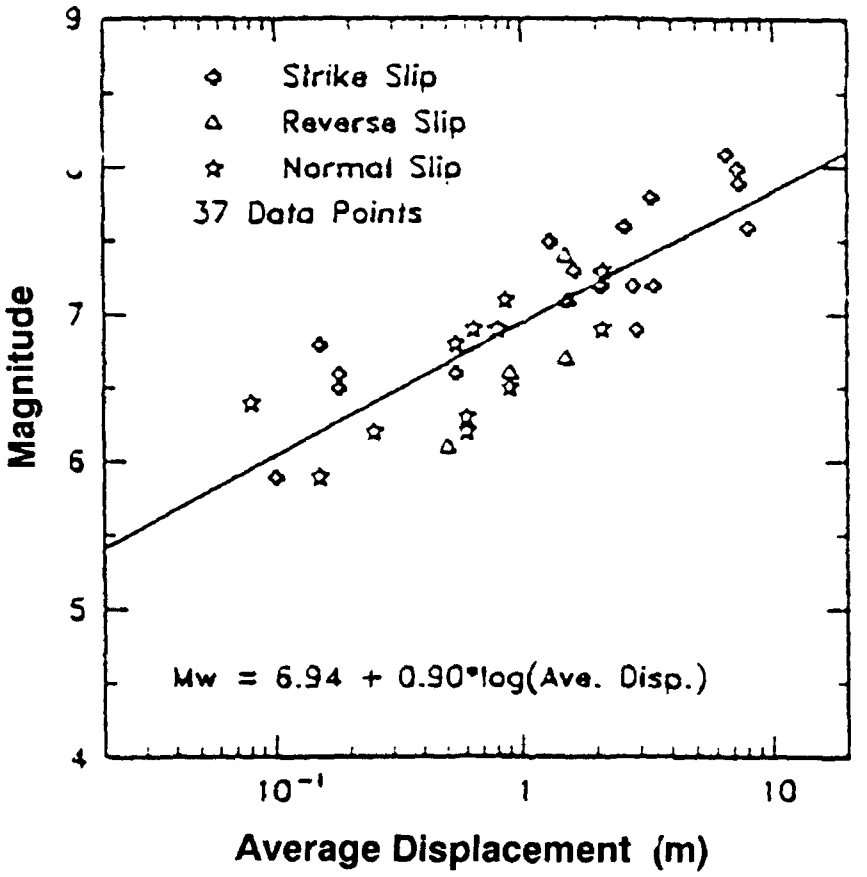

Figure 2-10. Earthquake magnitude versus average surface displacement (from Coppersmith, Proceedings Fourth International Conference on Seismic Zonation, 1991)

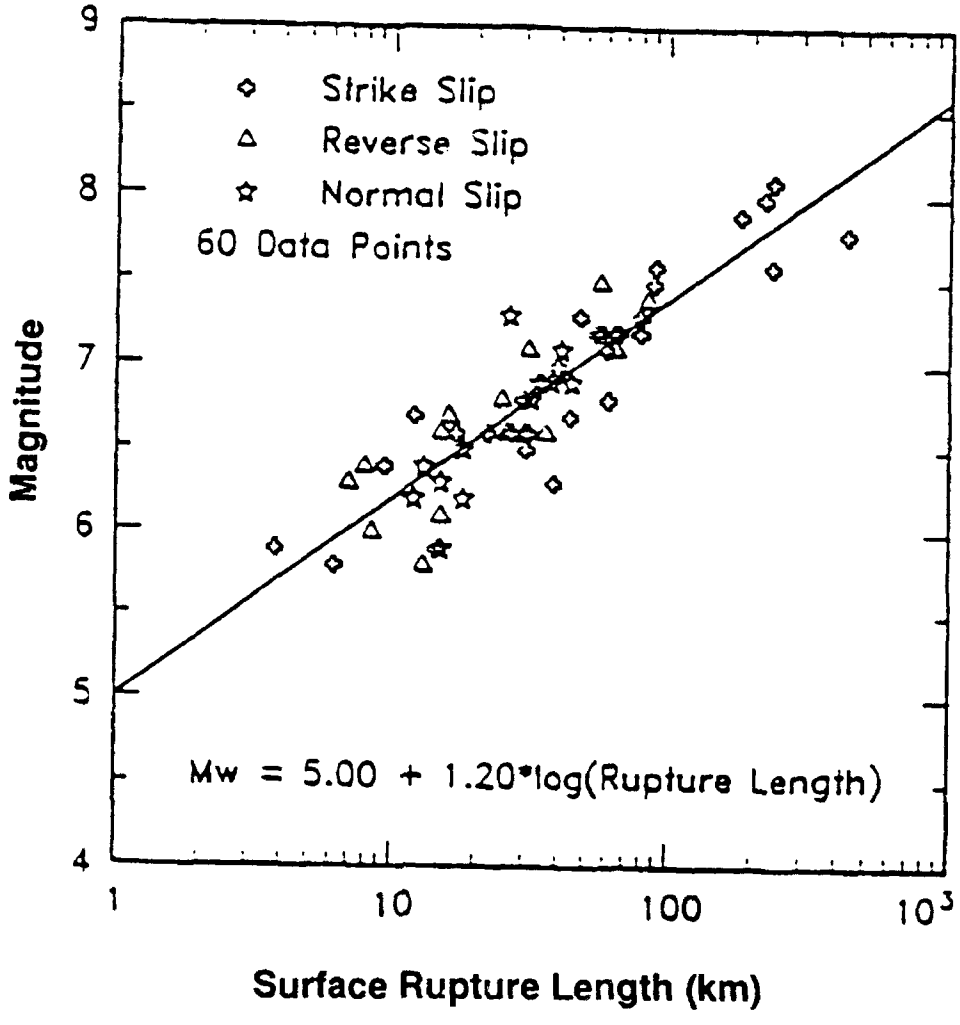

Figure 2-11. Earthquake magnitude versus fault surface rupture length. (from Coppersmith, Proceedings Fourth International Conference on Seismic Zonation, 1991)

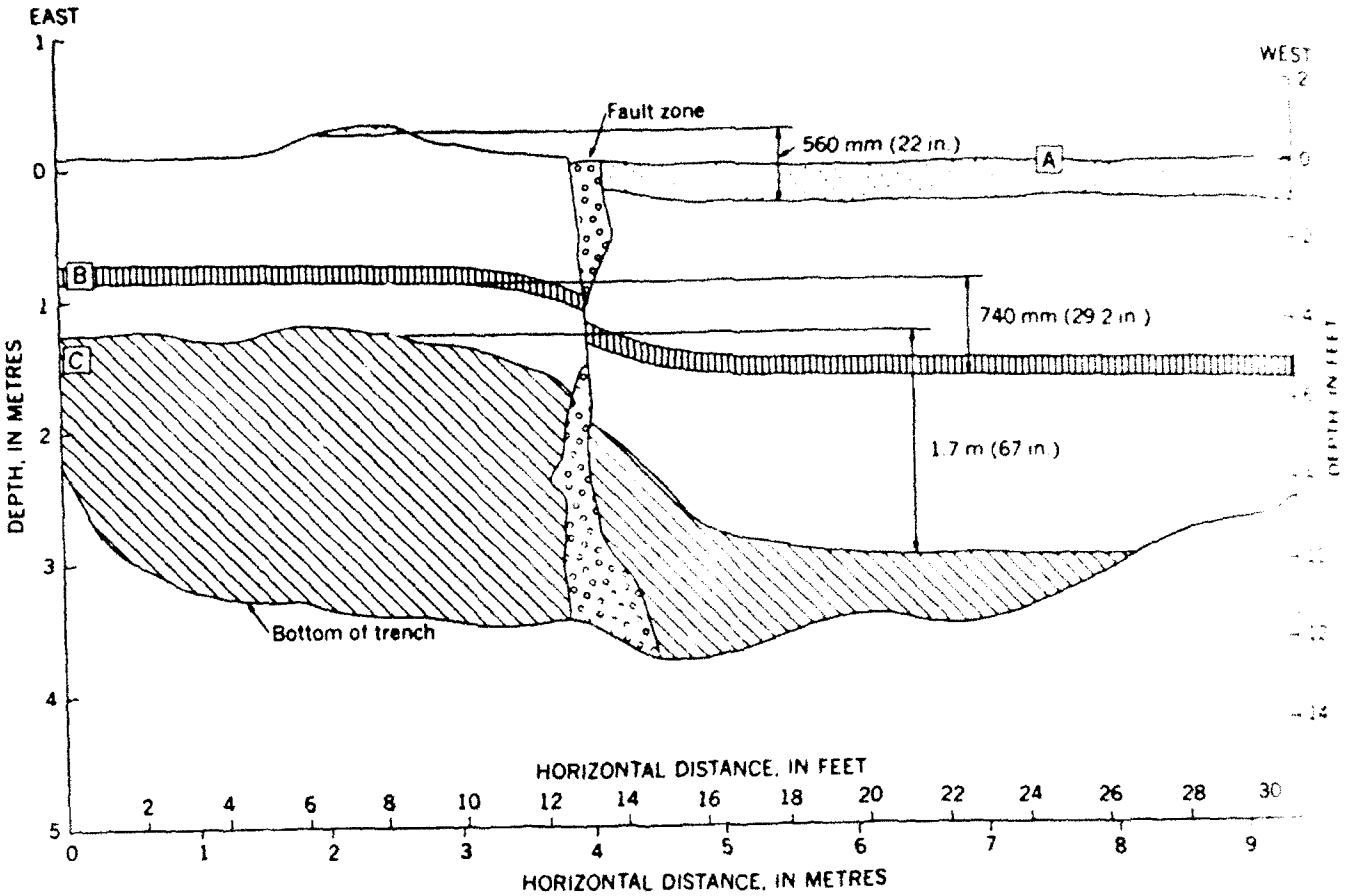

Figure 2-12. Sketch of trench wall (from Clark et al., 1972).

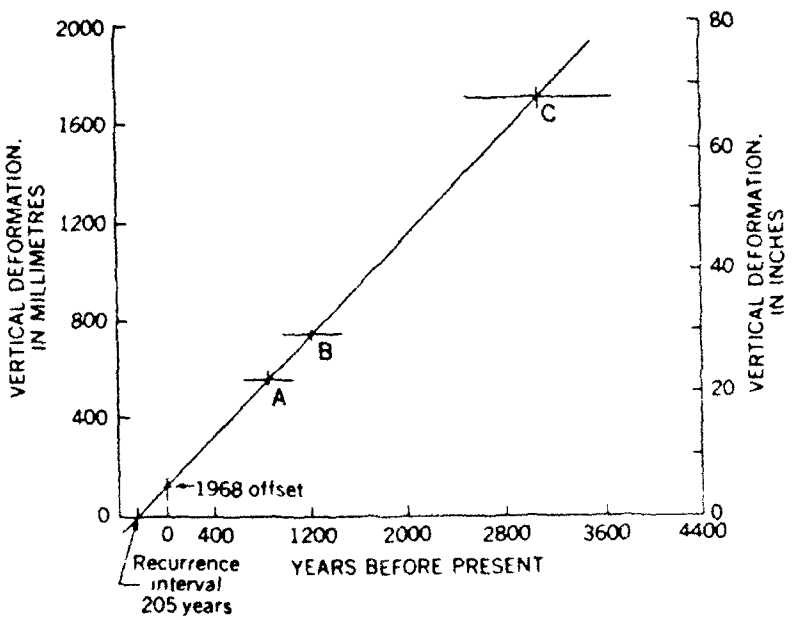

Figure 2-13. Estimated recurrence data (from Clark et al., 1972).

CHAPTER 3
EPICENTER DATA BASE

INTRODUCTION

The U.S. Geological Survey National Earthquake Information Center, Denver, Colorado has produced "The Global Hypocenter Data Base" CDROM which contains parameters for more than 438,000 earthquake events. Seven world-wide and 12 regional earthquake catalogs were assembled to produce this data base, spanning a time period from 2100 B.C. through 1990. Useful data for the United States is generally constrained to the period when instruments were available to compute event magnitude. Each earthquake is detailed where data are available with date, origin time, location, 4 magnitude estimates, intensity, and cultural effects.

DATA BASE SEARCHING

A computer program, EPIC, is available for searching the CDROM. EPIC makes data available to information users via a user-defined search request. The request determines which steps are necessary to produce the desired output. It includes a search method, combination of search elements, and a destination output format, including:

- Global
- Rectangular grid
- Circle
- Irregular grid

Search elements include:

- Date interval (year/month)
- Magnitude range
- Catalog selection
- Depth interval
- Intensity range
- Magnitude range or intensity interval

- Duplicate earthquake eliminator
- Cultural effects (casualities/damage)
- Information (fault plane/moment tensor solutions)
- Associated seismic phenomena (e.g., faulting, ground response)

An automated plotting package that produces seismicity maps in multicolor or monochrome is incorporated into the EPIC software. The data to be mapped are extracted from the selected data and plotted in a global or regional format. The map may be delayed or cancelled at user's discretion.

The availability of the CDROM data base of epicenters and EPIC software greatly facilitates creation of the historical epicenter subset required for use of the automated seismicity analysis tools developed and presented in this report. Any data base can be used provided the data are in the same format as the CDROM and EPIC data. Details are presented in the EPIC user's manual, which will not be repeated here.

DATA BASE DISCUSSION

A number of data fields for some events are unfilled because the information is not available. Information on cultural effects, intensity, and other phenomena associated with the event has been included for earthquakes in the United States. This information has sometimes been entered for non-United States earthquakes, particularly since May 1968, although significant gaps still exist.

The quality of epicenter determinations varies significantly with the time period studied. Before 1900, locations are usually noninstrumentally determined and are given as the center of the macroseismic effects. Most instrumental epicenters prior to 1961, excluding local earthquakes in California, were located to the nearest 1/4 or 1/2 degree of latitude and longitude. Reliable information on the quality of many epicenter determinations is lacking. Beginning in 1960, epicenters have been determined by computer, and the accuracy is generally better. However, although stated to tenths or hundredths of a degree, the location accuracy is usually a few tenths of a degree. Since May 1968, the latitude and longitude values for most events have been listed to three decimal places. This precision is not intended to reflect the accuracy of the location of events except for local California earthquakes and special epicenter determinations. Where several sources have determined an epicenter for the same earthquake, one solution has been designated as the most reliable. Usually it is the source believed to contain the best data set for the earthquake. In some cases, data from two sources were combined to provide a more complete record.

Magnitudes from a number of different sources are included in the earthquake data file. Gutenberg and Richter (1954) and Richter (1958) discuss the development of the magnitude scale. Many magnitudes published by Gutenberg and Richter (1954) were later revised by Richter (1958). The revised magnitudes are used in the file even though the source is identified as Gutenberg and Richter (1954). The concept of earthquake magnitude is not restricted to one value. Several definitions are possible, depending on which seismic waves are measured. Three different magnitude scales, BODY WAVE (MB), SURFACE WAVE (MS), and LOCAL (ML),

are distinguished in this file. In addition, another data field, OTHER MAGNITUDE, was included when it was unclear which scale was used. Richter (1958) and other modern seismology references provide detailed discussions of this topic. The different scales do not give exactly comparable results, and different values frequently are given for the same earthquake. It is common practice to average the individual magnitudes from different stations to get a more uniform value within each scale (MB, MS, and to a lesser extent ML).

In general, the file contains earthquakes of magnitude 4.0 or less only for the United States region and for areas within dense seismic station networks. However, no claim is made for the statistical homogeneity of these events. Inclusion of earthquakes of magnitude 4.0 to 5.0 also is influenced by the proximity of seismic stations to the source or epicenter.

A maximum intensity is listed for many of the earthquakes. Each is assigned according to the Modified Mercalli Intensity Scale of 1931. Some of these values have been converted from reported intensities on other scales.

CORRECTION OF EPICENTERS

Early records of earthquakes may show inaccurate epicentral locations. Also, magnitudes or intensities may differ from values that would now be assigned. As an example, Krinitzsky (1974) reports the following:

> "The location of a listed earthquake of 15 May 1909 in southern Saskatchewan is shown in [Figure 3-1]. It has a maximum intensity of VIII and is the largest recorded event in this general area. Its location was made when seismograph stations were few, and those that operated were far less accurate than they are today. The intensity of VIII was assigned on the basis of the large felt area. The event was checked by referring to the newspaper accounts of this time. This was not too formidable a task. State archives, state university collections, and national archives often have collections of local newspapers gathered in central depositories. One may request microfilm copies of these papers for the dates of interest, review them, and assign intensity values based on their descriptions. This exercise provided intensities for more than 50 communities though this was, and still is, a thinly populated area. The resulting iso-intensity map shows there was no intensity VIII. The greatest was VI. Also, the region of VI had its center to the east by about 1 degree from the NOAA location. In [Figure 3-1], the revised location is shown in relation to three other earthquakes of 1956, 1968, and 1972. Their locations were accurate to begin with because of better instrumental capability. One is associated with a seismically interpreted fault that also agrees with a geologically mapped fault. Its trend is toward the three other events. Thus, the revised location for the 1909 event helps to interpret a fault trend."

SEISMIC ARRAYS

Seismometers have been installed near known active faults to record microearthquakes. Figures 3-2 and 3-3 show the location of recorded microearthquakes for a year, and major fault

zones in California. The events recorded range in magnitude from 0.5 to 1.5. The figures show areas where the microearthquakes closely trace the faults. There are also regions where few microearthquakes occurred. The San Andreas fault north of the Sargent fault exhibits less activity than southern portions, perhaps indicating it is locked. However, sufficient microearthquakes have occurred to show the continuation of the fault. It may be reasoned that small failures might occur before a major rupture occurs; alternatively, the large number of microearthquakes demonstrate active creep which may be sufficient to prevent sizable strain accumulation and preclude a large event.

Since earthquakes are associated with faults, it might be thought that they should precisely overlay the fault location. This is not the case because the distribution of seismometers is uneven and has changed with time. There are limitations in the accuracy of the techniques used to locate epicenters, principally from variations in the assumed propagation velocities. Further explanation for the location of epicenters being off their associated fault comes from the simplified model used to locate them. This is explained in Figure 3-4. Note that the center of earthquake energy is located at the focus. For an inclined fault, the surface location (epicenter) is a distance removed from the surface fault location. It is only in vertical faults that one might expect the epicenter to lay on the fault.

Krinitzsky (1974) concludes that earthquakes can be related to existing faults and that the possibility of formation of new faults should not be considered in design. Large earthquakes require fault breaks of considerable distance. The uncertainties that occur in the association of earthquakes with faults can occur only for small events. Generally, in the Western United States the extent of geologic investigation precludes the omission of a large fault remaining unknown. However, there are uncertainties associated with eastern earthquakes. For example, causative faults responsible for the New Madrid earthquake of 1811 and 1812 have not yet been identified. This may be the result of insufficient geologic investigations. The importance of considering the extent and quality of geologic investigations is evident.

LIMITATIONS TO HISTORIC DATA

A period of demonstrated quiescence over a geological time period indicates inactivity of the fault and probable continued inactivity. However, inactivity over a period of historic recording (50 to 100 years) does not imply future inactiviy. Rather, it may point to a region which is locked and through which a major fault rupture may propagate. A number of earthquakes producing damage in southern California occurred on faults lacking historic activity. Caution must be exercised to recognize that the accuracy of an incomplete data base is very limited when extrapolated for return periods greatly exceeding the length of the period of recorded data. Furthermore, aftershocks must be distinguished from main shocks. An area having recently undergone a large event releasing strain built up for hundreds or thousands of years is probably safe against a large release in the near future. Thus, a recent large event on a fault might actually indicate safety in the immediate future, rather than an indication of activity. A single event by itself cannot give an accurate measure of return time.

Krinitzsky (1974) is quoted below:

> "In the United States the history of earthquake activity ' greatly truncated. At best the record covers less than 350 years. This it does in very few places. For most of the country it is about 150 years. This, however, is general

earthquake history and not the record of movement on specific faults or in fault zones. In other parts of the world the record for both earthquake history and interpreted fault activity is better.

N.N. Ambraseys (1971).... has studied the record of damaging earthquakes for the past two millennia in some portions of the Near East. [Figure 3-5].... shows the cumulative distribution during this time of damaging earthquakes along (a) the Border Zone, which is a northeast-southwest trend of faults that extends toward the Dead Sea along the border of Israel; and (b) the Anatolian Zone that is roughly an east-west zone of faulting. It intersects with the Border Zone. Ambraseys points out that during the first five centuries the Border Zone was quiescent while the Anatolian Zone was active. For the following six centuries the pattern was reversed only to be reversed again during the eleventh century. In this case there is a factor of dependence of activity along one zone on that of the other. The two join to encompass a miniplate, and movement tends to shift from one side to another on a cyclical basis. This tends to discredit the validity of probabilistic projections based only on a short history."

Also, as noted in Krinitzsky (1974), there are likely to be:

.... "variations in rates of slippage along various segments of any one long active fault or fault zone. This is known to be the case along the San Andreas. During its relatively short historic period, it was noted that major earthquakes moved from place to place along the fault. Portions that once moved, notably the segment that slipped during the San Francisco earthquake of 1906, have become locked while slippages occurred elsewhere. [Figure 3-6] is a schematic statement of variations in rates of slippage in inches per year.... The slippage is that which has occurred during an interval of 60 years. Though this is instructive of irregularities in the rates of movement, it is not intended as a guide to the future. If anything, the future is very likely to be different. The segment between Cholame and Camp Dix appears to be in a locked position. Stresses are building up. One day this segment will rupture suddenly."

REFERENCES

Ambraseys, N.N. (1971). "Value of historical records of earthquakes," Nature, vol 232, no. 5310, 1971, pp 375-379.

Guttenberg, B. and C.F. Richter (1954). Seismicity of the earth and associated phenomena, Second Ed. Princeton, NJ, Princeton University Press, 1954.

Krinitzsky, E. (1974). Fault assessment in earthquake engineering, Army Engineering Waterways Experiment Station, Miscellaneous Paper S-73-1. Vicksburg, MS, May 1974.

Lamar, D.L., P.M. Merifield, and R.J. Proctor (1973). Earthquake recurrence intervals on major faults in southern California, geology seismicity and environmental impact, Association of Engineering Geologists, Special Publication. Los Angeles, CA, University Publishers, 1973.

National Earthquake Information Center (1992). EPIC, retrieval software of the Global Hydrocenter Data Base CDROM, User's Guide, U.S. Geological Survey. Denver, CO, 1992.

Richter, C.F. (1958). Elementary seismology. San Francisco, CA, W.H. Freeman Co., 1958, p 768.

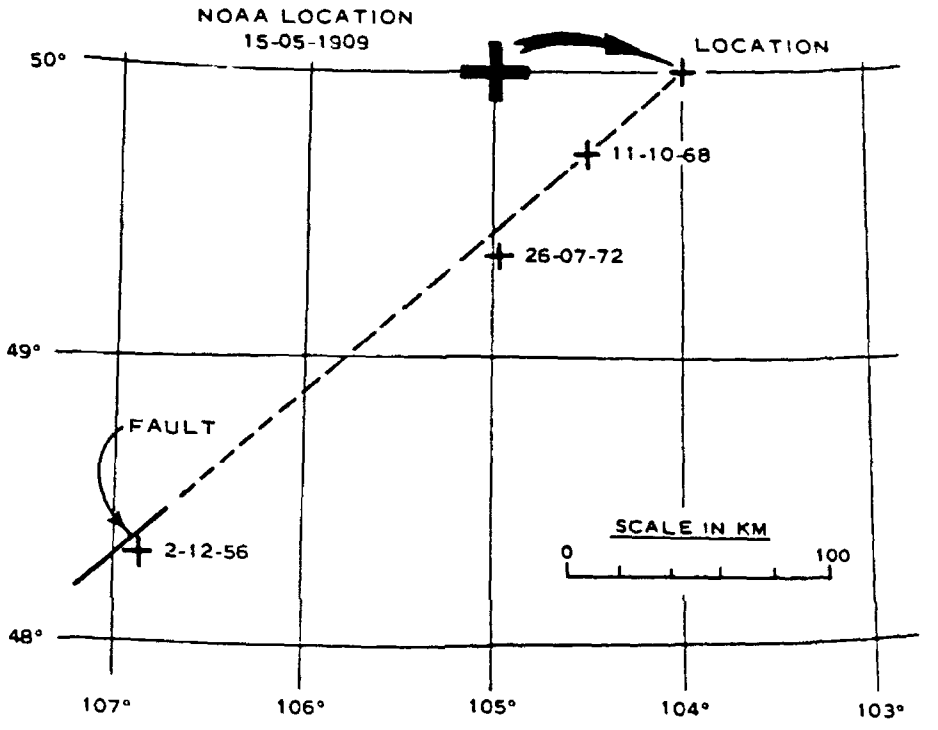

Figure 3-1. Revision of epicentral location based on association with fault (from Krinitzsky, 1974).

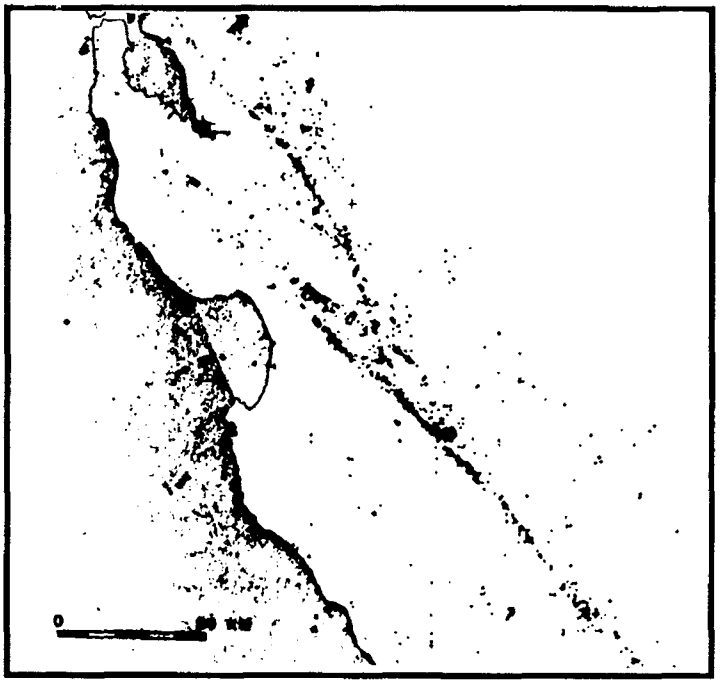

Figure 3-2. Micro earthquakes indicating fault trend, see Figure 3-3 (from Krinitzsky, 1974).

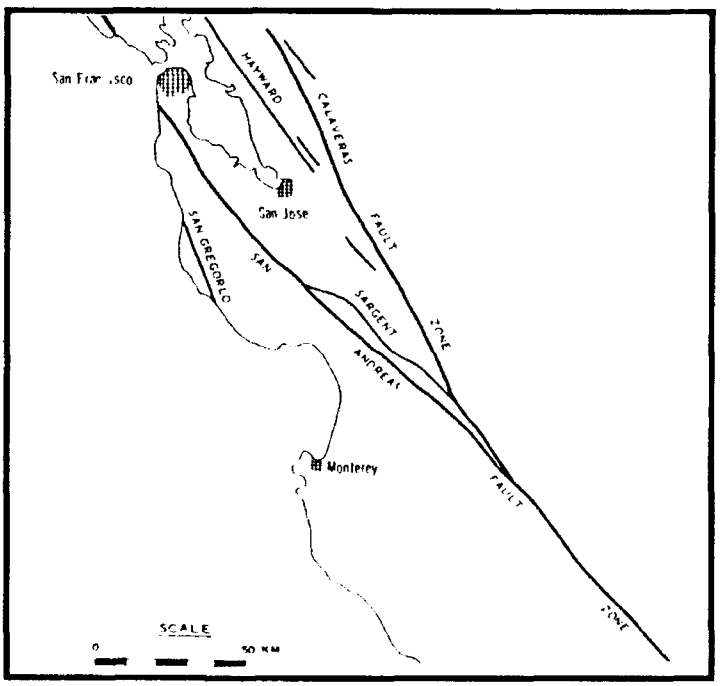

Figure 3-3. Major fault zones in central california (rom Krinitzsky, 1974).

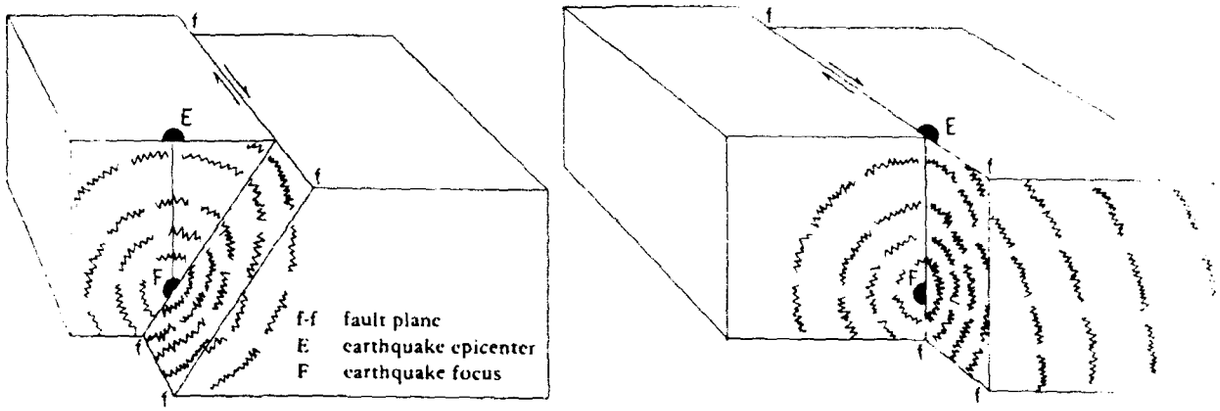

Figure 3-4. Epicenters (from US Gelogical Survey , 1975)

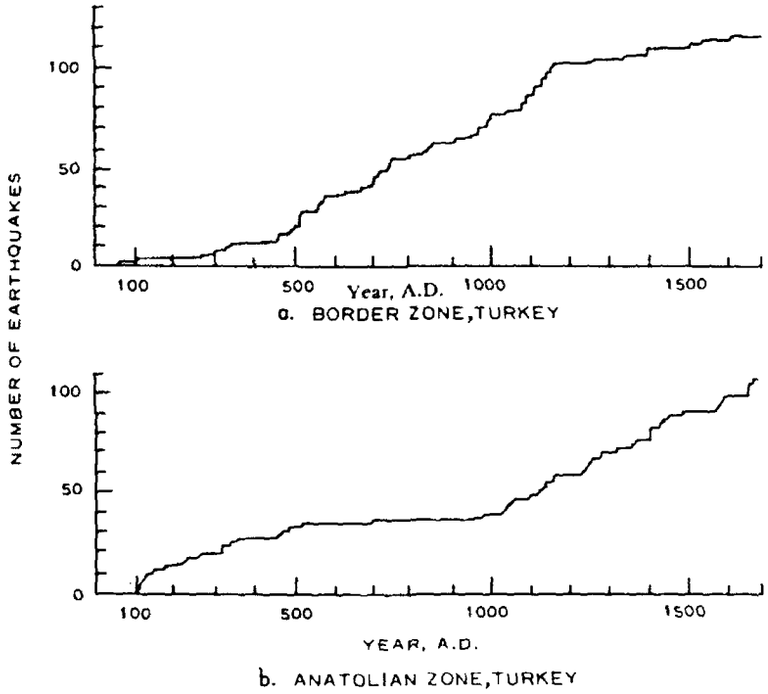

Figure 3-5. Time distribution of damaging earthquakes in Turkey (from Ambraseys, 1971)

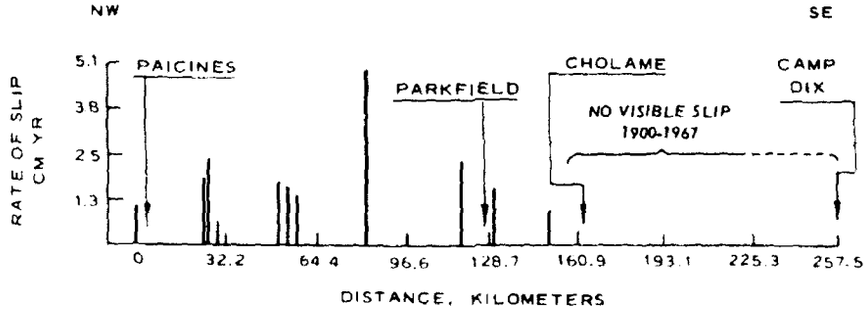

Figure 3-6. Variation in rate of slippage along san Andreas Fault (from Krinitzsky, 1974).

CHAPTER 4
ESTIMATING EARTHQUAKE RECURRENCE

EXPONENTIAL MAGNITUDE DISTRIBUTION

A fundamental step in the estimation of seismic hazard is the definition of recurrence interval of possible earthquakes as quantification of site exposure. In 1954 Guttenberg and Richter developed an exponential frequency magnitude relationship:

$$\log N(m) = a - b\,m \tag{4-1a}$$

where: N (m) = cumulative number of earthquakes greater than m
a = constant
b = constant

Equation 4-1a can be written in the form of an exponential distribution:

$$N(m) = \exp(a - \beta m) \tag{4-1b}$$

where: $\alpha = a \ln(10)$
$\beta = b \ln(10)$

A lower bound, m_l, can be selected as an arbitrary reference point. The following can be developed:

$$N(m) = N(m_l) \exp(-\beta(m - m_l)) \tag{4-2}$$

where: m_l = arbitrary reference magnitude

Equations 4-1 and 4-2 are constrained by an upper limit magnitude associated with the capability of a specific fault to generate such an event based on the fault's length and maximum rupture possible. The physical limitations of an upper limit truncate the magnitude distribution.

To estimate frequency with less error, a magnitude frequency relation in the form of:

$$\log_{10} N(m) = a_o + b_1 m + b_2 m^2 \qquad (4\text{-}3)$$

has been used. This quadratic form has an advantage of not overestimating the occurrence of large events and avoids the discontinuity of the function from a truncated linear frequency distribution.

Another generalized formulation of the Guttenberg-Richter relation is of the form:

$$\ln N(m) = A - B \exp(\alpha m)$$

CHARACTERISTIC MAGNITUDE

Coppersmith and Youngs (1990) report that recent geologic studies of late quaternary faults strongly suggest that the exponential recurrence model is not appropriate for expressing earthquake recurrence on individual faults. Their studies suggest many individual faults tend to generate essentially the same size or characteristic earthquakes having a relatively narrow range of magnitudes at or near the maximum. This conclusion is based upon evaluating the amount of displacement per event for studies of the Wasatch and south-central San Andreas faults. This implies that earthquake recurrence does not conform to an exponential recurrence model but rather one that has a variable b value. The type of geologic recurrence interval data developed for the Wasatch and San Andreas faults are not generally available for most faults in the Western United States. Fault slip rate data are required.

Youngs and Coppersmith (1985) note that when geologically derived recurrence intervals for characteristic earthquakes are compared with relationships derived from seismicity data, a marked mismatch occurs. The characteristic earthquake was found to include a band of events of about one-half magnitude width. For events less than the characteristic event magnitude, the exponential recurrence behavior was found to be a satisfactory representation. The increment between the minimum characteristic magnitude and the portion of the recurrence curve showing exponential behavior at recurrence rates greater than the rate for characteristic events is about one magnitude in width. The magnitude range showing nonexponential behavior is about 1.5 magnitudes in width. Figure 4-1 shows the generalized function. To simplify application, Δm_c is 0.5 magnitude units, m' is set at $m^u - \Delta m_c$, and the value of n (m^c) = n (m'-1).

EVENT RETURN TIME

The Poisson process has been used to describe earthquake occurrences and represents a basic model with only a single parameter to define. A Poisson process is a continuous time, integer-valued counting process with stationary independent increments. This means the number of events occurring in an interval of time depends only on the length of the interval. The

probability of an event occurring in the interval is independent of the history. The probability distribution of the number of earthquakes is given by:

$$P_N(n, \lambda t) = \frac{e^{-\lambda t}(\lambda t)^n}{n!} \quad (4\text{-}4)$$

where: P_N = probability of occurrence of n events of a given magnitude range

λ = mean rate of occurrences per unit of time t

The expected value of the numbers of earthquakes in time t is:

$$E(t) = \lambda t \quad (4\text{-}5)$$

A characterization of the Poisson process is that the time between events is independent, identically and exponentially distributed with a constant rate of occurrence, λ. The density function of the time between events is:

$$f(t) = \lambda e^{-\lambda t} \quad (4\text{-}6)$$

A consequence of Equation 4-6 is the hazard rate for the Poisson process is constant. In general, the hazard rate is defined as:

$$h(t) = \frac{f(t)}{1-F(t)} \quad (4\text{-}7)$$

where F(t) is the cumulative distribution function of the time between events. The quantity h(t)dt is the conditional probability of an event occurring in (t, t+dt) given there are no events in the interval (0,t). For the Poisson process,

$$h(t) = \frac{\lambda e^{\lambda t}}{1 - (1 - e^{\lambda t})} = \lambda \quad (4\text{-}8)$$

The constant hazard rate implies that the occurrence of an event in (t,t+dt) is independent of the time since the last event. This means that whether an earthquake of size m just occurred or whether there is a significant gap in events, the probability of an event occurring is independent

of past history. Physically, the energy released during event m does not affect the reservoir of stored energy available for subsequent events.

A significant advantage of the Poissan process is that it is based only on the epicenter data base. Thus, when additional information is lacking, it may be applied. Other models, as will be discussed in subsequent sections, will require additional parameters which may not be available, and will require substantial effort to acquire.

Weinbull Distribution

An improvement over the Poisson distribution is the Weinbull distribution suggested by Chou and Fisher (1975):

$$P(t) = 1 - e^{-ut^{\gamma}} \tag{4-9}$$

where u and γ are scale and shape parameters, respectively. Several methods are available to estimate the parameters. The maximum likelihood method is recommended because it utilizes the available information in the most appropriate manner. The shape factor γ is estimated by solving the general equation:

$$\frac{n}{\gamma} + \sum_{i=1}^{n} (\ln t_i) - n \left[\frac{\sum_{i=1}^{n} (t_i^{\gamma} \ln t_i)}{\sum_{i=1}^{n} (t^{\gamma})} \right] = 0 \tag{4-10}$$

and the scale parameter μ is obtained by equating:

$$\mu = \frac{n}{\sum_{i=1}^{n} (t_i^{\gamma})} \tag{4-11}$$

where n is the size of the sample and t_i is the time interval involved.

A graphical method of plotting historic earthquake data is very useful and widely used in practice. A new random variable is introduced as $Z = \ln (\mu t^{\gamma})$, and,

$$F(Z) = 1 - e^{-e^{Z}} \tag{4-12}$$

The list of earthquake occurrence data is arranged in groups of intensity or magnitude ranges. Within each group of earthquake events of the same magnitude range, the data are ordered by time intervals between occurrences, with the most frequent first. The plotting position of any data point within a group is $[t_i, F(i)]$ where t_i is the i^{th} longest time interval and,

$$F(i) = \frac{i}{n + 1} \tag{4-13}$$

where: i = position of the list; i.e., first, second, etc.
n = total number of events in the group

The parameters μ and γ are determined by the intercept and slope, respectively, of the plotted data following the relationship:

$$Z_i = \ln \mu + \gamma \ln t_i \tag{4-14}$$

where t_i is the i^{th} longest time interval and Z_i is given by:

$$\ln \ln \left[\frac{1}{1 - F(Z)}\right] \tag{4-15}$$

or

$$\ln \ln\left(\frac{n + 1}{n - i + 1}\right) \tag{4-16}$$

When $\gamma = 1$, the Weibull distribution is equivalent to the Poisson distribution.

Semi-Markov Process

A Markov or semi-Markov process can be defined as a process in which the occurrences of earthquakes make transitions from one range of earthquake magnitude to each of several other ranges. The transitions are probabilistic and have a one-step memory and the probability of moving to a given magnitude depends on the preceding magnitude. A semi-Markov process is also characterized by a probabilistic holding time between successive transitions. The probability that the holding time between two successive earthquakes is equal to a given value depends on the magnitude of the two events.

The semi-Markov process is consistent with the physical understanding of the earthquake process. That process consists of a gradual uniform accumulation and periodic release of significant strain energy within short periods of time following an earthquake of large magnitude.

The occurrence of another such sized event at the same location is less likely. As the time without occurrence of a large magnitude event increases, so does the probability of the occurrence of such an event. The size of the next large event and the holding time to that event are influenced by the amount of strain energy released in the previous event and the time during which strain energy has been accumulating.

Definition of the semi-Markov model requires specification of the most recent earthquake for a fault and the elapsed time since that event for various magnitude levels. Transition probabilities for each magnitude to other magnitudes must be specified. A probability distribution of holding times between the occurrence of two successive events must be determined. The exposure time or period of interest must be specified.

Woodward Clyde (1982) describes development of such a model that uses a Poisson process for events below a specified magnitude and a semi-Markov process for events above that level. This model requires a Bayesian approach for parameter estimation. The ability to use this class of model depends on the ability to quantify input data. The Bayesian approach will be discussed in the next section. The Markov process utilizes subsets of the epicenter data base for earthquake occurrences. This analysis of windows into the data requires a large catalog of events which are often not available. For this reason, semi-Markov models incorporate other techniques.

Bayesian Process

One method that has been used to supplement data is the use of Bayes' Theorem. Subjective information can be combined with historical data to develop parameters for a seismic model. Since the time interval or holding times between large magnitude earthquakes may be several hundred years, the historical seismicity data above are not sufficient to provide reliable estimates of parameters for a semi-Markov model. A Bayesian procedure with both historical seismicity data and subjective expert input has been used. From the seismicity data, estimates of transition time can be made from statistical examination of the time interval of the magnitudes of events which follow an event of magnitude m_i for all increments of i. The holding times between earthquakes of magnitude m_i and m_j can be evaluated. Subjective expert input takes the form of specification of fractiles of similar transition probabilities and holding times.

The Woodward Clyde (1982) study was done for a specific region. Obtaining data required is a major impediment from general adoption of Bayesian techniques into an easily useable general model for engineering applications.

Kiremidjian, et al. (1990) also developed a Bayesian procedure using a semi-Markov model. They note that at plate boundaries there are two types of forces: relatively uniform continuous tectonic forces and time-dependent forces from the asthenosphere. The coupling of the two forces causes nonlinear stress accumulation. They developed a random slip stochastic model to represent the nonlinear stress accumulation. To estimate the interarrival time distribution, a Weibull distribution is used. The parameters for the distribution are difficult to determine and subjective geophysical information is used to supplement the data. This model has been applied to the Middle America Trench and again is not thought adaptable for general engineering application.

RENEWAL MODELS

A renewal process consists of a set of independent, positive random variables with identical distribution. In a Poisson process, the sequence of arrival times is a renewal process with exponentially distributed random variables. In a Markov process, the time between entry to a fixed state form a renewal process. Whenever an event occurs, the process starts over. This process attempts to characterize the underlying physical process of strain buildup and release.

One approach using this process is to assume a Poisson process with a constant occurrence rate over some time period. If an earthquake of the same set magnitude has not occurred during this period, the rate of occurrence increases to a larger value. After an event, the rate decreases to the original value.

Cornell and Winterstein (1988) describe a renewal model. A general analytical form for the frequency-magnitude relation in the form of an approximate Weibull distribution is used:

$$\ln [N(m)] \approx \alpha - [\beta (m - m_t)]^{1/V_m} \quad m \geq m_t \tag{4-17}$$

where: α = $\ln [N(m_t)]$ reflects the recurrence rate of significant events, m_t

V_m = $(\text{var } [M]^{1/2}/(E [M] - m_t)$ is the coefficient of variation of $M - m_t$

β = 51

The log-linear relation of the Guttenberg-Richter law follows from Equation 4-17 when V_m = 1. The duration between events is not constrained to be exponentially distributed as implied by the Poisson process. This permits inclusion of characteristic time or event models. There is a dependence between time between events and the size of the last event.

The characteristic interevent time is represented by a Weibull model.

Anagnos (1993) developed a model using a Markov renewal process to describe earthquake states. Since specific stress release data are not available, specific magnitude ranges are selected and correlated with slip. It assumes stress builds up linearly at constant rate, and change depends only on the present state. An associated semi-Markov process is used to establish the duration of the visits to the states. Given that an earthquake of given magnitude just occurred, the associated semi-Markov process enters a specific state and remains in that state for some time until accumulated stress reaches a threshold level. The process then moves onto the next state. Event probabilities are defined for each transition state. The stress release, occurrence of an earthquake, and drop to another state are random events. The shape of the release distribution is based on the seismicity of the fault or region defined by the Guttenberg-Richter frequency-magnitude relation. A characteristic repeat event may also be used to define the magnitude distribution. A Weibull distribution is used to compute the holding time distribution, which is the probability of the time to the next event. The mean and variance of the Weibull distribution can be estimated from interarrival time data and slip rate data. Probability of occurrence of an earthquake greater than a specific magnitude and the expected number of events can be calculated using recursive relations for the associated discrete time semi-Markov process.

Application of this model requires specification of the lower-bound fault magnitude, mean magnitude and associated standard deviation, and upper-bound magnitude. The parameters of the Weibull distribution for time to the next event must be established. This may be based on data from a least squares regression analysis of magnitude, or must be developed for the specific site. The time-predictable model reflects the dependence on the time since, and the size of, the last event. When the gap in event occurrence becomes much larger than the mean interevent time, the behavior of the process approaches a Poisson process. For small gaps, the Poisson process gives higher probability of occurrence estimates. However, if the gap is sufficiently large, the Poisson model will underestimate the hazard from future events. The time predictable model exhibits a correlation between interevent time and the preceding magnitude level, although both remain independent of subsequent magnitude. The time predictable renewal process gives higher hazard predictions than a simple renewal process.

DISCUSSION

The Poisson process has a distinct advantage in its ability to be used with available data to characterize its single parameter. The independence assumptions associated with the Poisson process do not permit it to characterize the underlying physical process of strain buildup and release. The time dependence feature is lacking. It was found to be unconservative when a long gap occurred since the last event occurred on a fault. Cornell and Winterstein (1988) give an excellent evaluation of the limitations and applicability of the Poisson model. They studied a broad set of models with temporal and magnitude dependence, including time and slip predictable models. They considered agreement acceptable for engineering hazard studies when results agreed within a factor of three for a 50-year time window and magnitude levels with annual exceedance probabilities of 0.001 or less. According to Cornell and Winterstein (1988):

> "The Poisson model has been commonly used for several reasons. These include: (1) some successful comparisons of its predictions with observations..., (2) rather broad acceptance that, lacking evidence to the contrary, the model is not unreasonable physically (especially for the less-than-the-largest events that may govern hazard); and, more formally, (3) the fact that the sum of non-Poissonian processes may be approximately Poisson. But perhaps most importantly, it is the simplest model that captures the basic elements of the problem. ...Significantly, these parameters of the standard hazard model are those that the engineering seismologist commonly estimates and is therefore best prepared to specify. Should an alternative model be considered, questions arise, first, as to which alternative model should be considered and, second, as to how in practice to estimate both the additional model parameters and the initial conditions (e.g., size and time of the last significant event) upon which non-Poissonian prediction may depend. Therefore, the practical application on non-Poissonian models requires much more detailed knowledge of specific tectonic features. If the engineering conclusions are not substantively different, the implied effort may not be justified.
>
> Cases in which the Poisson estimate is insufficient are limited practically to those in which the hazard is controlled by a single feature for which the elapsed time since the last significant event exceeds the average time between such events. Moreover, this situation creates a problem only if there is reason to believe that

the fault displays strongly regular, "characteristic time" behavior. In particular, the Poisson estimate will generally be adequate if the mean interevent time between significant events exceeds either the seismic "gap" (elapsed time since the last such event) or the length of the historical record, whichever is less. For strongly regular earthquakes, the mean gap length under random entry is roughly half of the mean interevent time; therefore, this gap with higher than Poisson hazard may be rather unusual in engineering design practice.

Finally, in many practical situations, two or more features will be important hazard contributions at a particular site. In these cases, the combined hazard is better estimated by the Poisson model than is the hazard from any single feature."

Lomnitz (1989), in a discussion of the Cornell and Winterstein (1988) paper, makes the following comment:

"Cornell and Winterstein found that the fit to the Poisson model improved as the number of discrete sources increased. If there are two or more faults, "the combined hazard is better estimated by the Poisson model than is the hazard from any single feature." This result is not altogether unexpected. An elegant theorem... proves that the sum of any number of random point processes tends to a Poisson process. The larger the number of arbitrary component processes, the better the Poisson fit.

Hence, it is not quite fair to state that the effects of temporal and magnitude dependence "are ignored in the conventional Poisson earthquake model" (Cornell and Winterstein, 1988). The model is not that unsophisticated. The Poisson process is a limiting process for the sum of many point processes - all of which exhibit time and magnitude dependence!

For example, the earthquake hazard in North China is governed by a few large faults, both on land and in the Gulf of Bo, plus an unknown number of small faults. The capital city of Beijing, which appears to be somewhat removed from the major faults, may be adequately planned on the basis of a Poissonian earthquake hazard (which in effect means that the ground conditions dominate the hazard). But I would be concerned about applying the same criterion to a site on the Tangshan Fault - event though a significant earthquake occurred on that fault as recently as 27 July 1976."

For engineering hazard studies using the historical data base and available slip data, a Poisson model may be used as a starting point. Geologic data should then be used to adjust recurrence data computed from the historical data base. Characteristic event data can easily be incorporated, and this should be done where required. This represents an "engineering" solution for a range of studies where the exposure time is 50 years or less and the risk levels of interest are in the range of 0.001. Studies where the risk range is 0.0001 require more detailed analysis.

REFERENCES

Anagnos, T. (1993). Time predictable stochastic earthquake recurrence model, prepared for the Naval Civil Engineering Laboratory, Memorandum to files. Port Hueneme, CA, 1993.

Chou, E.H., and J.A. Fisher (1975). "Earthquake hazards and confidence," in Proceedings of the U.S. National Conference on Earthquake Engineering, Ann Arbor, MI, Jun 1975.

Coppersmith, K.S., and R.R. Youngs (1990). "Improved methods for seismic hazard analysis in the Western United States," in Proceedings of the Fourth U.S. National Conference on Earthquake Engineering, Palm Springs, CA, May 20-24, 1990.

Cornell, C.A., and S.R. Winterstein (1988). "Temporal and magnitude dependence in earthquake recurrence models," in Bulletin of the Seismological Society of America, vol 28, no. 4, Aug 1988, pp 1522-1537.

Guttenberg, B., and C.F. Richter (1954). Seismicity of the earth and associated phenomena. Princeton, NJ, Princeton University Press, Second Edition, 1954.

Kiremidjian, A.S., et al. (1990). "A random strain accumulation model for earthquake occurrences with Bayesian parameters," in Proceedings of the Fourth U.S. National Conference on Earthquake Engineering, Palm Springs, CA, May 20-24, 1990.

Lomnitz, C. (1989). "Comments on temporal and magnitude dependence in earthquake recurrence models by C.A. Cornell and S.R. Winterstein," in Bulletin of the Seismological Society of America, vol 79, no. 5, Oct 1989, p 1662.

Woodward Clyde Consultants (1982). Development and initial application of software for seismic exposure evaluation, prepared for National Oceanic and Atmospheric Administration. San Francisco, CA, May 1982.

Youngs, R.R., and K.J. Coppersmith (1985). "Implications of fault slip rate and earthquake recurrence models to probabilistic seismic hazard estimates," in Bulletin of the Seismological Society of America, vol 75, 1985, pp 939-964.

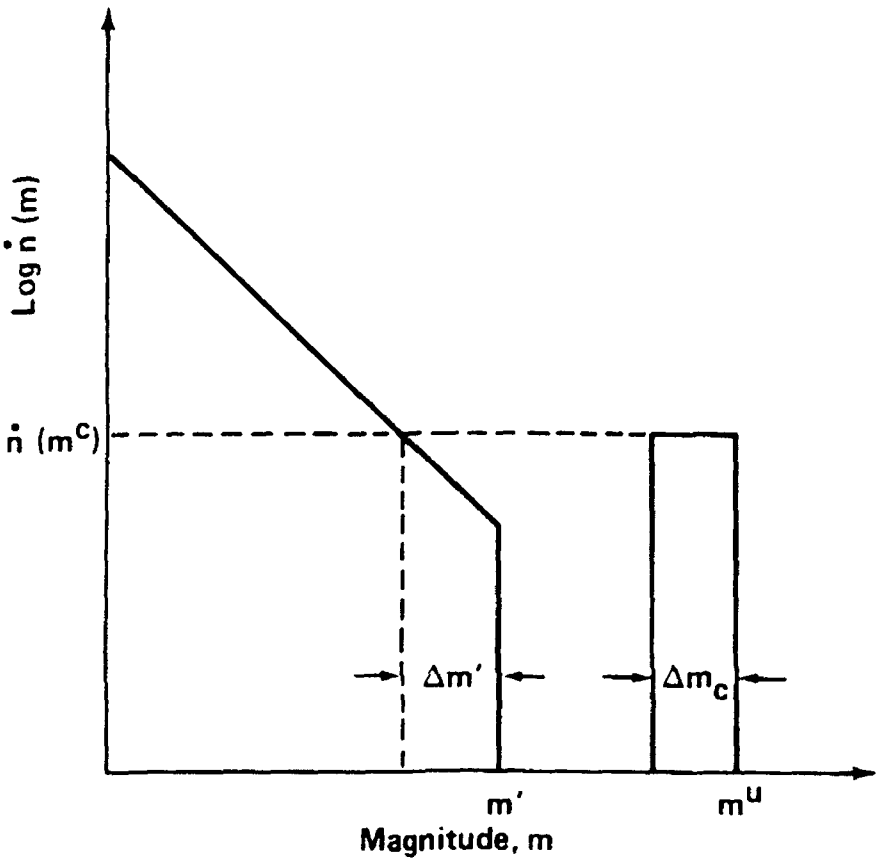

Figure 4-1. Generalized frequency magnitude density function.

CHAPTER 5
GROUND MOTION ESTIMATION

INTRODUCTION

This chapter will review ground motion attenuation equations which are used to determine levels of acceleration as a function of distance from the source and magnitude of the earthquake. The increased installation of strong motion data recording equipment has provided an accumulation of earthquake records. Correlations have been made of peak acceleration with distance for various events. These equations allow us to estimate the ground motion at a site from a specified event and the uncertainty associated with the estimate. This estimation is a key step in any seismic hazard analysis. There are a number of attenuation equations that have been developed by various researchers. As the data set expands and more data points are available, agreement among researchers improves.

JOYNER AND BOORE

Joyner and Boore (1988) developed an attenuation equation based on a regression analysis of a carefully selected set of events. The events are restricted to moment magnitude, M, greater than 5 and less than 7.7 and shallow fault rupture. Their equation is:

$$\log y = a + b(M - 6) + c(M - 6)^2 + d(\log (r)) + k\,r + s$$
$$r = (r^2 + h^2)^{1/2} \qquad (5\text{-}1)$$

where a, b, c, d, k, s, and h are given in Table 5-1 for estimating quantities corresponding to the randomly oriented horizontal component, and in Table 5-2 for estimating quantities corresponding to the larger of the two horizontal components.

Tables 5-1 and 5-2 also give estimates of the standard deviation (σ) of an individual prediction of log y using the equations.

CROUSE, ET AL.

Crouse, et al. (1984) developed the following equation for peak horizontal acceleration and horizontal pseudovelocity response at 5 percent damping. It was developed from data recorded at deep soil sites (generally greater than 60 m in thickness) during shallow crustal earthquakes in southern California (Crouse 1984, 1987; Vyas, et al., 1988):

$$\ln y = a + b M_S + c M_S^2 + d \ln(r + 1) + k r \qquad (5\text{-}2)$$

where: y = peak horizontal acceleration (gal) or horizontal pseudovelocity response (cm/s)
M_S = surface-wave magnitude
r = closest distance (km) from rupture surface to recording site

Coefficients a, b, c, d, and k are given in Table 5-3. Both horizontal components were used so that the values of y predicted by Equation 5-2 correspond to the randomly oriented horizontal component.

SADIGH, ET AL.

Sadigh, et al. (1986) developed an equation for peak horizontal acceleration and horizontal pseudoacceleration response at 5 percent damping from data from the Western United States supplemented by significant recordings of earthquakes at depth less than 20 km from other parts of the world. Both horizontal components were used:

$$\ln y = a + b M + c_1 (8.5 - M)^{c2} + d \ln [r + h_1 \exp (h_2 M)] \qquad (5\text{-}3)$$

where: y = peak horizontal acceleration (g) or horizontal pseudoacceleration (g)
M = moment magnitude
r = the closest distance (km) to the rupture surface
a, b, c_i, d, and h_i are given in Table 5-4.

The values in Table 5-4 were derived for strike-slip earthquakes. To obtain estimates for reverse-slip events, the strike-slip estimates should be increased by 20 percent. Sadigh, et al. (1989) used additional earthquake data through 1988 to develop a set of coefficients for short-period horizontal ground motion at rock sites in reverse-slip earthquakes (Table 5-5). Data from both horizontal components were used in developing the equations, and the results apply to reverse-slip earthquakes. The results should be reduced by 17 percent to give estimates for strike-slip events and by 9 percent to give estimates for reverse-oblique slip events. The shape of response spectra computed from Equation 5-3 does not change with distance for the coefficients in either Table 5-4 or 5-5.

DONOVAN AND BORNSTEIN

Donovan and Bornstein (1978) developed the following equation for peak horizontal acceleration from the Western United States data. Both horizontal components were used:

$$\begin{aligned} y &= a \exp(b\,M)\,(r + 25)^d \\ a &= 2{,}154{,}000(r)^{-2.10} \\ b &= 0.046 + 0.445 \log(r) \\ d &= 2.515 + 0.486 \log(r) \end{aligned} \qquad (5\text{-}4)$$

where: y = peak horizontal acceleration (gal)
M = any magnitude
r = distance (km) to the energy center, default at a depth of 5 km

Table 5-6 gives the standard deviation of the natural logarithm of an individual prediction of y.

CAMPBELL

Campbell (1987, 1989) developed equations for estimating peak acceleration, peak velocity, and pseudovelocity at 5 percent damping. He used a worldwide data set including earthquakes as recent as 1987 based on the following criteria:

> "(1) the largest horizontal component of peak acceleration was at least 0.02 g; (2) the accelerograph triggered early enough to record the strongest phase of shaking; (3) the magnitude of the earthquake was 5.0 or larger; (4) the closest distance to seismogenic rupture was less than 30 or 50 km, depending on whether the magnitude of the earthquake was less than or greater than 6.25; (5) the shallowest extent of seismogenic rupture was no deeper than 25 km."

Records from instruments on the abutments or toes of dams were excluded, as were records from "hard-rock" sites and shallow-soil sites, which were defined as sites with 1 to 10 m of soil overlying rock.

Campbell's (1989) equation is:

$$\ln y = a + b M + d \ln [r + h_1 \exp(h_2 M) + q F f_1 \tanh [f_2 (M + f_3)] + g_1 \tanh(g_2 D) + \sum_{i=1}^{3} l_i K_i \quad (5\text{-}5)$$

where: y = ground motion parameter of interest, the vertical component or the mean of two horizontal components.

M = surface wave magnitude M_S if both local magnitude M_L and M_S are greater than or equal to 6.0 or M_L if both M_S and M_L are less than 6.0.

r = the shorest distance (km) to the zone of seismogenic rupture, identified from spatial distribution of aftershocks, from earthquake modeling studies, from regional crustal velocity studies, and from geodetic and geologic data.

D = depth to basement rock (km).

F and K are defined in Table 5-7.

Values for the coefficients of Equation 5-5 are given in Tables 5-8 and 5-9. Also given in Table 5-8 are the values of the standard deviation of an individual prediction of ln y. The standard deviations are substantially less than those in Tables 5-1 and 5-2 after conversion from natural to common logarithms. The shape of response spectra computed from Equation 5-5 does not change with distance.

IDRISS

Idriss (1985, 1987) developed the following for the randomly oriented horizontal component of peak horizontal acceleration:

$$\ln y = \ln a + d \ln(r + 20) \quad (5\text{-}6)$$

where: y = peak horizontal acceleration (g)

M = surface-wave magnitude for M greater than or equal to 6 and local magnitude otherwise.

r = closest distance (km) to the source for M greater than 6 and hypocentral distance otherwise.

a and d are given in Table 5-10.

Idriss proposed that peak acceleration be used to scale the response spectral shapes for different site conditions with magnitude- and period-dependent correction factors. The shape of response spectra computed by Idriss' method does not change with distance.

COMPARISON OF EQUATIONS

According to Joyner and Boore (1988):

> "....to properly compare the different relationships, adjustments must be made for the different definitions of distance. [Figure 5-1] compares peak horizontal acceleration for the randomly oriented horizontal component at magnitude 6.5 as estimated by Donovan and Bornstein (1978), Joyner and Boore (1988), Idriss (1987), and Campbell (1989). The definition of distance used in [Figure 5-1] is the closest distance to the vertical projection of the rupture on the surface of the earth. The curves of Donovan and Bornstein and Campbell were adjusted assuming a source depth of 5 km. The curve shown for Idriss is that for deep soil sites. The curve shown for Campbell is that for strike-slip earthquakes recorded at free-field sites.
>
> At short distances, where it matters the most, the different relationships agree to within a fraction of the uncertainty of an individual estimate as given by any of the authors. This suggests that the short-distance estimates at magnitude 6.5 are controlled by the data. The differences at large distances are not of much practical importance."

Figure 5-1 gives the same comparison for magnitude 7.5. The agreement at short distance is not as good as at magnitude 6.5, reflecting the scarcity of data points, but it is within the uncertainty of an individual estimate.

From Figure 5-1, the Donovan and Bornstein equation yields an almost upper bound and is a conservative estimate. This equation was selected for further study. The study included the following attenuation equations:

1. McGuire (1978)
2. Trifunac and Brady (1975)
3. Campbell (west) (1982)
4. Campbell (east) (1982)
5. Donovan and Bornstein (1978)
6. Joyner and Boore (1988)

Figure 5-2 shows the attenuation relationships along with events selected from the catalog of strong motion records cited by Chang (1978). Records on buildings and vertical records were

excluded. As can be seen, there is significant scatter. The standard deviation in equation prediction to date is given as:

Equation	Mean Deviation*	Standard Deviation
McGuire	-0.005	0.089
Trifunac and Brady	+0.008	0.105
Campbell (west)	-0.059	0.111
Campbell (east)	-0.041	0.101
Donovan and Bornstein	-0.042	0.104
Joyner and Boore	-0.056	0.111

*Minus = equation underestimates.

Another data set used by Joyner and Boore (1988) is shown in Figure 5-3. The mean and standard deviations of the equations are:

Equation	Mean Deviation*	Standard Deviation
McGuire	+0.001	0.0901
Trifunac and Brady	+0.076	0.1885
Campbell (west)	-0.027	0.0936
Campbell (east)	-0.013	0.0913
Donovan and Bornstein	-0.014	0.0844
Joyner and Boore	-0.021	0.0830

*Minus = equation underestimates.

The McGuire equation has the least overall bias. The standard deviations except for the Trifunac and Brady equations are statistically about the same. From the above, there is little difference between McGuire's equation and Donovan's equation.

The significance of selection of the earthquake attenuation equation is primarily in the determination of separation distances. McGuire and Donovan, for example, define the relationship in hypocentral distance; Trifunac and Brady in terms of epicentral distance; and Campbell and Joyner and Boore in terms of the closest distance to the fault. For risk analysis of faults where the site tends to be located near one end of the fault, the selection of a relationship based on the shortest distance will tend to give higher values. To illustrate the significance of the attenuation relationship, a study was made of a site 0.5 miles from the Hayward fault. Results for the 225-year return time are:

Joyner and Boore	0.535 g
Campbell	0.540 g

McGuire	0.396 g
Donovan and Bornstein	0.382 g

The equations shown in Figure 5-1 represent the current consensus of top researchers in the field and show good agreement.

DATA FROM THE LOMA PRIETA EARTHQUAKE

The Loma Prieta, California earthquake of 17 October 1989 brought a significant addition to the strong motion data base. Figure 5-4, with equations from Joyner and Boore (1988) and Loma Prieta data, shows the larger of the two horizontal components of peak acceleration plotted against the closest distance to the vertical projection of the rupture on the surface of the earth. The solid curves in Figure 5-4 are Joyner and Boore (1988) for the larger of two horizontal components for a moment magnitude of 6.9 (Kanamori and Helmberger, 1990), and the dashed curves are the curves corresponding to plus and minus one standard deviation of an individual estimate. The recorded data are plotted with different symbols for rock, alluvium, and bay-mud sites. The values for the three site categories are factors of 1.6, 1.8, and 4.5 higher on the average than the estimates from the equations, which were derived from a data set that included rock and alluvium sites, but not bay-mud sites. The larger values for rock and alluvium may represent ordinary earthquake-to-earthquake variability, but the values for bay mud clearly represent a local site effect.

DISCUSSION

Table 5-11 summarizes the earthquake attenuation equations reviewed above. The earthquake epicenter data base records a surface magnitude, a local magnitude, a body magnitude, and another magnitude. There is uncertainty in each magnitude since events often do not have all magnitudes established. Averages of the individual magnitudes from each station are made to get a more uniform value. Specification of a moment magnitude would complicate use of the existing epicenter data base. All the equations give similar values (Figure 5-1).

REFERENCES

Campbell, K.W. (1982). "A preliminary methodology for the regional zonation of peak ground acceleration," in Proceedings of the Third International Earthquake Microzonation Conference, University of Washington, Seattle, WA, Jun 1982.

Campbell, K.W. (1987). "Predicting strong ground motion in Utah," in Assessment of Regional Earthquake Hazards and Risk Along the Wasatch Front, Utah, P.L. Gori and W.W. Hays, Editors, U.S. Geological Survey Open-File Report 87-585, vol 2, LI-L90, 1987.

Campbell, K.W. (1989). Empirical prediction of near-source ground motion for the Diablo Canyon power plant site, San Luis Obispo County, California, U.S. Geological Survey Open-File Report 89-484. Menlo Park, CA, 1989.

Chang, F.K. (1978). MPS73-1 State of the art for assessing earthquake hazards in the United States catalog of stray motion earthquake records, Waterways Experiment Station. Vicksburg, MS, Apr 1978.

Crouse, C.B., G.C. Liang, and G.R. Martin (1984). "Experimental study of soil-structure interaction at an accelerograph station," in Bulletin of Seismocological Society of America, vol 74, 1984, pp 1995-2013.

Crouse, C.B., and B. Hushmand (1987). "Experimental investigations of soil-structure interaction at CDMG and USGS accelerograph stations (abs.)," Seismic Research Letter 58, no. 10, 1987.

Donovan, N.C., and A.E. Bornstein (1978). "Uncertainties in seismic risk procedures," in Proceedings of the American Society of Civil Engineers, Journal of Geotechnical Engineering Division, vol 104, 1978, pp 869-887.

Idriss, I.M. (1985). "Evaluating seismic risk in engineering practice," in Proceedings of the Eleventh International Conference on Soil Mechanics and Foundation Engineering, Aug 12-16, San Francisco, CA, vol 1, pp 255-320, A.A. Balkema, Rotterdam, 1985.

Idriss, I.M. (1987). "Earthquake ground motions," Lecture notes on course on strong ground motion, Earthquake Engineering Research Institute, Pasadena, CA, Apr 10-11, 1987.

Joyner, W.B., and B.M. Boore (1988). "Measurement, characterization, and prediction of strong ground motion," Earthquake Engineering and Soil Dynamics II, in Proceedings of the American Society of Civil Engineers, Geotechnical Engineering Division. Specialty Conference, Park City, Utah, Jun 27-30, 1988, pp 43-102.

Joyner, W.B., and B.M. Boore (1993). Telephone conversation, NCEL Code L51, J. Ferritto, 1993.

Kanamori, H., and D.V. Helmberger (1990). "Semi-realtime study of the 1989 Loma Prieta earthquake, using teleseismic and regional data (abs.)," EOS, Transcriptions American Geophysical. Union 71, 1990, p 291.

McGuire, R.K. (1978). "Seismic ground motion parameter relations," in Proceedings of the American Society of Civil Engineers, Journal of Geotechnical Engineering Division, vol 104, 1978, pp 481-490.

Sadigh, K., J. Egan, and R. Youngs (1986). "Specification of ground motion for seismic design of long period structures (abs.)," Earthquake Notes 57, vol 13, 1986.

Sadigh, K., C.Y. Chang, F. Makdisi, and J. Egan (1989). "Attenuation relationships for horizontal peak ground acceleration and response spectral acceleration for rock sites (abs.)," Seismic Research Letter 60, no. 19, 1989.

Trifunac, M.D., and A.G. Brady (1975). "On the correlation of peak acceleration of strong motion with earthquake magnitude, epicentral distance and site conditions," in Proceedings of the U.S. National Conference on Earthquake Engineering, University of Michigan, Ann Arbor, MI, 1975.

Vyas, Y.K., C.B. Crouse, and B.A. Schell (1988). "Regional design ground motion criteria for the southern Bering Sea," Conference for Offshore Mechanical and Arctic Engineering, Houston, TX, Feb 7-12, 1988.

TABLE 5-1. COEFFICIENTS IN THE EQUATIONS OF JOYNER AND BOORE FOR THE RANDOMLY ORIENTED HORIZONTAL COMPONENT OF GROUND MOTION

Period (s)	a	b	c	h	d	k	s	V_{S0}	e	$\sigma_{\log y}$
Pseudovelocity response (cm/s)										
0.1	2.16	0.25	-0.06	11.3	-1.0	-0.0073	-0.02			0.28
0.15	2.40	.30	- .08	10.8	-1.0	- .0067	- .02			.28
0.2	2.46	.35	- .09	9.6	-1.0	- .0063	- .01			.28
0.3	2.47	.42	- .11	6.9	-1.0	- .0058	.04	590	-0.28	.28
0.4	2.44	.47	- .13	5.7	-1.0	- .0054	.10	830	- .33	.31
0.5	2.41	.52	- .14	5.1	-1.0	- .0051	.14	1020	- .38	.33
0.75	2.34	.60	- .16	4.8	-1.0	- .0045	.23	1410	- .46	.33
1.0	2.28	.67	- .17	4.7	-1.0	- .0039	.27	1580	- .51	.33
1.5	2.19	.74	- .19	4.7	-1.0	- .0026	.31	1620	- .59	.33
2.0	2.12	.79	- .20	4.7	-1.0	- .0015	.32	1620	- .64	.33
3.0	2.02	.85	- .22	4.7	-0.98	.0	.32	1550	- .72	.33
4.0	1.96	0.88	-0.24	4.7	-0.95	0.0	0.29	1450	-0.78	0.33
Peak acceleration (g)										
	0.43	0.23	0.0	8.0	-1.0	-0.0027	0.0			0.28
Peak velocity (cm/s)										
	2.09	0.49	0.0	4.0	-1.0	-0.0026	0.17	1190	-0.45	0.33

TABLE 5-2. COEFFICIENTS IN THE EQUATIONS OF JOYNER AND BOORE FOR THE LARGER OF TWO HORIZONTAL COMPONENTS OF GROUND MOTION

Period (s)	a	b	c	h	d	k	s	V_{S0}	e	$\sigma_{\log y}$
Pseudovelocity response (cm/s)										
0.1	2.24	0.30	-0.09	10.6	-1.0	-0.0067	-0.06			0.27
0.15	2.46	.34	- .10	10.3	-1.0	- .0063	- .05			.27
0.2	2.54	.37	- .11	9.3	-1.0	- .0061	- .03			.27
0.3	2.56	.43	- .12	7.0	-1.0	- .0057	.04	650	-0.20	.27
0.4	2.54	.49	- .13	5.7	-1.0	- .0055	.09	870	- .26	.30
0.5	2.53	.53	- .14	5.2	-1.0	- .0053	.12	1050	- .30	.32
0.75	2.46	.61	- .15	4.7	-1.0	- .0049	.19	1410	- .39	.35
1.0	2.41	.66	- .16	4.6	-1.0	- .0044	.24	1580	- .45	.35
1.5	2.32	.71	- .17	4.6	-1.0	- .0034	.30	1780	- .53	.35
2.0	2.26	.75	- .18	4.6	-1.0	- .0025	.32	1820	- .59	.35
3.0	2.17	.78	- .19	4.6	-1.0	.0	.29	1620	- .67	.35
4.0	2.10	0.80	-0.20	4.6	-0.98	0.0	0.24	1320	-0.73	0.35
Peak acceleration (g)										
	0.49	0.23	0.0	8.0	-1.0	-0.0027	0.0			0.28
Peak velocity (cm/s)										
	2.17	0.49	0.0	4.0	-1.0	-0.0026	0.17	1190	-0.45	0.33

TABLE 5-3. COEFFICIENTS IN THE EQUATIONS OF CROUSE HORIZONTAL COMPONENT OF GROUND MOTION

Period (s)	a	b	c	d	k	$\sigma_{\ln y}$
Pseudovelocity response (cm/s)						
0.05	- 2.44178	0.84826	-0.02579	-0.52916	-0.00961	0.59914
0.10	- 0.61623	0.62660	- .00999	- .50106	- .01199	.68673
0.20	- 4.47801	2.00876	- .11673	- .32102	- .01423	.64716
0.40	- 1.35559	1.17453	- .04411	- .47398	- .00782	.62089
0.60	- 6.02161	2.66493	- .15619	- .52586	- .00548	.62275
1.00	- 5.89916	2.48235	- .13036	- .52261	- .00405	.62745
2.00	-11.48576	4.01914	- .23152	- .56791	- .00280	.63277
2.50	-12.33454	4.15828	- .23359	- .56280	- .00320	.66459
4.00	-14.90528	4.54962	- .24999	- .32351	- .00738	.73830
6.00	-14.77796	4.33959	-0.23491	-0.20849	-0.00791	0.79595
Peak acceleration (g)						
	2.48456	0.73377	-0.01509	-0.50558	-0.00935	0.58082

TABLE 5-4. COEFFICIENTS IN THE EQUATIONS OF SADIGH HORIZONTAL COMPONENT OF GROUND MOTION

								$M < 6.5$	$M \geq 6.5$		
Period (s)	a	b	c_1	c_2	d	h_1	h_2	$\sigma_{\ln y}$	h_1	h_2	$\sigma_{\ln y}$
Pseudoacceleration response (g) at soil sites											
0.1	-2.024	1.1	0.007	2.5	-1.75	0.8217	0.4814	1.332 – 0.148M	0.3157	0.6286	0.37
0.2	-1.696	1.1	.0	2.5	-1.75	.8217	.4814	1.453 – 0.162M	.3157	.6286	.40
0.3	-1.638	1.1	- .008	2.5	-1.75	.8217	.4814	1.486 – 0.164M	.3157	.6286	.42
0.5	-1.659	1.1	- .025	2.5	-1.75	.8217	.4814	1.584 – 0.176M	.3157	.6286	.44
1.0	-1.975	1.1	- .060	2.5	-1.75	.8217	.4814	1.62 – 0.18M	.3157	.6286	.45
2.0	-2.414	1.1	- .105	2.5	-1.75	.8217	.4814	1.62 – 0.18M	.3157	.6286	.45
4.0	-3.068	1.1	-0.160	2.5	-1.75	0.8217	0.4814	1.62 – 0.18M	0.3157	0.6286	0.45
Peak acceleration (g) at soil sites											
	-2.611	1.1	0.0	2.5	-1.75	0.8217	0.4814	1.26 – 0.14M	0.3157	0.6286	0.35
Pseudoacceleration response (g) at rock sites											
0.1	-0.688	1.1	0.007	2.5	-2.05	1.353	0.406	1.332 – 0.148M	0.579	0.537	0.37
0.2	-0.479	1.1	- .008	2.5	-2.05	1.353	.406	1.453 – 0.162M	.579	.537	.40
0.3	-0.543	1.1	- .018	2.5	-2.05	1.353	.406	1.486 – 0.164M	.579	.537	.42
0.5	-0.793	1.1	- .036	2.5	-2.05	1.353	.406	1.584 – 0.176M	.579	.537	.44
1.0	-1.376	1.1	- .065	2.5	-2.05	1.353	.406	1.62 – 0.18M	.579	.537	.45
2.0	-2.142	1.1	- .100	2.5	-2.05	1.353	.406	1.62 – 0.18M	.579	.537	.45
4.0	-3.177	1.1	-0.150	2.5	-2.05	1.353	0.406	1.62 – 0.18M	0.579	0.537	0.45
Peak acceleration (g) at rock sites											
	-1.406	1.1	0.0	2.5	-2.05	1.353	0.406	1.26 – 0.14M	0.579	0.537	0.35

TABLE 5-5. COEFFICIENTS IN THE ALTERNATIVE EQUATIONS OF SADIGH *ET AL.*(1989) FOR THE RANDOMLY ORIENTED HORIZONTAL COMPONENT OF SHORT-PERIOD GROUND MOTION AT ROCK SITES IN REVERSE-FAULT EARTHQUAKES

Period (s)	a	b	c_1	c_2	d	h_1	h_2	$\sigma_{\ln y}$
Pseudoacceleration response (g) $M < 6.5$								
0.1	0.218	1.00	0.006	2.5	-2.1	3.656	0.250	$1.29 - 0.14M$
0.2	0.418	1.00	-0.010	2.5	-2.1	3.656	0.250	$1.31 - 0.14M$
0.3	0.402	1.00	-0.023	2.5	-2.1	3.656	0.250	$1.33 - 0.14M$
0.5	0.181	1.00	-0.040	2.5	-2.1	3.656	0.250	$1.35 - 0.14M$
1.0	-0.409	1.00	-0.064	2.5	-2.1	3.656	0.250	$1.36 - 0.14M$
Peak acceleration (g) $M < 6.5$								
	-0.442	1.00			-2.1	3.656	0.250	$1.27 - 0.14M$
Pseudoacceleration response (g) $M \geq 6.5$								
0.1	-0.432	1.10	0.006	2.5	-2.1	0.616	0.524	0.38
0.2	-0.232	1.10	-0.010	2.5	-2.1	0.616	0.524	0.40
0.3	-0.248	1.10	-0.023	2.5	-2.1	0.616	0.524	0.42
0.5	-0.469	1.10	-0.040	2.5	-2.1	0.616	0.524	0.44
1.0	-1.059	1.10	-0.064	2.5	-2.1	0.616	0.524	0.45
Peak acceleration (g) $M \geq 6.5$								
	-1.092	1.10			-2.1	0.616	0.524	0.36

Reprinted from Joyner and Boore draft U.S. Geological Survey paper in publication.

TABLE 5-6. STANDARD DEVIATION GIVEN BY DONOVAN AND BORNSTEIN (1978) FOR THE NATURAL LOGARITHM OF AN INDIVIDUAL ESTIMATE OF PEAK HORIZONTAL ACCELERATION

Peak acceleration	0.01	0.05	0.10	0.15
Standard deviation of natural logarithm of peak acceleration	0.50	0.48	0.46	0.41

 Reprinted from Joyner and Boore (1988) with permission from American Society of Civil Engineers

TABLE 5-7. DEFINITION OF VARIABLES IN THE EQUATIONS OF CAMPBELL (1989)

Fault type	$F =$	1 reverse 0 strike-slip
Building effects	$K_1 =$	1 embedded buildings 3–11 stories 0 other
	$K_2 =$	1 embedded buildings greater than 11 stories 0 other
	$k_3 =$	1 nonembedded buildings greater than 2 stories 0 other

Reprinted from Joyner and Boore draft U.S. Geological Survey paper in publication.

TABLE 5-8. COEFFICIENTS IN THE EQUATIONS OF CAMPBELL (1989)

Period (s)	a	b	h_1	h_2	d	q	f_1	f_2	f_3	g_1	g_2	$\sigma_{\ln y}$
Mean horizontal pseudovelocity response at 5 percent damping (cm/s)												
0.04	-0.648	1.08	0.311	0.597	-1.81	0.382						0.42
0.05	-0.379	1.08	.311	.597	-1.81	.382						.44
0.075	0.251	1.08	.311	.597	-1.81	.382						.46
0.1	0.754	1.08	.311	.597	-1.81	.382						.48
0.15	1.424	1.08	.311	.597	-1.81	.382						.50
0.2	1.788	1.08	.311	.597	-1.81	.382						.50
0.3	2.170	1.08	.311	.597	-1.81	.382						.50
0.4	2.009	1.08	.311	.597	-1.81	.382	0.425	0.570	-4.7			.50
0.5	1.930	1.08	.311	.597	-1.81	.382	0.685	.570	-4.7			.50
0.75	1.612	1.08	.311	.597	-1.81	.382	1.27	.570	-4.7			.50
1.0	1.268	1.08	.311	.597	-1.81	.382	1.74	.570	-4.7			.50
1.5	0.487	1.08	.311	.597	-1.81	.382	2.43	.570	-4.7	0.344	0.553	.50
2.0	0.040	1.08	.311	.597	-1.81	.382	2.83	.570	-4.7	.469	.553	.50
3.0	-0.576	1.08	.311	.597	-1.81	.382	3.17	.570	-4.7	.623	.553	.50
4.0	-0.766	1.08	0.311	0.597	-1.81	0.382	3.08	0.570	-4.7	0.857	0.553	0.50
Mean horizontal peak acceleration (g)												
	-2.470	1.08	0.311	0.597	-1.81	0.382						0.421
Mean horizontal peak velocity (cm/s)												
	-1.974	1.34	0.00935	1.01	-1.32	0.327				1.16	0.0776	0.395
Vertical pseudovelocity response at 5 percent damping (cm/s)												
0.04	-2.082	0.978	0.0536	0.674	-1.45	0.239						0.62
0.05	-1.634	.978	.0536	.674	-1.45	.239						.62
0.075	-0.903	.978	.0536	.674	-1.45	.239						.62
0.1	-0.488	.978	.0536	.674	-1.45	.239						.62
0.15	-0.125	.978	.0536	.674	-1.45	.239						.62
0.2	0.157	.978	.0536	.674	-1.45	.239						.62
0.3	0.356	.978	.0536	.674	-1.45	.239						.62
0.4	0.188	.978	.0536	.674	-1.45	.239	0.214	0.546	-4.7			.62
0.5	0.038	.978	.0536	.674	-1.45	.239	0.435	.546	-4.7			.62
0.75	-0.035	.978	.0536	.674	-1.45	.239	0.719	.546	-4.7			.62
1.0	-0.448	.978	.0536	.674	-1.45	.239	1.37	.546	-4.7			.62
1.5	-1.287	.978	.0536	.674	-1.45	.239	2.18	.546	-4.7	0.344	0.553	.62
2.0	-1.580	.978	.0536	.674	-1.45	.239	2.36	.546	-4.7	.469	.553	.62
3.0	-1.741	.978	.0536	.674	-1.45	.239	2.24	.546	-4.7	.623	.553	.62
4.0	-1.975	0.978	0.0536	0.674	-1.45	0.239	2.46	0.546	-4.7	0.857	0.553	0.62
Vertical peak acceleration (g)												
	-4.003	0.978	0.0536	0.674	-1.45	0.239						0.569
Vertical peak velocity (cm/s)												
	-4.336	1.72	0.00594	1.14	-1.51	0.337						0.520

Reprinted from Joyner and Boore draft U.S. Geological Survey paper in publication.

TABLE 5-9. ADDITIONAL COEFFICIENTS FOR BUILDING EFFECTS IN THE EQUATIONS OF CAMPBELL (1989)

	Mean horizontal component			Vertical component		
Period (s)	l_1	l_2	l_3	l_1	l_2	l_3
Pseudovelocity response at 5 percent damping (cm/s)						
0.04	-0.180	-0.489			-0.392	-0.103
0.05	-0.180	-0.489		-0.083	-0.712	-0.264
0.075	-0.180	-0.489		-0.206	-0.582	-0.371
0.1	-0.180	-0.489		-0.197	-0.650	-0.370
0.15	-0.180	-0.489			-0.392	
0.2	-0.180	-0.489			-0.392	
0.3	-0.180	-0.489			-0.392	
0.4	-0.180	-0.489			-0.347	
0.5	-0.180	-0.489			-0.153	
0.75	-0.180	-0.489			-0.347	
1.0	-0.180	-0.219			-0.278	
1.5	-0.180	0.074			0.284	0.619
2.0	-0.180	0.072			0.437	0.992
3.0	0.218	0.391	0.663	0.291	0.691	1.15
4.0	0.330	0.503	0.759	0.085	0.722	1.10
Peak acceleration (g)						
	-0.180	-0.489			-0.392	
Peak velocity (cm/s)						
				0.366		0.388

Reprinted from Joyner and Boore draft U.S. Geological Survey paper in publication.

TABLE 5-10. PARAMETERS IN THE EQUATIONS OF IDRISS (1987) FOR THE RANDOMLY ORIENTED HORIZONTAL COMPONENT OF PEAK ACCELERATION (g)

	Rock and stiff soil sites		Deep soil sites		
M	a	d	a	d	$\sigma_{\ln y}$
4.5	606	-2.57	189	-2.22	0.70
5.0	617	-2.46	195	-2.13	.58
5.5	452	-2.28	147	-1.97	.48
6.0	282	-2.07	98	-1.79	.42
6.5	164	-1.85	61.6	-1.60	.38
7.0	91.7	-1.63	37.2	-1.41	.35
7.5	49.8	-1.41	22	-1.22	.35
8.0	28.5	-1.21	13.7	-1.05	.35
8.5	15.9	-1.01	8.4	-0.88	0.35

Table 5-11
Comparison of Equations

Equation	Magnitude	Distance	σ	Problems
Joyner & Boore	M_o	Shortest distance	0.28	Range magnitude limited 5 to 7.5
Crouse	M_S	Shortest distance	0.58	Uses M_S
Sadigh	M_o	Shortest distance	0.35 to 1.26-0.14M	Uses M_o
Donovan	M	Dist. to hypocenter	0.4 to 0.5	
Campbell	M_L/M_S	Shortest distance	0.421	Uses M_S and M_L
Idriss	M_S	Shortest distance	0.35 to 0.70	Range limited M = 1.5 to 8.5

M_o = Moment magnitude
M_S = Surface magnitude
M_L = Local magnitude
M = Any magnitude

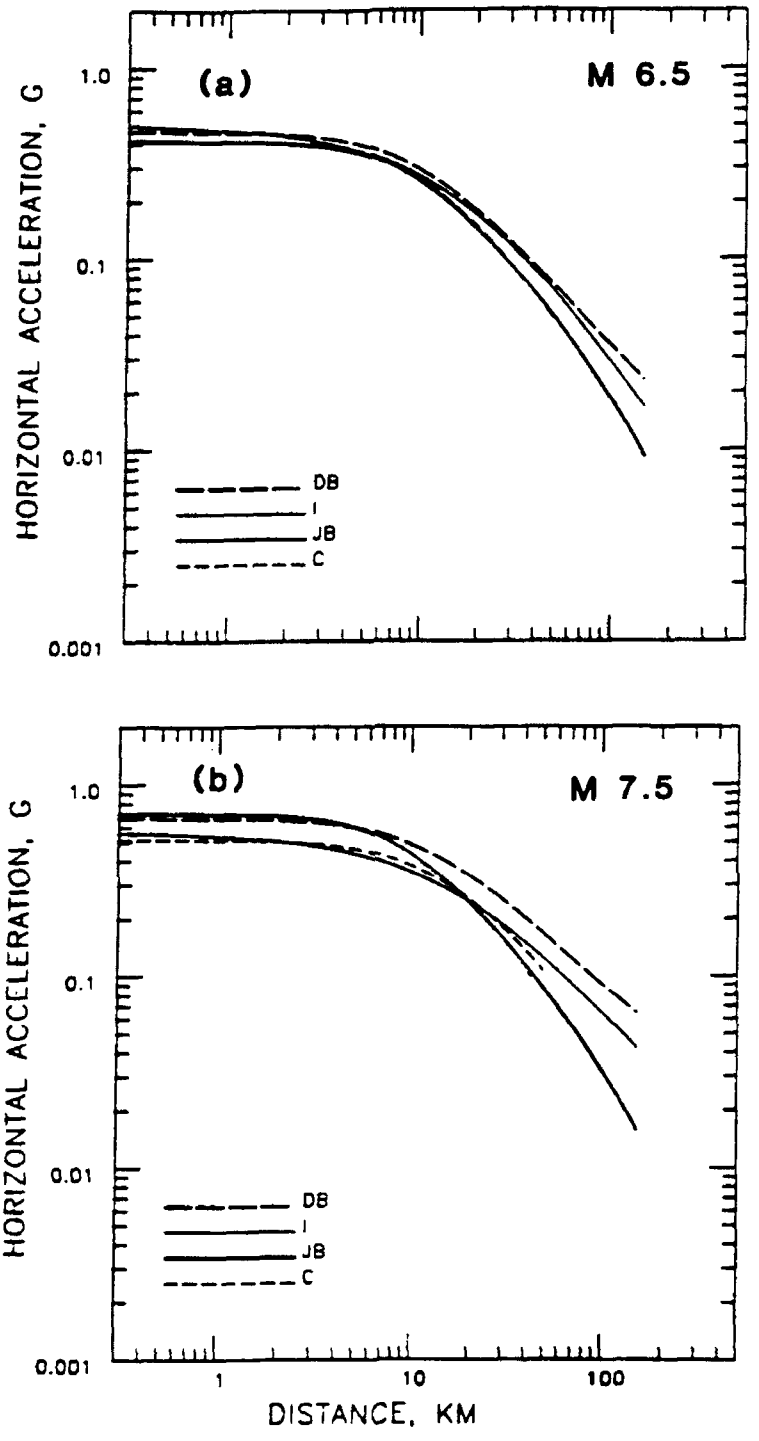

Figure 5-1.

Comparison of different relationships for peak horizontal acceleration at magnitude 6.5 (a) and 7.5 (b). DB, from Donovan and Bornstein (1978); I, from Idriss (1987) for deep soil sites; JB, from Joyner and Boore (1982), reduced by 13 percent so as to approximate the value for the randomly oriented horizontal component; C, from Campbell (1989) for a strike-slip earthquake recorded at a free-field site. For magnitude 6.5 the curve from Cambell is almost coincident with that from Joyner and Boore. The distance plotted is the closest distance to the vertical projection of the rupture on the surface of the earth. The curves of Donovan and Bornstein and those of Campbell are adjusted assuming a source depth of 5 km.

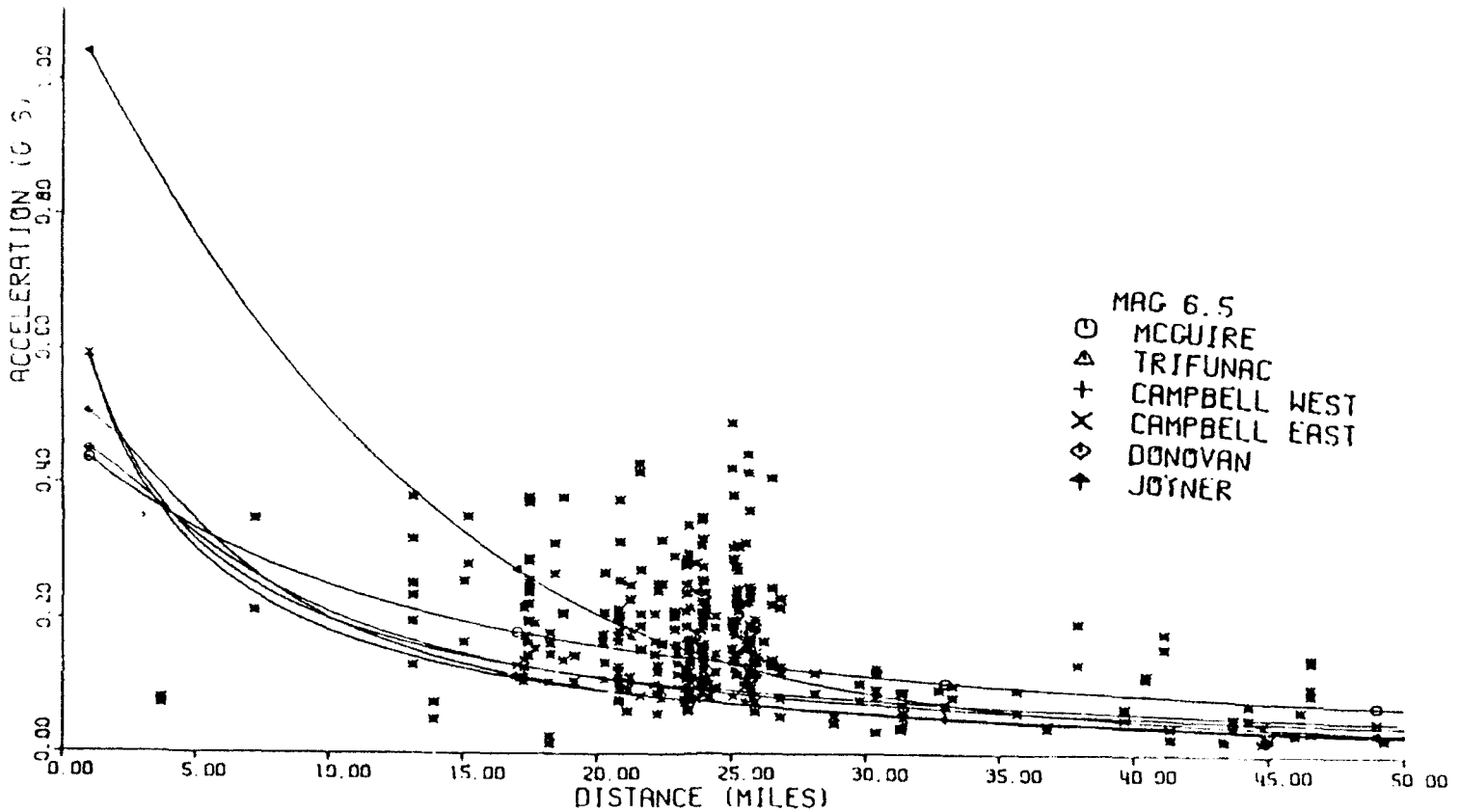

Figure 5-2. Attenuation equation and strong motion data, magnitude 6.5. Data set from Chang (1978)

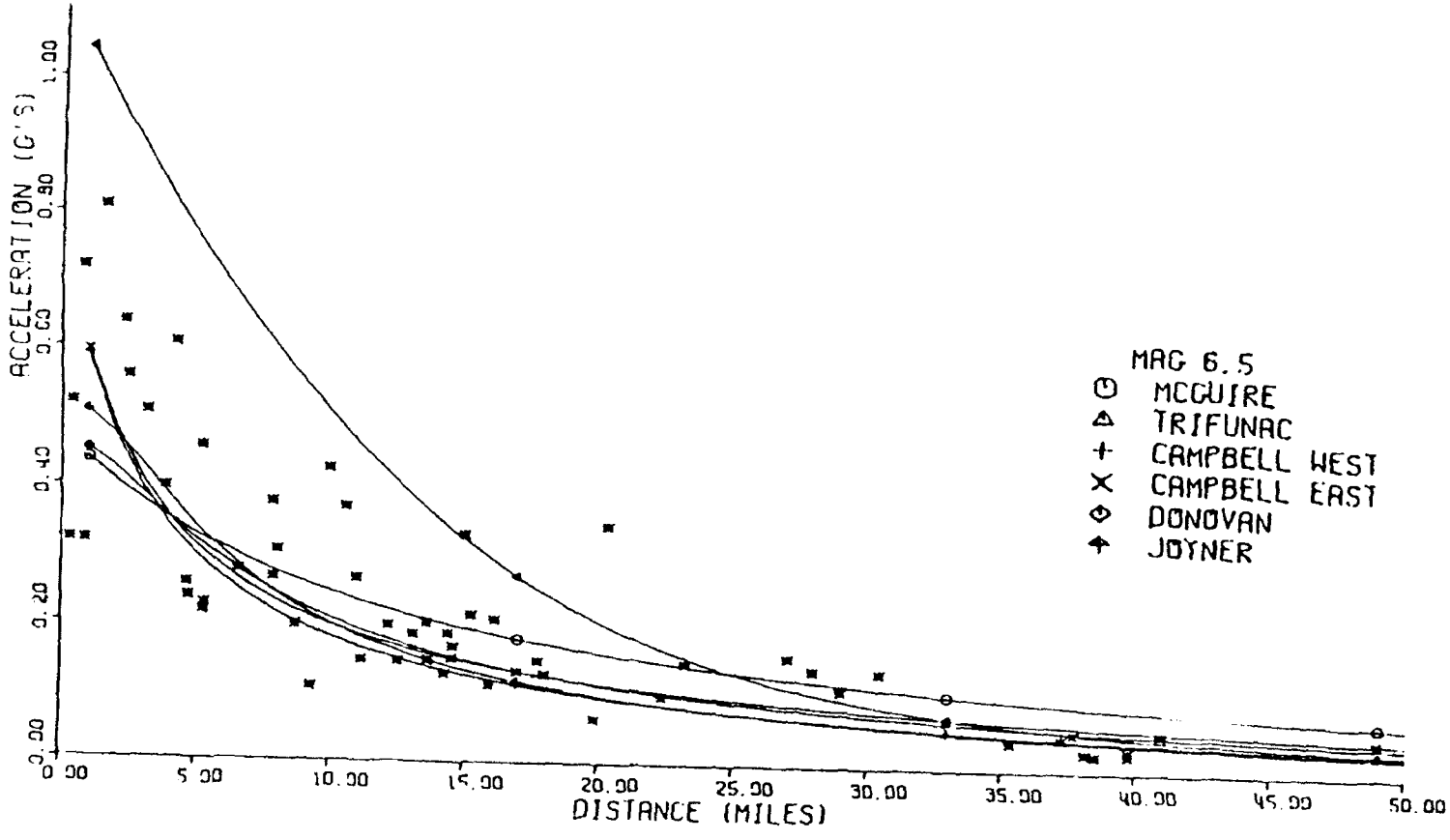

Figure 5-3. Attenuation equation and strong motion data, magnitude 6.5. Data set from Joyner and Boore

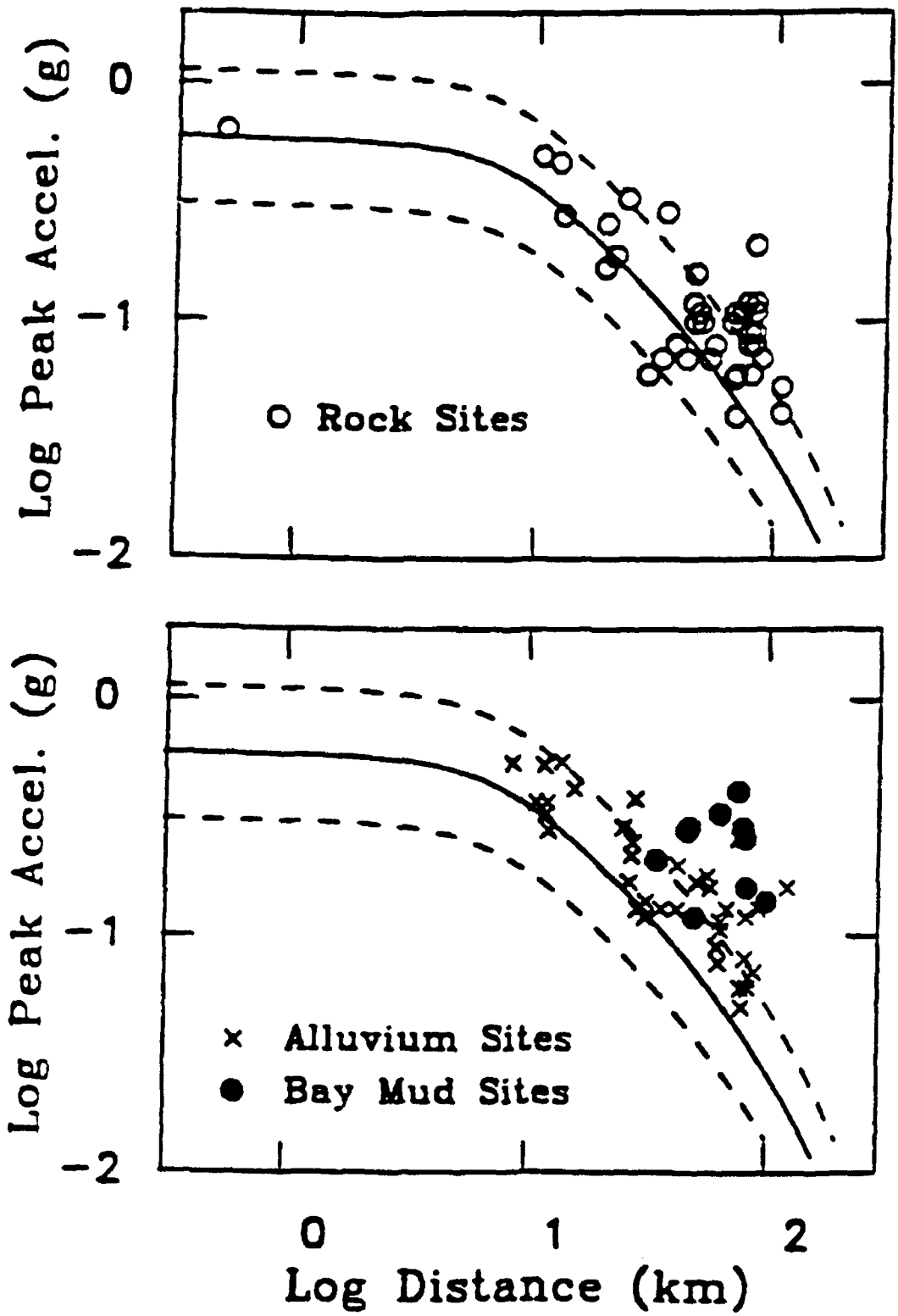

Figure 5-4.Loma Prieta earthquake and Joyner and Boore equation (from draft USGS paper)

CHAPTER 6
DEVELOPING A SEISMIC MODEL

INTRODUCTION

This chapter discusses the process of constructing a seismic model and, using data presented in previous chapters, describes a new procedure for computing the probability of site ground motion. As mentioned previously, our objective is to develop an engineering procedure that will give results of sufficient accuracy to estimate site motion for events with return time on the order of 1,000 years. As an engineering procedure, it is intended to use historical data and geologic data where available. Procedures that require panels of experts or extensive geologic investigation are not considered practical or feasible for limited scope engineering investigations. Nonetheless, given that such data exist, the conclusions regarding seismic activity should be useable.

BUILDING A SEISMIC SOURCE MODEL

As noted by Coppersmith (1991), many elements of seismic source characterization depend on the tectonic environment. In the Western United States, the tectonic environment is such that earthquakes are associated on known faults. However, in the Eastern United States, the causative geologic structures are generally not known. A seismic model must be based on the knowledge of the local area. It can consist of an area source zone for eastern sites or a detailed fault definition region for western sites.

In the Western United States, it is recognized that large earthquakes are associated with faults. For a magnitude 8 event, a rupture of 200 miles is required to release that level of energy. A 200-mile fault exhibits visual evidence of its existence and is unlikely to remain undiscovered. It is possible for lower magnitude events that require considerably less fault rupture to occur on faults lacking recent evidence of activity, or on faults that have not been identified.

Where faults are identified as sources, the area contained within the source zone is defined to have relatively uniform seismic potential in terms of maximum magnitude and event recurrence. A fault is modeled as a line source encompassing a distance or region surrounding the fault, such that the activity of this region can be associated with events on the fault. Where a fault exhibits variations of activity along its length, it can be divided into subelements containing regions where activity is uniform.

For the procedures developed here, a fault consists of two line segments defined by three points. The events to include or associate with the fault are defined by specification of a distance from the fault line, such that all those events within the distance are grouped with the fault. Alternatively, a region can be designated by four points to bound the fault. Again, note a fault can be divided into pieces where activity or geometry so dictates.

CHAPTER 6
DEVELOPING A SEISMIC MODEL

INTRODUCTION

This chapter discusses the process of constructing a seismic model and, using data presented in previous chapters, describes a new procedure for computing the probability of site ground motion. As mentioned previously, our objective is to develop an engineering procedure that will give results of sufficient accuracy to estimate site motion for events with return time on the order of 1,000 years. As an engineering procedure, it is intended to use historical data and geologic data where available. Procedures that require panels of experts or extensive geologic investigation are not considered practical or feasible for limited scope engineering investigations. Nonetheless, given that such data exist, the conclusions regarding seismic activity should be useable.

BUILDING A SEISMIC SOURCE MODEL

As noted by Coppersmith (1991), many elements of seismic source characterization depend on the tectonic environment. In the Western United States, the tectonic environment is such that earthquakes are associated on known faults. However, in the Eastern United States, the causative geologic structures are generally not known. A seismic model must be based on the knowledge of the local area. It can consist of an area source zone for eastern sites or a detailed fault definition region for western sites.

In the Western United States, it is recognized that large earthquakes are associated with faults. For a magnitude 8 event, a rupture of 200 miles is required to release that level of energy. A 200-mile fault exhibits visual evidence of its existence and is unlikely to remain undiscovered. It is possible for lower magnitude events that require considerably less fault rupture to occur on faults lacking recent evidence of activity, or on faults that have not been identified.

Where faults are identified as sources, the area contained within the source zone is defined to have relatively uniform seismic potential in terms of maximum magnitude and event recurrence. A fault is modeled as a line source encompassing a distance or region surrounding the fault, such that the activity of this region can be associated with events on the fault. Where a fault exhibits variations of activity along its length, it can be divided into subelements containing regions where activity is uniform.

For the procedures developed here, a fault consists of two line segments defined by three points. The events to include or associate with the fault are defined by specification of a distance from the fault line, such that all those events within the distance are grouped with the fault. Alternatively, a region can be designated by four points to bound the fault. Again, note a fault can be divided into pieces where activity or geometry so dictates.

GEOLOGIC SLIP-BASED RECURRENCE

Chapter 2 presented procedures for calculating recurrence based on the geologic slip rate data. Once the seismicity is estimated from the historical data, the geologic data can be compared. The procedure allows the user to adjust the A and B values replacing the historical data values with values based on the longer span geologic data.

Should other studies be available, the results of these individual fault studies can be used here by adjusting the recurrence parameters.

CHARACTERISTIC MAGNITUDE

As discussed in Chapter 4, geologic data may show the presence of history of a characteristic event at some average return time. The seismicity defined by the historical data fails to capture this activity, so it is important to include it within the set of events developed for the fault. Once the size of the event and the effective average return time is defined, it becomes a simple task to randomly add these events into the magnitude list of events. Again, if studies with more advanced models are available to define temporal distributions, that data can be used here.

COMPUTATIONAL PROCEDURE

In Chapter 4, various approaches were presented to determine the probability of earthquake occurrence. As shown above, various amounts of data are required, some of which are beyond the scope of an engineering investigation. A new approach was taken in the formulation of a Monte Carlo simulation procedure. The procedure uses the fault model and regional model discussed earlier in this chapter, together with the recurrence procedure. As stated above, the A and B parameters combined with geologic slip rate data and characteristic magnitude form the basis for the recurrence function.

Once the recurrence function for a fault is defined, the magnitude distribution can be computed. The process is done for each fault individually. A list of 5,000 events representing the largest magnitudes expected to occur in 50,000 years is computed. For each magnitude, a fault break length is determined using data by Coppersmith (1991). A random epicenter location is selected along the fault. The fault break is then assigned to the random epicenter. Various distances are computed, such as epicentral distance, hypocentral distance, and closest distance of fault break to site. The choice of distance depends on the acceleration attenuation equation chosen by the user.

Using the magnitude and separation distance, a site acceleration and standard deviation are computed. A random acceleration is then determined. Associated with each acceleration is the causative event and distance. The process is repeated 5,000 times for each fault. The random fault data are then combined for a total site probability distribution.

The procedure described above has the advantage that historical data are augmented with available geologic slip data. Where characteristic events are defined, they may be easily incorporated at the appropriate return time. The effective nonlinear recurrence function attempts to capture the temporal characteristics of the data without complex estimates of Markov or Bayesian parameters.

REFERENCE

Coppersmith, K.J. (1991). "Seismic source characterization for engineering seismic hazard analyses," in Proceedings of the Fourth International Conference on Seismic Zonations, vol 1, 1991, pp 1-60.

CHAPTER 7
RESPONSE SPECTRA AND ANALYTICAL TECHNIQUES

SPECTRA

Engineers have found it useful to examine the frequency content of earthquake-induced ground motion. Strong motion accelerograms have been analyzed as a means of obtaining further insight into ground motion.

The first technique available is Fourier analysis. The Fourier spectrum of an acceleration shows the significant frequency characteristics of the recorded motion. The Fourier spectrum is defined as:

$$F(w) = \int_0^T z(t)\, e^{-iwt}\, dt \qquad (7\text{-}1)$$

over the interval $O<t<T$. The acceleration is zero outside the limits O to T. The Fourier amplitude spectrum is given by the square root of the sum of the squares of the real and imaginary parts of F(w). Associated with the magnitude F(w) is the phase angle $\rho(w)$, defined as the arc tangent of the imaginary part divided by the real part. Units of the spectrum reflect the time integration; thus, for an acceleration in ft/sec^2, the spectrum magnitude will be in feet per second and the phase angle will be in radians. The Fourier spectrum magnitude and phase angle represent only the input motion. Through convolution this may be combined with transfer functions for other elements (such as soil structure interaction) assuming elastic behavior. The Fourier spectrum magnitude and phase are a complete record that is unique and maintains the total time history record. The time history record may be recreated by reverse transformation. Generally, only the magnitude of the Fourier spectrum is shown in reference illustrations.

In earthquake engineering it is important to be able to determine the magnitude of maximum response of a structure. This has given rise to the response spectra technique. A single-degree-of-freedom, spring-mass-damper system can be analyzed and its time history of displacement calculated to determine relative displacement between the mass (the structure) and the excited base (the ground). Relative velocity and relative acceleration may also be calculated. However, of primary interest for engineering applications is the maximum absolute values of structure relative-displacement, structure relative-velocity, and absolute structure acceleration. These values SD, SV, SA are functions of the critical damping. Plots of SD, SV, SA versus the undamped natural period of vibration and for various fractions of critical damping are called

response spectra. In typical engineering structures the damping is small and for harmonic excitation the following holds:

$$SD = \left(\frac{T}{2\pi}\right) SV$$

$$SA = \left(\frac{2\pi}{T}\right) SV \qquad (7\text{-}2)$$

For earthquake-like excitations that are not strictly harmonic excitation, an engineering assumption is made that the above is still accurate. The following definitions are used:

$$PSV \equiv \left(\frac{2\pi}{T}\right) SD$$

$$PSA \equiv \left(\frac{2\pi}{T}\right)^2 SD \qquad (7\text{-}3)$$

where PSV is the pseudo-relative velocity and PSA is the pseudo-absolute acceleration. The term "pseudo" is used to recognize the assumptions made concerning small damping and harmonic motion. Thus, SD, PSV, PSA, and T make up a set of data; knowing any two makes it possible to determine the other two. This unique relationship makes it possible to plot response spectra in tripartile form. The response spectra shows the response of a single-degree-of-freedom system (structure) as a function of damping of the system and period for the given input acceleration.

A comparison of Fourier and pseudo-velocity response spectrum reveals that both are of the same units. For an undamped oscillator, a similar mathematical relationship exists between the Fourier amplitude spectrum and exact relative velocity response spectrum. (The Fourier spectrum may be viewed as the maximum velocity of the undamped oscillator in the free vibration following the earthquake; however, the exact velocity response spectrum is the maximum velocity during both the earthquake and the subsequent free vibration.)

The Fourier amplitude spectrum is the quantity most frequently used by seismologists in their investigations of the earthquake ground motion. The response spectrum is generally used by structural engineers in the design of structures. Generally, the pseudo-velocity response spectrum is the upper envelope of the Fourier spectrum.

In summary, the most representative measure of the driving ground motion is the Fourier spectrum, which may be plotted in tripartile form. The response spectrum gives the response of a single-degree-of-freedom structure to the ground motion. Amplification of motion occurs where resonant components of motion interact with the structure. The response spectrum is most widely used in structural engineering with the modal analysis technique. This approach determines the eigenvalues and mode shapes for a number of the modes of structure, and using the modal period determines the acceleration to be used in computing an equivalent maximum static force to be applied to the structure. A response spectrum cannot be used directly as input to a dynamic structural analysis to generate a time history response because the response

spectrum does not contain a measure of the duration of excitation. The Fourier spectrum does contain the full earthquake representation and may be used in conjunction with transfer functions to compute the structure response. This technique is not used in general structural engineering because of the difficulty in determining the transfer function. The more common structural analysis techniques that produce dynamic time histories of response require input acceleration histories. Random analysis programs exist to generate time histories from a given spectral envelope; however, the duration must be specified. The resulting randomly generated signal is not unique, and any number may be generated from a single spectral envelope.

Time history records of actual earthquakes are available from the California Institute of Technology National Earthquake Information Center. These may be used when required for time history input of ground motion. Care is needed in selection since most records are recorded in structures that may influence the recording. Also, the region around the site may influence the site response. The propagation of seismic waves is influenced by the local geology and soil conditions. The greater the extent of softer soils over bedrock, the less the boundary effects of the bedrock will have on the site. The depth of soil overlaying bedrock affects the period of vibration of the ground. This establishes a fundamental soil frequency of particular importance on soil-structure interaction. Further, this is a factor in determining the frequencies of waves filtered out by the soil, thus directly affecting the time history record.

SITE-INDEPENDENT SPECTRA

Based on studies of response spectra, Newmark (1970) noted that response spectra could be related to peak ground acceleration, velocity, and displacement. From this study it was possible to develop standard shapes for use in structural analysis. The standard ground motion spectra (defined as lg, 48 inches/second, 36 inches) could be scaled, based on peak horizontal ground acceleration expected at the site. Figure 7-1 gives amplification factors that could then be applied to estimate structural response.

McGuire (1977) also demonstrates ratios of damped spectra. He found that the 5 percent damped pseudo-velocity spectra have value approximately 70 to 80 percent of the 2 percent damped spectra and that the 10 percent damped spectra have values of approximately 55 to 65 percent of the 2 percent damped spectra. These ratios are constant throughout frequency range independent of the type of earthquake distance from site and magnitude. This confirms the Newmark-Hall (1969) approach, Newmark, et al. (1973).

At a frequency of about 6 cps, the amplitude acceleration region line intersects a line sloping down toward the maximum ground acceleration value and intersecting that line at various frequencies, depending on the damping. The intersection is at a frequency of about 30 cps for 2 percent damping. These lines are designated as the acceleration transition region of the spectra. Finally, beyond the intersection with the maximum ground acceleration line, the response spectrum continues with the maximum ground acceleration value for higher frequencies.

The spectra so determined can be used as design spectra for elastic responses. The spectra are completely described when the maximum ground motion values are given for the three components of ground motion, and the damping is known. When only the maximum ground acceleration is given, the values used for maximum ground velocity and displacement are taken as proportional to those in the figure, or as scaled by the same scale factor relative to the maximum ground acceleration compared with it.

An assumption is made that acceleration, velocity, and displacement values are proportional to one another, independent of magnitude of motion. The shape is thought correct for sites on firm ground, soft rock, or competent sediments. However, for soft sediments, the velocities and displacements must be increased. Garcia and Roesset (1970) performed studies comparing actual spectra with those estimated by the Newmark-Hall procedure. Results show favorable comparison indicating the utility of the Newmark-Hall procedure.

Vertical spectra may be estimated by taking two-thirds of the horizontal spectra when fault movements are horizontal and by taking horizontal spectra when large vertical motions are expected.

Newmark (1970) has studied the response of elasto-plastic systems; one set of results shows the response of an elasto-plastic system to the El Centro earthquake. For low frequency systems, the total displacement varies approximately inversely with the ductility factor. In a high frequency (stiff) structure, the mass acceleration approaches the driving ground acceleration.

The following generalizations were developed by Newmark (1970):

1. For low frequency systems, the total displacement for the inelastic system is the same as for an elastic system having the same frequency.

2. For intermediate frequency systems, the total energy absorbed by the spring is the same for the inelastic system as for an elastic system having the same frequency.

3. For high frequency systems, the force in the spring is the same for the inelastic system as for an elastic system having the same frequency.

Newmark (1970) has outlined a method for selecting the response spectrum to use (Figure 7-2):

> "The elastic spectrum, designated by the symbol $\mu = 1$, for displacement and acceleration (D and A) represents slightly amplified values, corresponding to an elastic response spectrum for the ground motion considered. The curve marked D for $\mu = 5$ is the displacement spectrum for a ductility factor of 5, and the curve marked A for $\mu = 5$ is the acceleration or force spectrum for the same conditions. These are drawn so as to conserve displacement on the left-hand side, force on the right-hand side, and energy in the central part. An elastic analysis made for the reduced acceleration spectrum therefore would correspond to the ductility values derived for the conditions described. The relations between the various bounding lines in [Figure 7-2], for an elasto-plastic resistance function, are the same and the acceleration is one-fifth as much for the elasto-plastic spectrum as for the elastic spectrum. Along a constant velocity line, the displacement is five-thirds as great and the acceleration one-third as great for the elasto-plastic spectrum compared with the elastic spectrum. Finally, along a line of constant acceleration, the displacement is five times as great and the acceleration value is the same as the value for elastic response."

The elastic spectrum discussed above may be adjusted to approximate inelastic behavior of a structure. The displacement region and the velocity region are divided by the structure ductility μ to obtain yield displacement D' and velocity V' (Figure 7-3). The acceleration region

(right side) is relocated by choosing it at a level which corresponds to the same energy absorption for elasto-plastic behavior as for elastic for the same period of vibration.

The extreme right-hand portion of the spectrum, where the response is governed by the maximum ground acceleration, remains at the same acceleration level as for the elastic case and, therefore, at a corresponding increased total displacement level. The frequencies at the corners are kept at the same values as in the elastic spectrum. The acceleration transition region of the response spectrum is now drawn also as a straight line transition from the newly located amplified acceleration line to the ground acceleration line, using the same frequency points of intersection as in the elastic response spectrum.

In all cases, the "inelastic maximum acceleration" spectrum and the "inelastic maximum displacement" spectrum differ by the factor μ at the same frequencies. The design spectrum so obtained is shown in Figure 7-3. Both the maximum displacement and maximum acceleration bounds are shown for comparison with the elastic response spectrum.

The solid line $DVAA_o$ shows the elastic response spectrum. The heavy circles at the intersections of the various branches show the frequencies that remain constant in the construction of the inelastic design spectrum.

The line $D'V'A'A_o$ shows the inelastic acceleration, and the line $DVA"A_o$ shows the inelastic displacement. These two differ by a constant factor μ for the construction shown, but A and A' differ by the factor $2\mu - 1$, since this is the factor that corresponds to constant energy.

A study by Newmark and Riddell (1979) investigated the response of elasto-plastic systems to numerous earthquake records. Based on this effort, the preceding work was found to be unconservative for damping larger than 5 percent and for ductilities greater than 3.

SITE-MATCHED SPECTRA

The data base of strong motion records can be a useful source of seismic data. Records may be selected to represent seismologic, geologic, and local site conditions. Selection is complicated by a number of factors. Ideally, the records should be selected to match source-site transmission path, source mechanism, and local site conditions. These are not readily quantifiable. Thus, reliance is made on earthquake magnitude site acceleration level, site classification, and duration of motion. Judgment is an important factor in selecting and scaling records.

Ferritto (1992) describes a desktop computer program for computing optimized earthquake time histories and response spectra. The program has the data base of about 1,000 records provided by the National Oceanographic and Atmospheric Administration. The user may select specific records and obtain time histories and spectra or may specify a ground acceleration level, site distance, and magnitude and the program will search the data base and provide the user with a list of the closest matching records. The user may then combine a number of spectra and obtain average, average plus one standard deviation, and envelope spectra.

It is suggested that site-matched groups of spectra be used to develop the mean and mean-plus-1-standard-deviation spectra. These should be compared with standard spectral shapes and typical results for soft, intermediate, or rock sites to denote regions where the spectra may be deficient. This is particularly important for Eastern sites since the spectra are recorded in the West. Significant variations in attenuation have been noted between Western and Eastern ground motion.

The same nominal ground motion level can be produced by different magnitude earthquakes at different distances. As an example of this, a nominal ground motion of 0.15 g was caused by the following earthquakes:

Earthquake	Magnitude	Separation Distance (miles)
A	5	14
B	6	18
C	7	30

Using response spectra programs, the closest matching ten spectral records for each earthquake (intermediate soil class) were used to generate average and maximum spectra (Figure 7-4). Each spectrum represented the characteristics of the magnitude and separation distance.

In the response spectra program, the closest matching ten spectral records for each earthquake (intermediate soil class) were used to generate average and maximum spectra (Figure 7-4). Each spectrum represented the characteristics of the magnitude and separation distance.

The response spectra data base and accelerograms have been categorized by soil site conditions: alluvium, intermediate, or rock. It was of interest to evaluate this effect on the response of the structure. Ten spectra of each site type for a magnitude 6.6 event at 20 miles having a 0.15 g nominal ground motion were combined to produce average and maximum spectra (Figure 7-5).

Two alternative procedures used to determine site specific ground motion are as follows.

Surface Motion

This technique utilizes attenuation relationships based on surface motion. The computed motion is then used as a scaling value for the response spectra. The specific response spectrum may be based on a group selected for similar site properties or a spectral shape determined by researchers to be applicable to specific site conditions.

Bedrock Motion

This technique utilizes an attenuation relationship based on bedrock motion. The motion may be brought to the surface either from empirical data or by use of wave propagation computation programs.

An automated-analysis technique, widely used today for treating horizontal soil layers, has been developed by Schnabel, Lysmer, and Seed (1972), based on the one-dimensional wave propagation method. This program, SHAKE, can compute the responses for a given horizontal earthquake acceleration specified anywhere in the system. The analysis incorporates nonlinear soil behavior, the effect of the elasticity of the base rock, and variable damping. It computes the responses in a system of homogeneous viscoelastic layers of infinite horizontal extent, subject to vertically traveling shear waves. The program is based on the continuous solution of the wave equation adapted for use with transient motions through the Fast Fourier Transform algorithm.

Equivalent linear soil properties are obtained by an iterative procedure for values of modulus and damping compatible with the effective strains in each layer. The following assumptions are made:

1. The soil layers extend infinitely in the horizontal direction.

2. The layers are completely defined by shear modulus, critical-damping ratio, density, and thickness.

3. The soil values are independent of frequency.

4. Only vertically propagating, horizontal shear waves are considered.

The soil model is similar to that developed by Seed and Idriss (1970), using data similar to Hardin and Drnevich (1970). The absolute range of soil parameter variation may be stipulated by merely inputting factors whose numerical values may be derived from simple soil strength properties. These strength properties may be the undrained shear strength of a clay or the relative density for sands. The program requires the definition of the soil profile down to bedrock (defined as seismic velocity 2,500 ft/sec) as well as an earthquake time history record in digital form.

The motion used as a basis for the analysis can be given in any layer in the system, and new motions can be computed in any other layer. Maximum stresses and strains, as well as time histories, may be obtained in the middle of each layer. Response spectra may be obtained and amplification spectra determined.

Using the site soil properties, a one-dimensional wave propagation analysis was performed. The time histories of the records selected were used in the one-dimensional analysis. The ground motion was applied to the surface. The average shear velocity of the site was 125 m/sec with a natural period of 1.7 seconds. The site responded as anticipated, as a deep, soft site showing attenuation of the acceleration. The surface motion (input at 0.5 g) was increased to about 1.0 g at a depth of 57 meters. The site attenuated bedrock motion by a factor of about two. This is in general agreement with empirical data.

Figure 7-6 shows input surface response spectrum and computed bedrock response spectrum. The bedrock spectrum has its peak value at a period of 0.13 second. The shape of this spectrum, location of peak value, and relative magnitudes are very much in agreement with standard spectral data based on records recorded in rock sites. The soil layer responds as a filter. Thus, it is also possible to generate surface motion using a scaled rock-site spectrum as input. The magnitude of the spectra would be based on attenuation relations developed for rock. Figure 7-7 gives a flow chart of two approaches for determining an average surface response spectrum.

The approach of using surface-recorded scaled, response spectra matched to the site conditions is thought to be a better representation of actual conditions than the alternative of attempting to compute ground motion propagation from bedrock to the surface. The limitations in the accuracy of the attenuation equation show no statistical difference between peak accelerations recorded on rock and those on soil at comparable distances. Thus, the problem of what level of motion to input must be based on uncertain data. Motion must be artificially brought to bedrock by deconvolution. Unfortunately, motions are usually recorded on the surface and not at bedrock depth. Without at-depth experimental records, one-dimensional wave

propagation calculations, although very useful, may have error. Spectral shapes from such calculations cannot be used with absolute certainty. The extent of site amplification is a significant parameter. However, it cannot be computed from wave propagation analysis in absolute certainty. It should be looked at as relating relative soil behavior. Uncertainty is introduced by the choice of material properties used to characterize the site. The assumptions made in one-dimensional analysis are perhaps more hidden and, thus, create a greater confidence in the results.

It is important to consider the major assumption made in wave propagation analysis: that vertically propagating shear waves travel through horizontal layers. For sites close to the fault, the inclined nature of the fault and the close horizontal proximity to the energy source must be considered. The energy released, which is composed of surface and body waves, cannot be represented by a simplified one-dimensional model. Thus, it is questionable whether any attentuation of motion would actually occur. The one-dimensional model is best suited for sites at distances from the source where propagation is essentially through the more competent subsurface (bedrock) layers refracting to the surface. This site may indeed show attenuation to motion originating from distant sources. However, little is known about close-in behavior; there is not enough known to justify a reduction in ground motion without loss of confidence in the results.

REFERENCES

Ferritto, J.M. (1992). Optimized earthquake time-history and response spectra, Naval Civil Engineering Laboratory, User Guide UG-0025. Port Hueneme, CA, Oct 1992.

Garcia, F., and J.M. Roesset (1970). Influence of damping on response spectra, Massachusetts Institute of Technology, Department of Civil Engineering, R70-4. Cambridge, MA, Jan 1970.

Hardin, B., and V. Drnevich (1970). Shear modulus and damping in soils, University of Kentucky, College of Engineering, Soil Mechanics Series Technical Report UKY 26-70-CE2. Lexington, KY, Jul 1970.

McGuire, R. (1977). "Seismic design spectra and mapping procedures," Earthquake Engineering and Structural Dynamics, vol 5, New York, NY, Wiley Publications, 1977, pp 211-234.

Newmark, N.M. (1970). Current trends in the seismic analysis and design of high-rise structures in earthquake engineering, Chapter 16, R.L. Wiegel, editor. Englewood Cliffs, NJ, Prentice-Hall, 1970.

Newmark, N.M., and R. Riddell (1979). "A statistical study of inelastic response spectra," in Proceedings of the Second U.S. National Conference on Earthquake Engineering, Stanford University, Stanford, CA, Aug 1979.

Newmark, N.M., J.A. Blume, and K.K. Kapur (1973). "Seismic design spectra for nuclear power plants," Journal of the Power Division, ASCE, vol 99, no. P02, Nov 1973.

Newmark, N.M., and W.J. Hall (1969). "Seismic design criteria for nuclear reactor facilities," in Proceedings of the Fourth World Conference on Earthquake Engineering, Santiago, Chile, 1969.

Schnabel, P.B., J. Lysmer, and H.B. Seed (1972). SHAKE, a computer program for earthquake response analysis of horizontally layered sites, University of California, Earthquake Engineering Research Center, EERC Report No. 72-12. Berkeley, CA, Dec 1972.

Seed, H.B., and I.M. Idriss (1970). Soil moduli and damping factors for dynamic response analysis, University of California, Earthquake Engineering Research Center, EERC Report No. 70-10. Berkeley, CA, Dec 1970.

Percent of Critical Damping	Displacement	Velocity	Acceleration
0	2.5	4.0	6.4
0.5	2.2	3.6	5.8
1	2.0	3.2	5.2
2	1.8	2.8	4.3
5	1.4	1.9	2.6
7	1.2	1.5	1.9
10	1.1	1.3	1.5
20	1.0	1.1	1.2

(a) Relative values of spectrum amplification factors (from "Seismic design spectra for nuclear power plants," by N. M. Newmark, J. A. Blume, and K. K. Kapur, in Journal of the Power Division, ASCE, vol 99, no. PO2, Nov 1973, table 5).

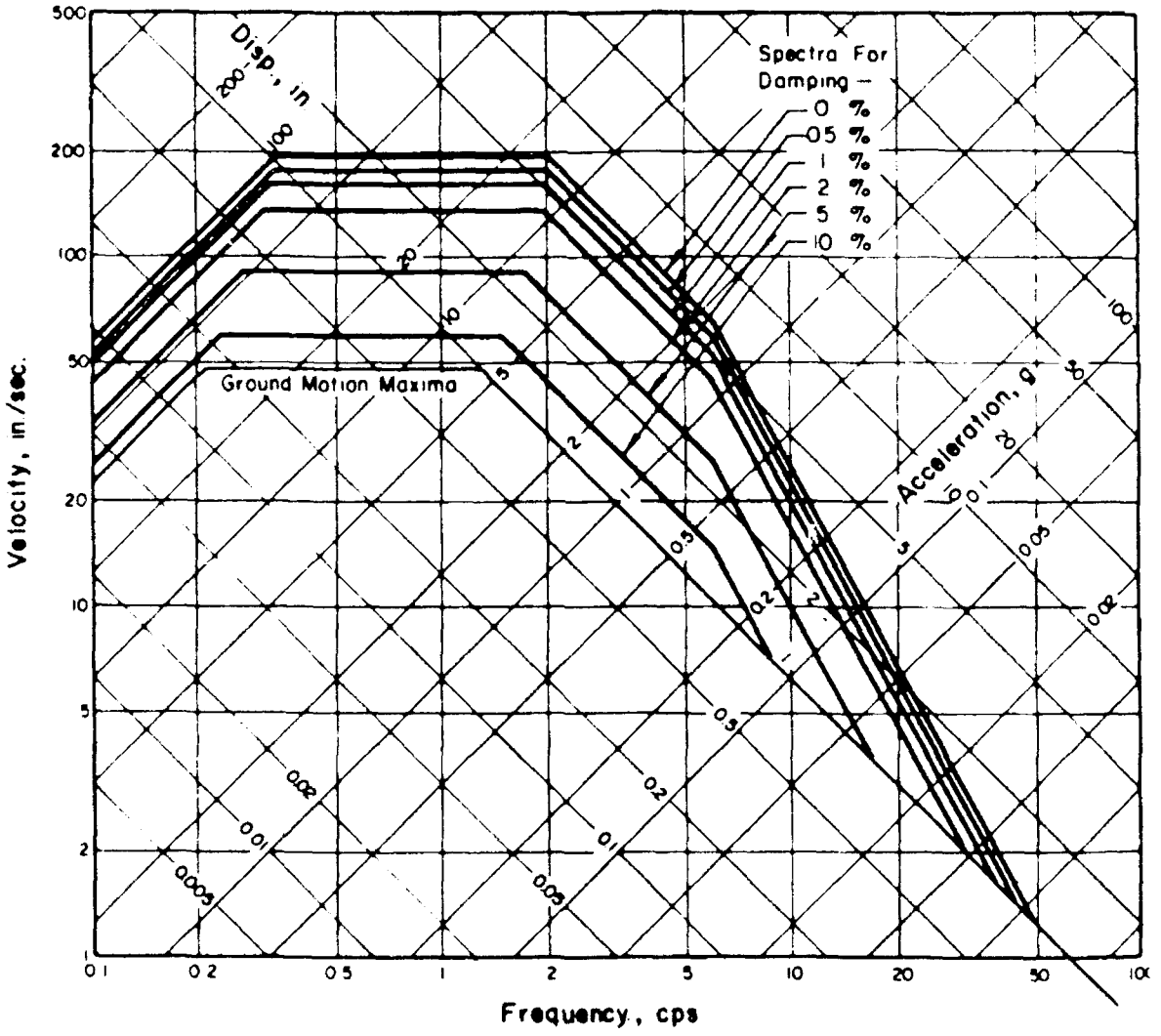

Figure 7-1 Design Spectra normalized to 1.0 g (from Applied Technology Council, 1974)

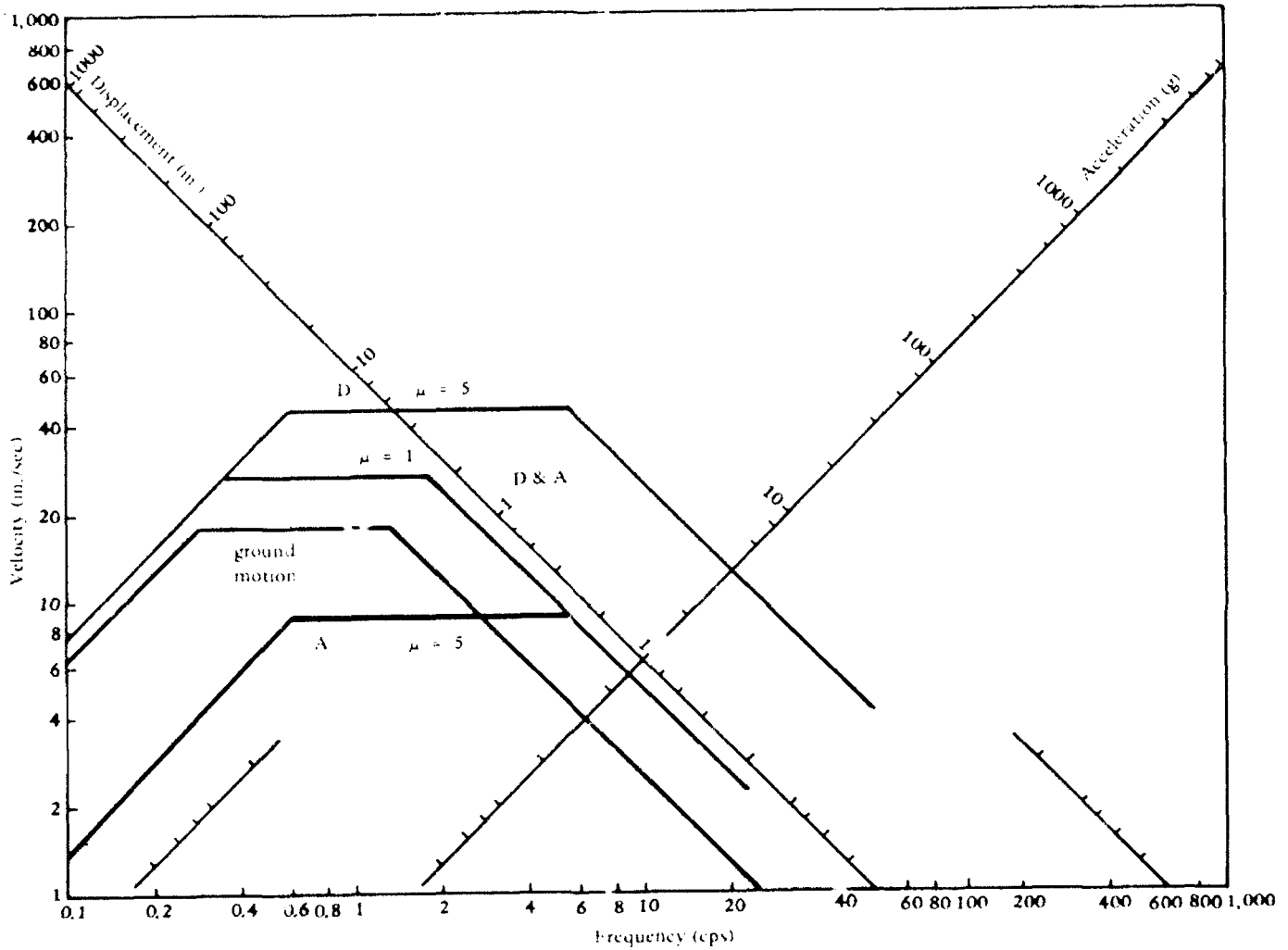

Figure 7-2. Comparison of elastic and elasto-plastic spectra. (Natan M. Newmark, "Current Trends in the Seismic Analysis and Design of High Rise Sructures", in Earthquake Engineering, edited by Robert L. Weigel, copy right 1970, pp 419. reprinted by permission of Prentice Hall, Inc. Englewood Cliffs, New Jersey.

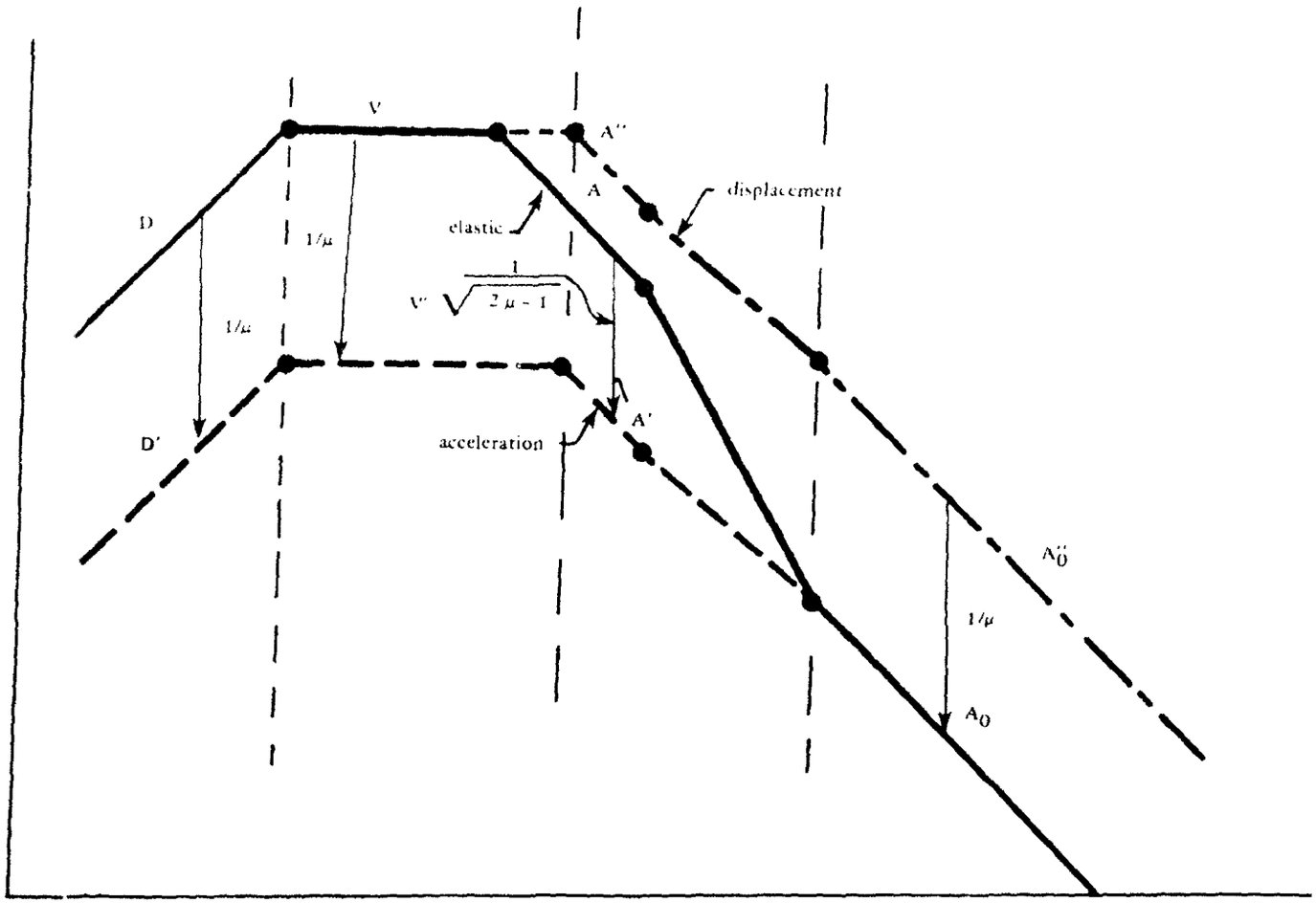

Figure 7-3 Design spectra for inelastic analysis.

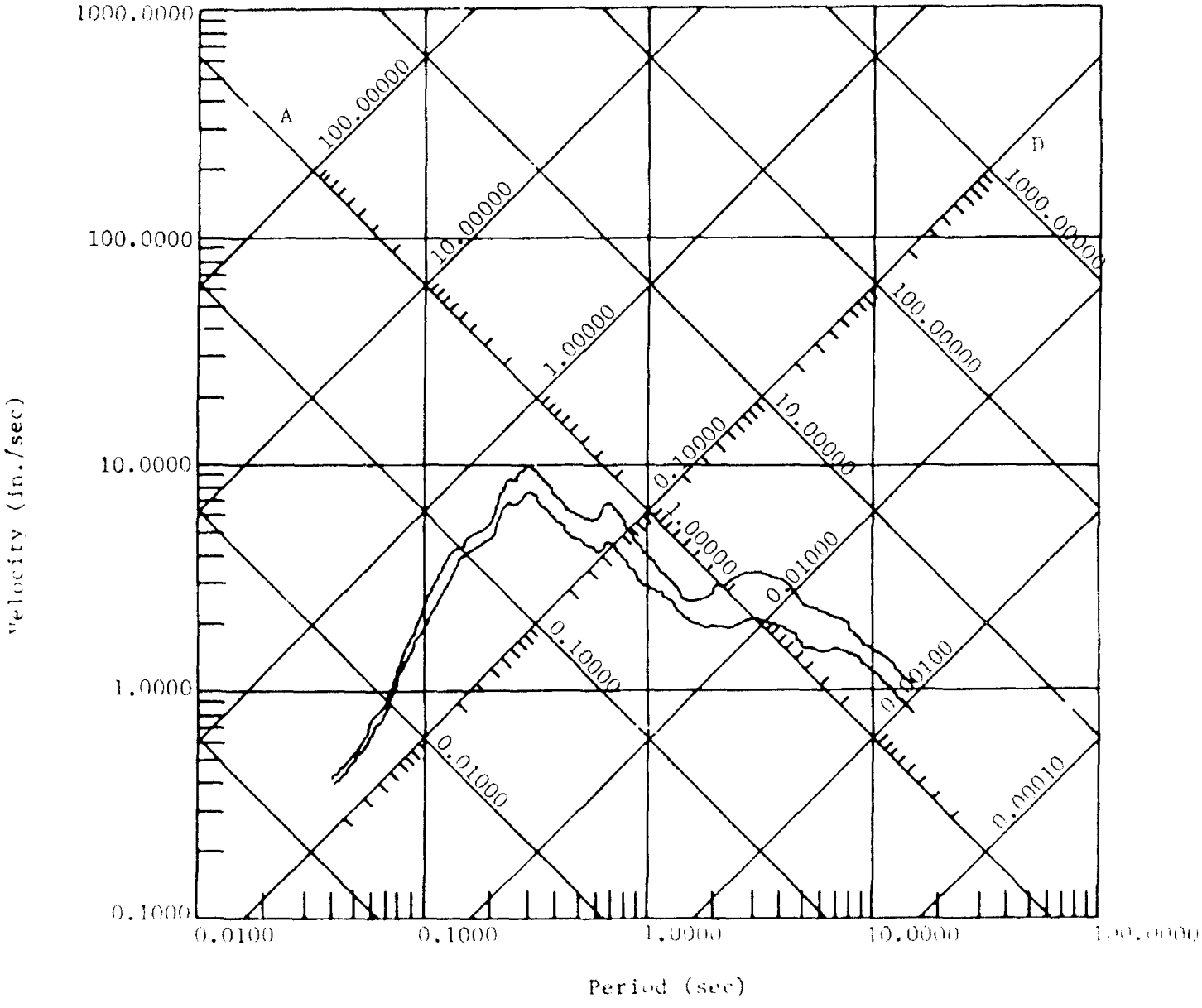

Figure 7-4a. Magnitude 5 at 14 miles.

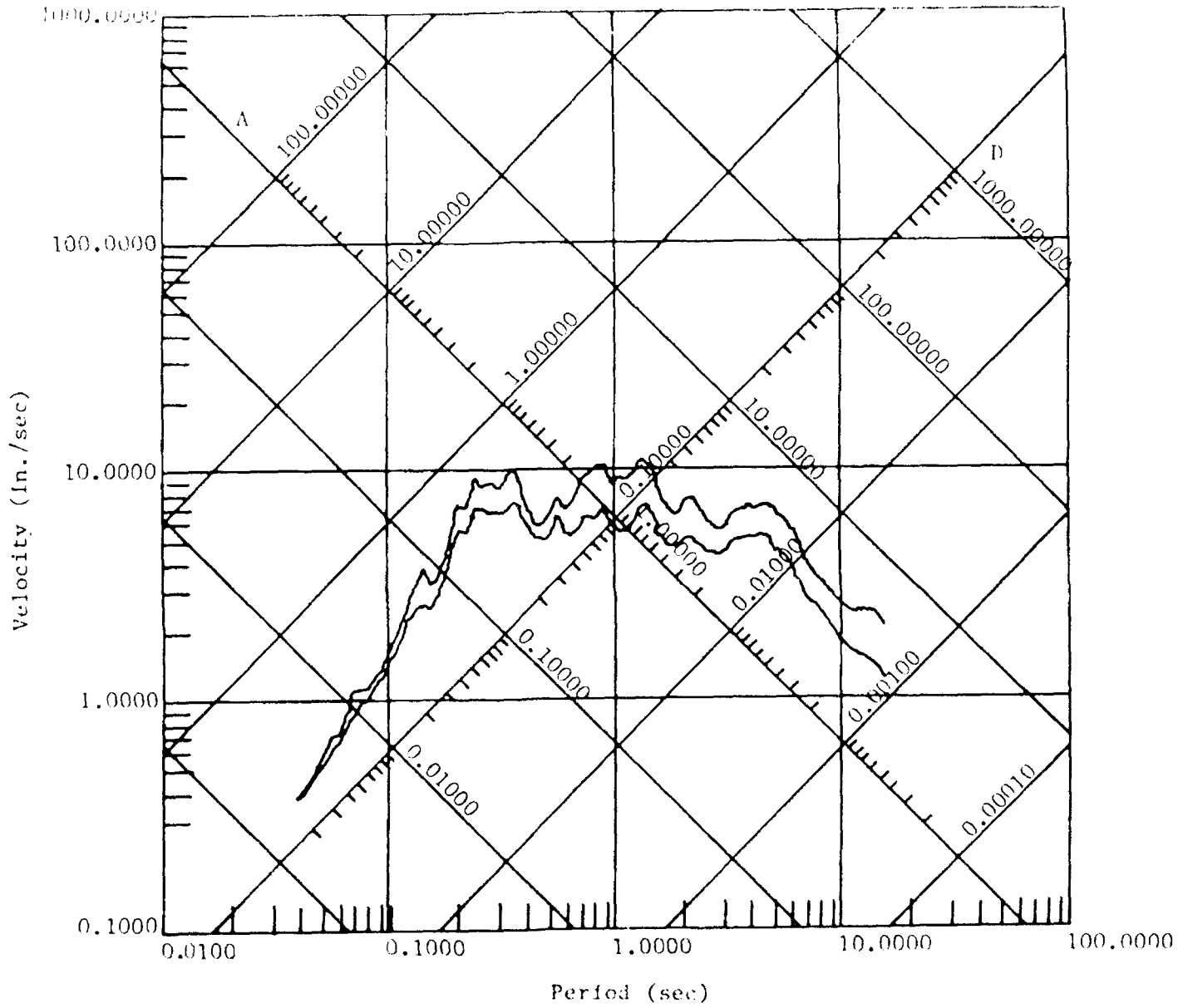

Figure 7-4b. Magnitude 6 at 17 miles.

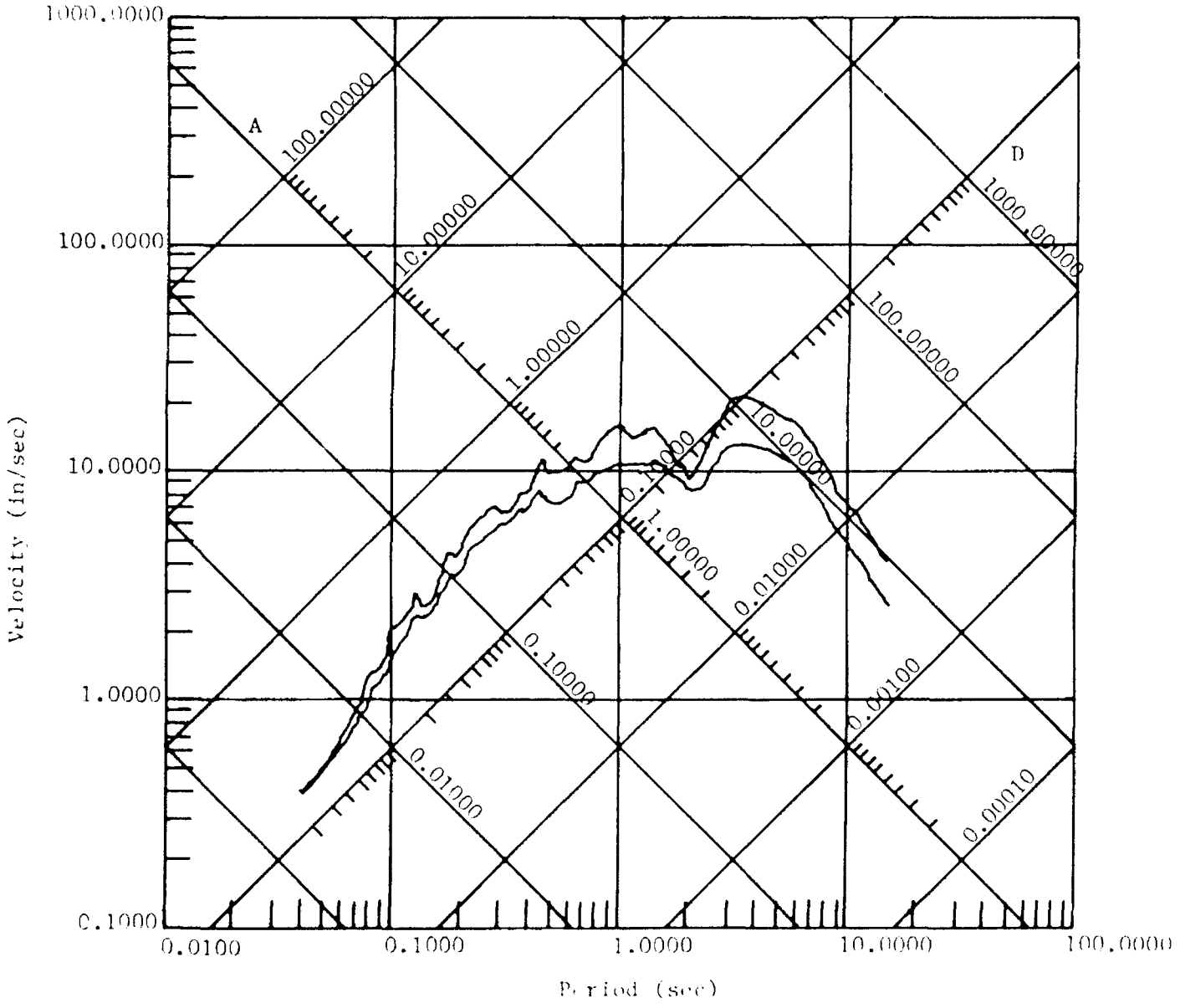

Figure 7-4c. Magnitude 7 at 30 miles.

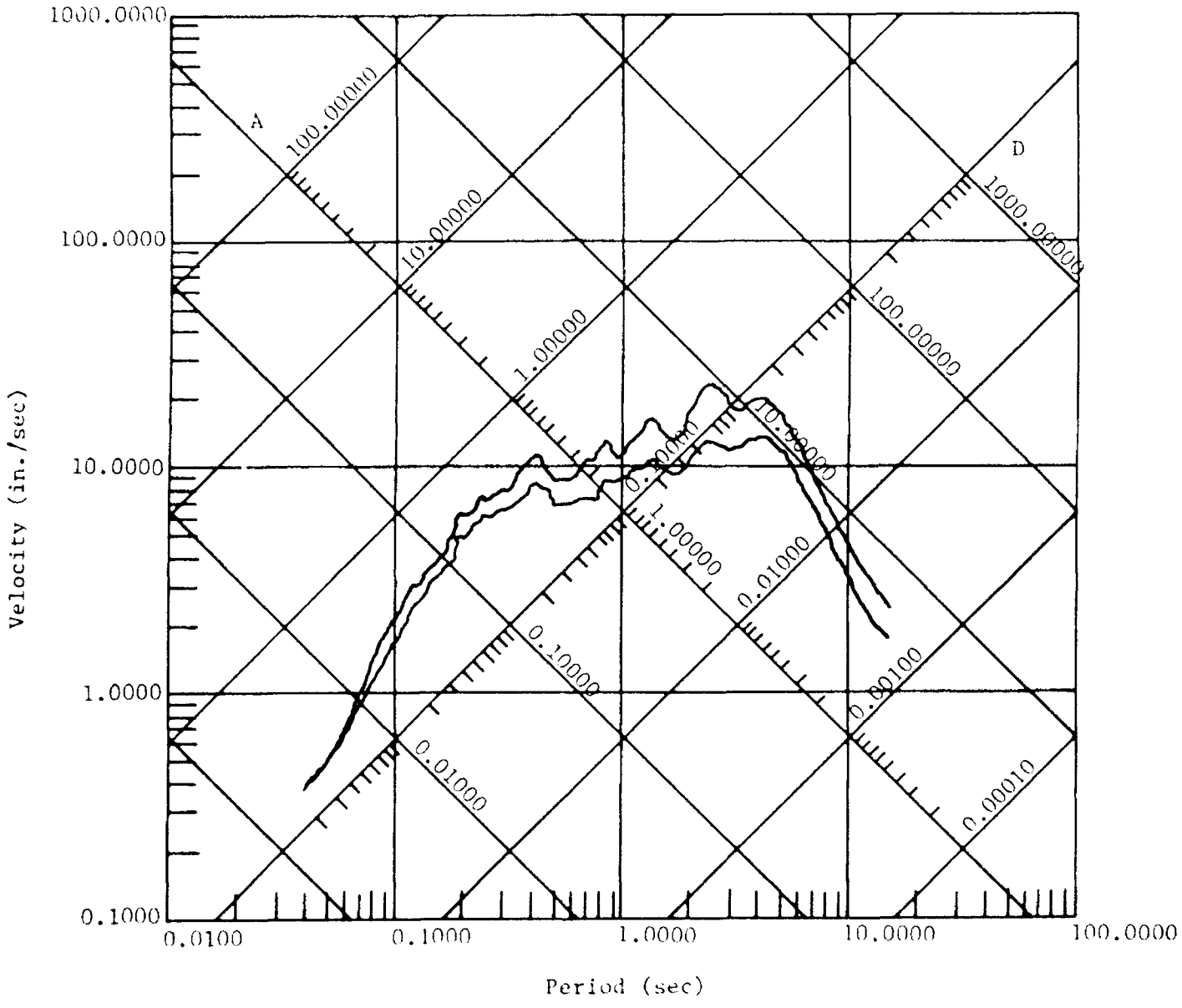

Figure 7-5a. Magnitude 6.6 at 20 miles, 0.15g, alluvium site.

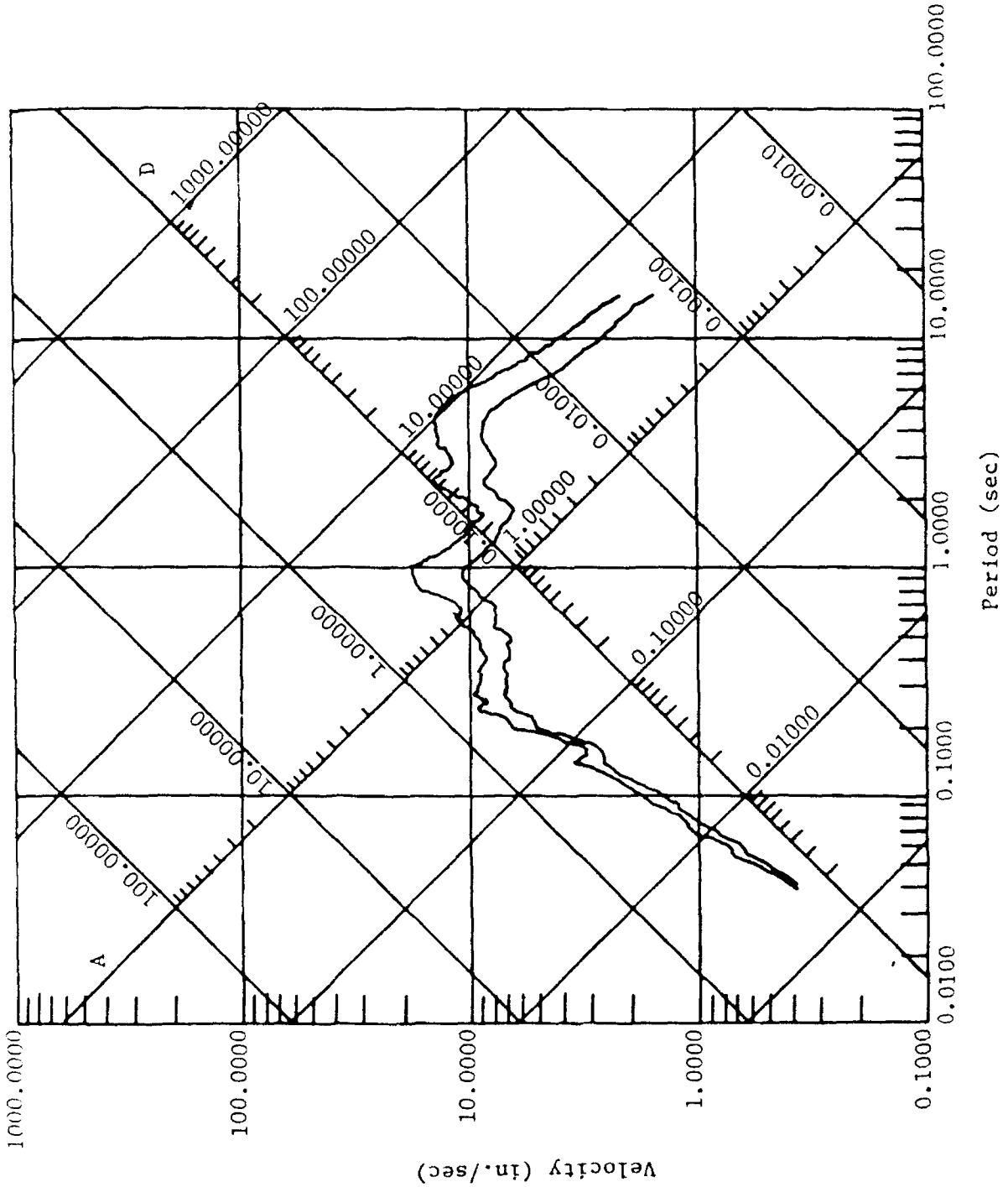

Figure 7-5b. Magnitude 6.6 at 20 miles, 0.15g, intermediate site.

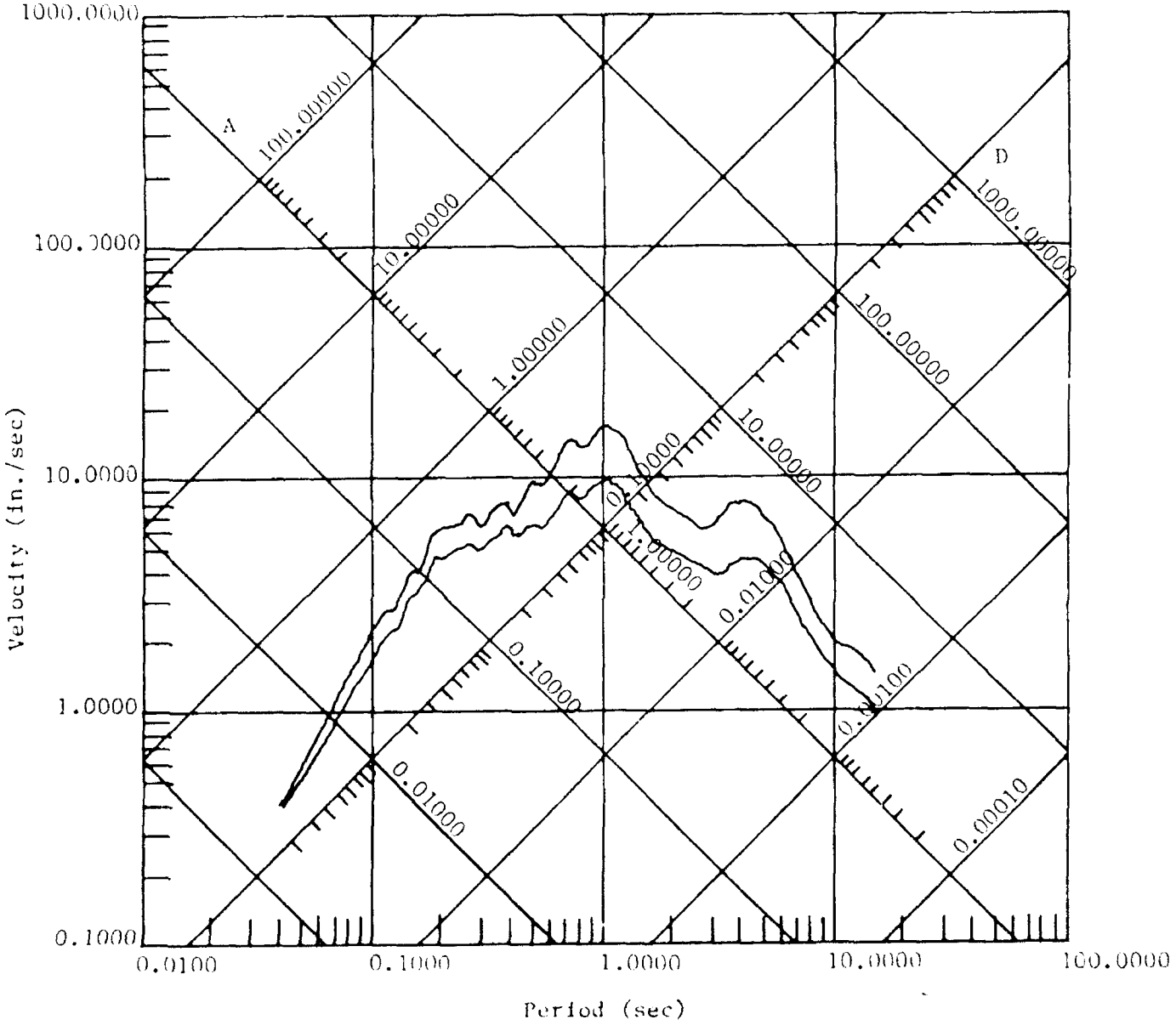

Figure 7-5c. Magnitude 6.6 at 20 miles, 0.15g, rock site.

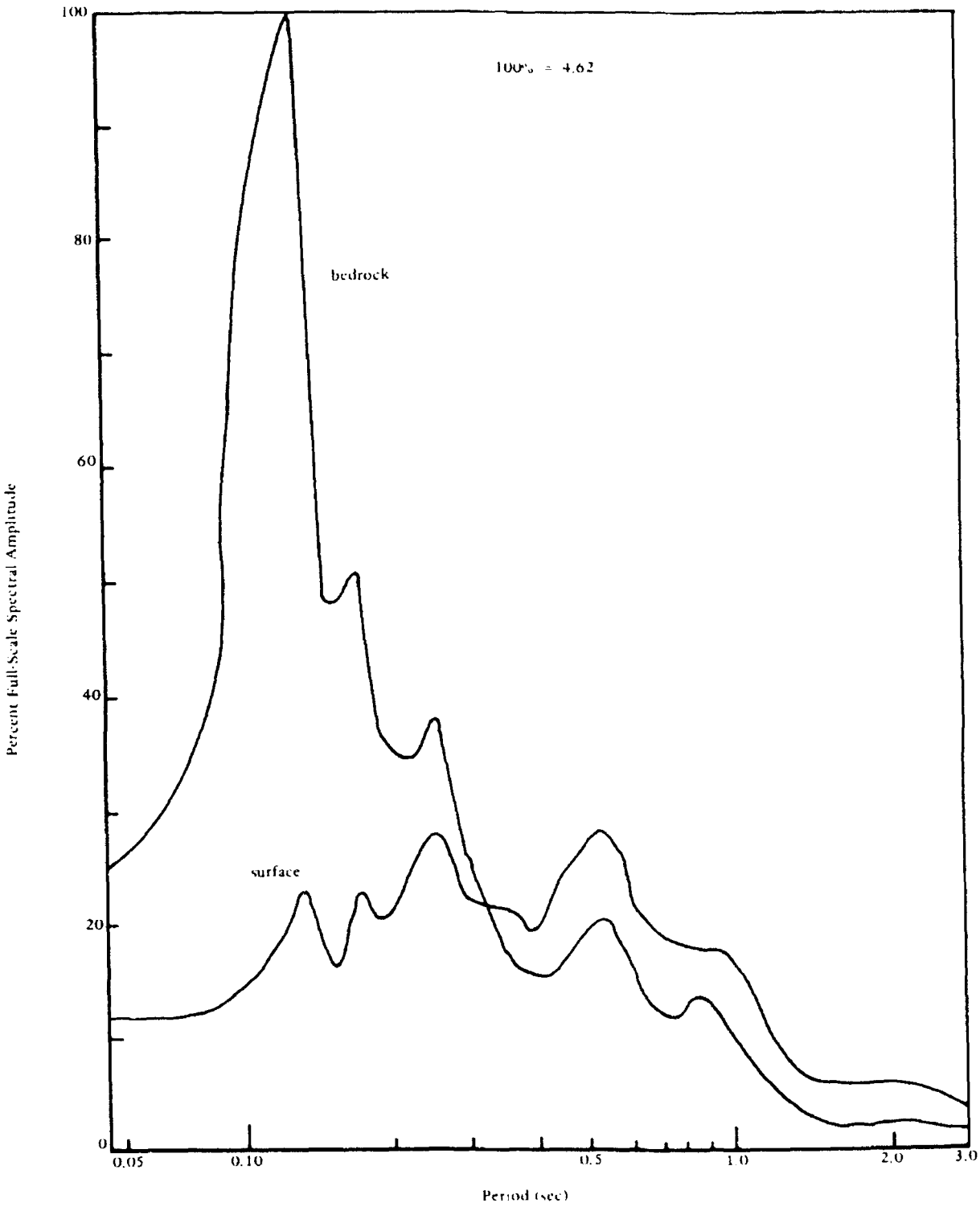

Figure 7-6 Plot of acceleration response spectra.

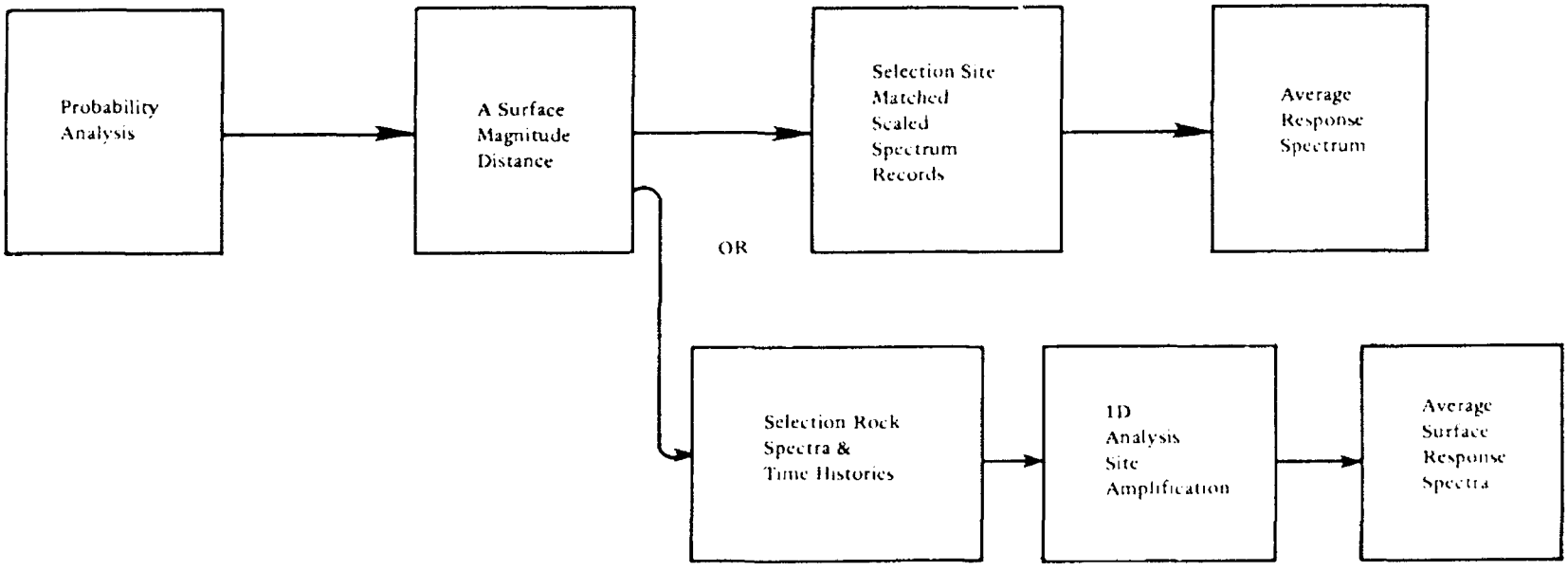

Figure 7-7. Flow chart of analysis.

CHAPTER 8
EARTHQUAKE ACTIVITY FOR ENGINEERING ANALYSIS IN THE SAN DIEGO AREA

SEISMICITY

The seismicity and regional geologic structure of the San Diego area can be interpreted in light of current plate tectonic theory. California is believed to lie on the junction of two relatively rigid plates of the earth's crust that respond to movement of subcrustal material. The main evidence of this juncture is the San Andreas fault. These same forces that tend to move the portion of California on the westerly side of the San Andreas fault northward have resulted in the formation of other faults, such as the San Jacinto, Whittier-Elsinore and Newport-Inglewood faults.

Distant faults that must be considered significant to the site region include the Elsinore and San Jacinto fault zones to the northeast and the San Clemente fault zone to the west. Local faults include the Rose Canyon and La Nacion. The San Andreas fault zone is not considered very significant because of its great distance from the study area.

The San Diego Bay contains cretaceous, tertiary, and quaternary strata, which is generally flat but locally folded and cut by normal and right lateral faults. This area is called the Rose Canyon zone (Lamar, et al., 1973). A bottom survey of the bay revealed numerous faults which were difficult to correlate. The quaternary deformations observed along the Rose Canyon fault zone attest to the tectonic importance of the zone. Although no major earthquakes have occurred near San Diego recently, several earthquakes of about magnitude 3.5 have been recorded during the past 41 years. Eleven took place near the Rose Canyon fault. The magnitude 3.5 earthquake is associated with a fault rupture length of 1 km. The geologic structure of this area shows evidence of previous movement. Surface traces of more than 24 km in length and vertical separation of hundreds of feet are visible. Table 8-1 shows the key faults and the maximum credible earthquake.

San Jacinto Fault

The San Jacinto fault system extends from its junction with the San Andreas southeast of Palmdale to the Colorado River Delta. Geodetic data indicate an average slip rate of 0.3 cm/yr. Seventeen large earthquakes have occurred since 1890 along the 290-km long fault. The magnitudes determined were in the range of 5.7 to 7.1.

This is one of the most active faults. In the 33-year period from 1890 to 1923, the northern portion of this fault system averaged an event each 5.5 years. Large earthquake activity in the northern half of the fault system has lapsed during the past 52 years. Movement in faults in the Imperial Valley caused an earthquake in 1915 and again in 1940 (25-year span). The last event was 35 years ago, and it is thought that significant strain has not been released since that event.

Whittier-Elsinore Fault

This fault system is composed of the Elsinore and Whittier fault zones, Agua Caliente fault, and Earthquake Valley fault. Five recent earthquakes of unknown magnitudes have occurred on this fault, the last one in 1935. No historical data exist to construct a recurrence relationship. A slip rate of 0.08 cm/yr was determined and used to calculate a recurrence interval. It is believed that sufficient elastic strain to produce a magnitude 6 or greater earthquake has accumulated along the fault in recorded historic time (several hundred years).

San Clemente Fault

This fault, with a verified length of 176 km, extends from the eastern side of San Clemente Island to the Cabo Colonet area of Baja California, Mexico. A magnitude 5.9 earthquake occurred off the southeast tip of San Clemente Island in 1951. The maximum credible event for a fault of this length is 7.7 on the Richter scale. A significant consequence of an earthquake on this fault is the possible production of a tsunami or seismic sea wave, but such is not likely with magnitudes less than 6.3. Seven percent of southern California earthquakes have submarine epicenters, yet only two or three locally-generated tsunamis are known to have occurred since 1800, and none in the San Diego area.

Rose Canyon Fault

The Rose Canyon fault zone forms a belt of fractures about a mile wide. The zone on shore can be traced southwestward for a distance of more than 16 km and then projects under San Diego Bay and continues to the Mexican border and possibly beyond. An investigation of the bay (Moore, 1972) revealed many faults. North of La Jolla an offshore extension of the fault exists, suggesting that Rose Canyon is part of a much larger northwest trending zone of deformation that extends at least 240 km from Santa Monica, California to Baja, California and includes the New-Inglewood zone.[1] Geologic evidence suggests that the most recent movement was less than 500,000 years ago. Fault displacements as recently as early Holocene time (10,000 years ago) cannot be precluded; Moore (1972) cites evidence of faulting through Pleistocene deposits. No large earthquakes have been associated with the Rose Canyon fault during historic time. During 1964, however, three earthquakes in the magnitude range of 3.5 to 3.7 were felt in the vicinity of San Diego Bay. Uplift has been noted near the fault in La Jolla in sediments that overlie the Linda Vista formation and are considered to be late Pleistocene (1,000,000 years old).

La Nacion Fault

This fault extends for 24 km southward from La Mesa. The fault dips 60 to 70 degrees toward the west and consists of two or more branches; several are tens of feet apart. Offsets of Holocene deposits along the fault have been noted but not confirmed. There is definite evidence that Linda Vista formations (50,000 years) have been displaced. Evidence (McEuen and Pinckney, 1972) suggests a change in the history of the San Diego area, previously thought to

[1]Possible locus of the 1933 Long Beach earthquake, magnitude 6.3.

be stable. Test borings approximately 30 meters deep show open faults in sedimentary rock, suggesting the area is in tension. McEuen and Pinckney (1972) also note that 1 km north of the Otay Valley the La Nacion fault offsets Pliocene formations, late Pleistocene terrace deposits, and Holocene alluvium (dating 10,090 $\pm$ 190 years).

PROBABILITY ANALYSIS

This study is intended as a demonstration of the procedure. The bounds of the study area are 117.0 to 119.0 W longitude, 34.5 to 31.0 N latitude. The coordinates of the site are 117.125N, 32.708N. A set of historical data was prepared for the site containing over 6,000 events with magnitudes of 3 or greater.

Figure 8-1 shows the region of interest with the epicenters plotted. Figure 8-2 shows a similar plot with only the faults shown. Figure 8-3 shows the computed recurrence for the La Nacion fault. All other faults utilized the default data in the program. Figure 8-4 shows the individual contributions of each fault on the site probability. Figure 8-5 shows the total probability of not exceeding the acceleration for a 50-year exposure. Figure 8-6 shows a generalized site-independent spectra normalized to 0.33 g.

RESPONSE SPECTRA

The site has been characterized as an intermediate site. The closest ten records matching a 6.5 event 16 km from this site producing 0.33 g acceleration were used to produce the response spectra shown in Figures 8-6 and 8-7. These are useful in structural design.

REFERENCES

Lamar, D.L., P.M. Merifield, and R.J. Proctor (1973). Earthquake recurrence intervals on major faults in southern California, geology seismicity and environmental impact, Association of Engineering Geologists, Special Publication. Los Angeles, CA, University Publishers, 1973.

McEuen, R.B., and C.J. Pinckney (1972). "Seismic risk in San Diego," in Transactions of the San Diego Society of Natural History, vol 17, no. 4, Jul 1972.

Moore, G. (1972). Offshore extension of the Rose Canyon fault, San Diego, California, geological survey research, U.S. Geological Survey, Professional Paper 800 C. Washington, DC, 1972, pp C113-C116.

Table 8-1
Fault Systems of Interest to NAS North Island

Fault	Maximum Credible Magnitude
Coyote Creek	7.0
Elsinore	7.5
Imperial	7.0
La Nacion	6.8
Malibu	7.5
Newport-Inglewood	7.0
Palos Verdes	7.0
Pinto Mountain	7.5
Raymond Hills	7.5
Rose Canyon	7.1
San Clemente	7.7
San Gabriel	7.7
San Jacinto	7.5
Santa Susana	6.5
Sierra Madre	6.5
South San Andreas	7.5
Superstition Mountain	7.0

Figure 8-1. San Diego region showing epicenters.

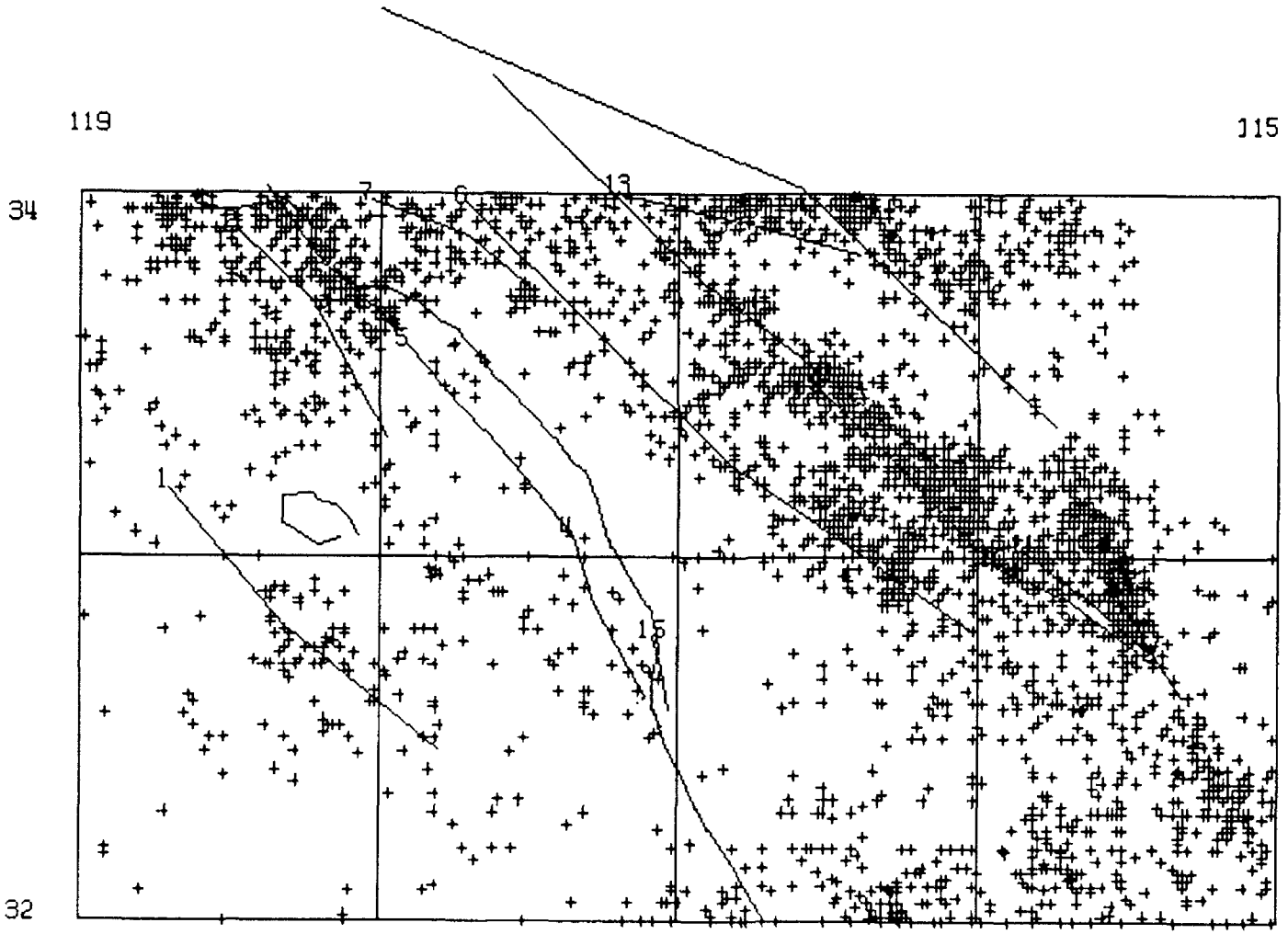

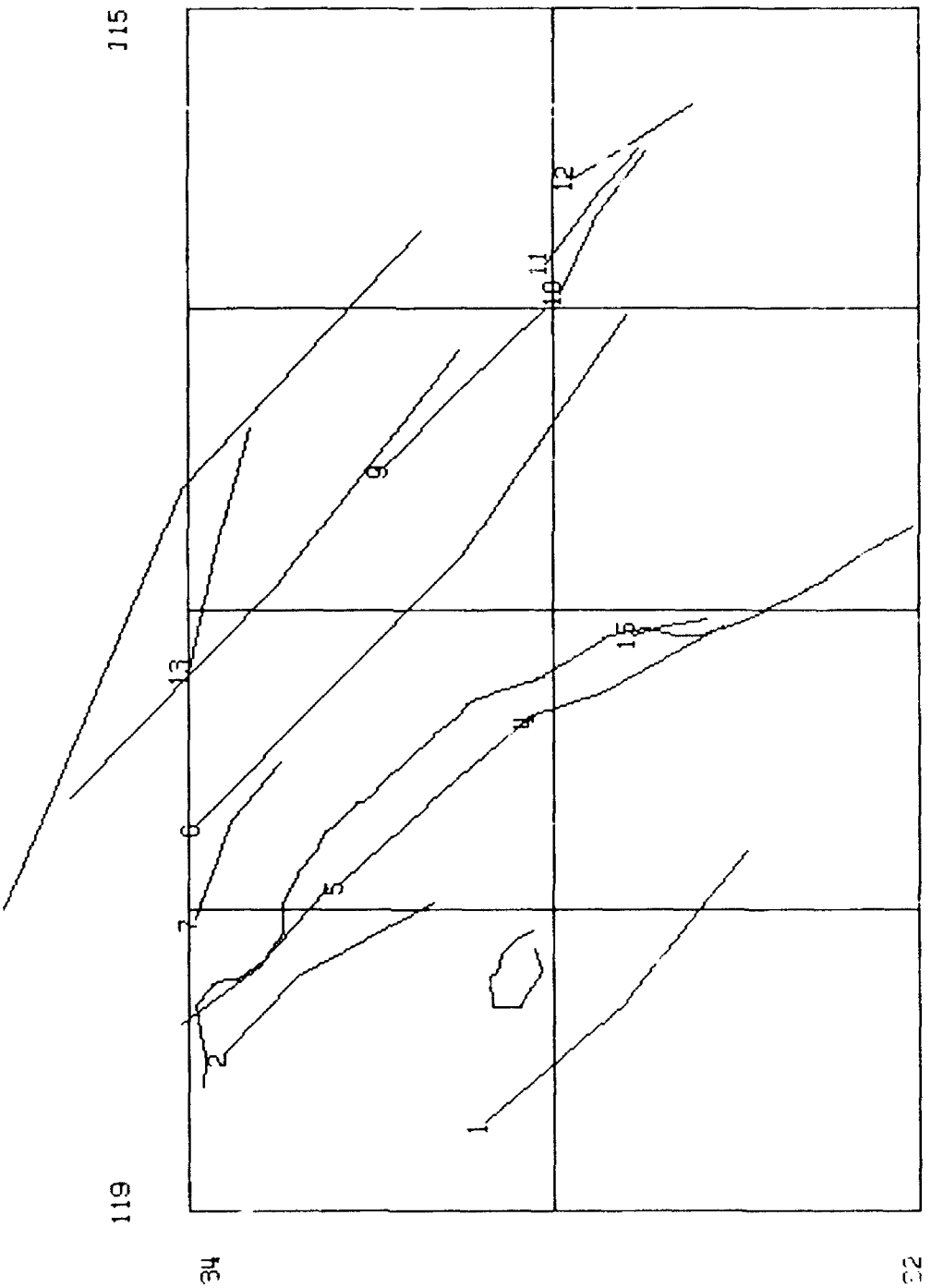

Figure 8-2. San Diego region showing faults.

Figure 8-3. Recurrence plot for La Nacion Fault

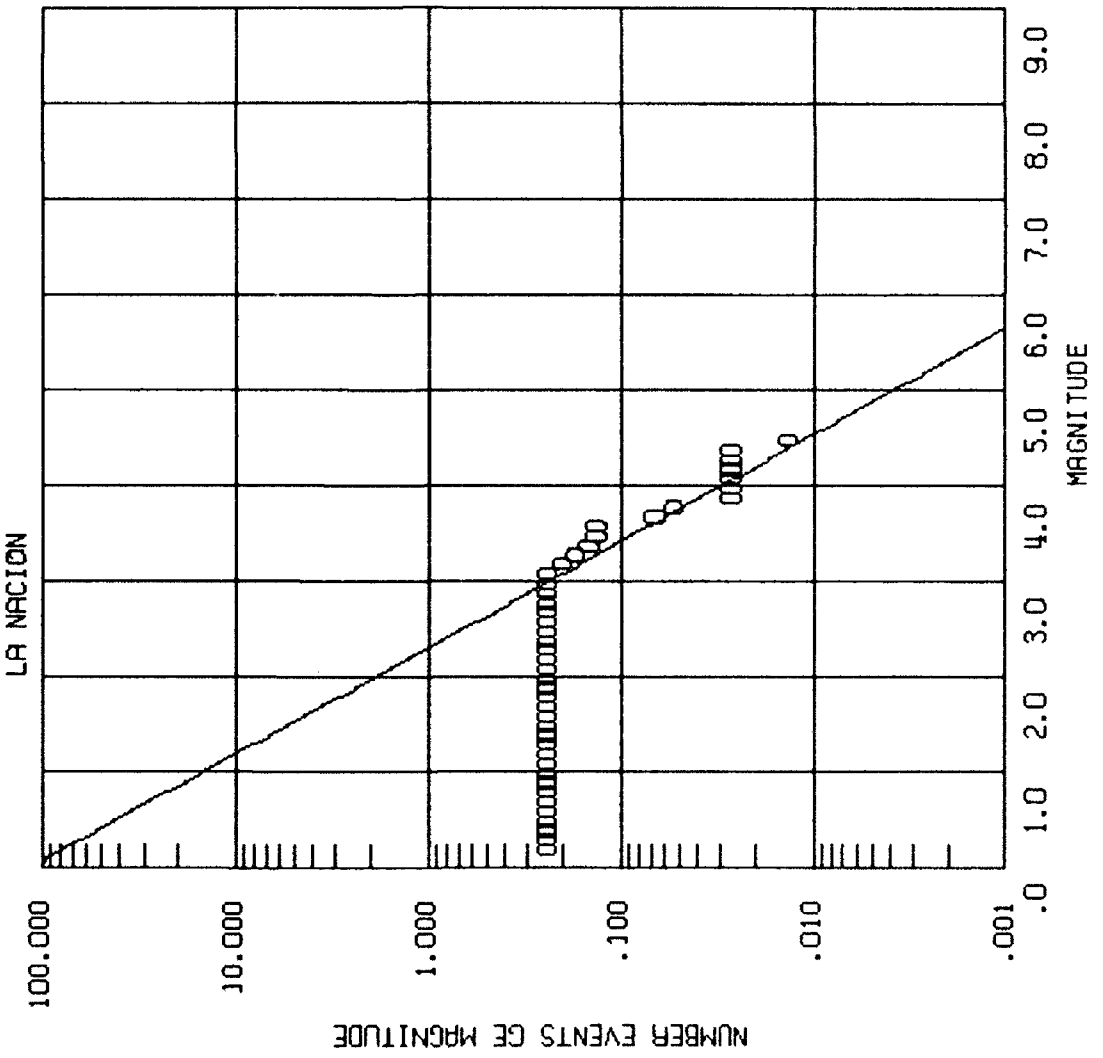

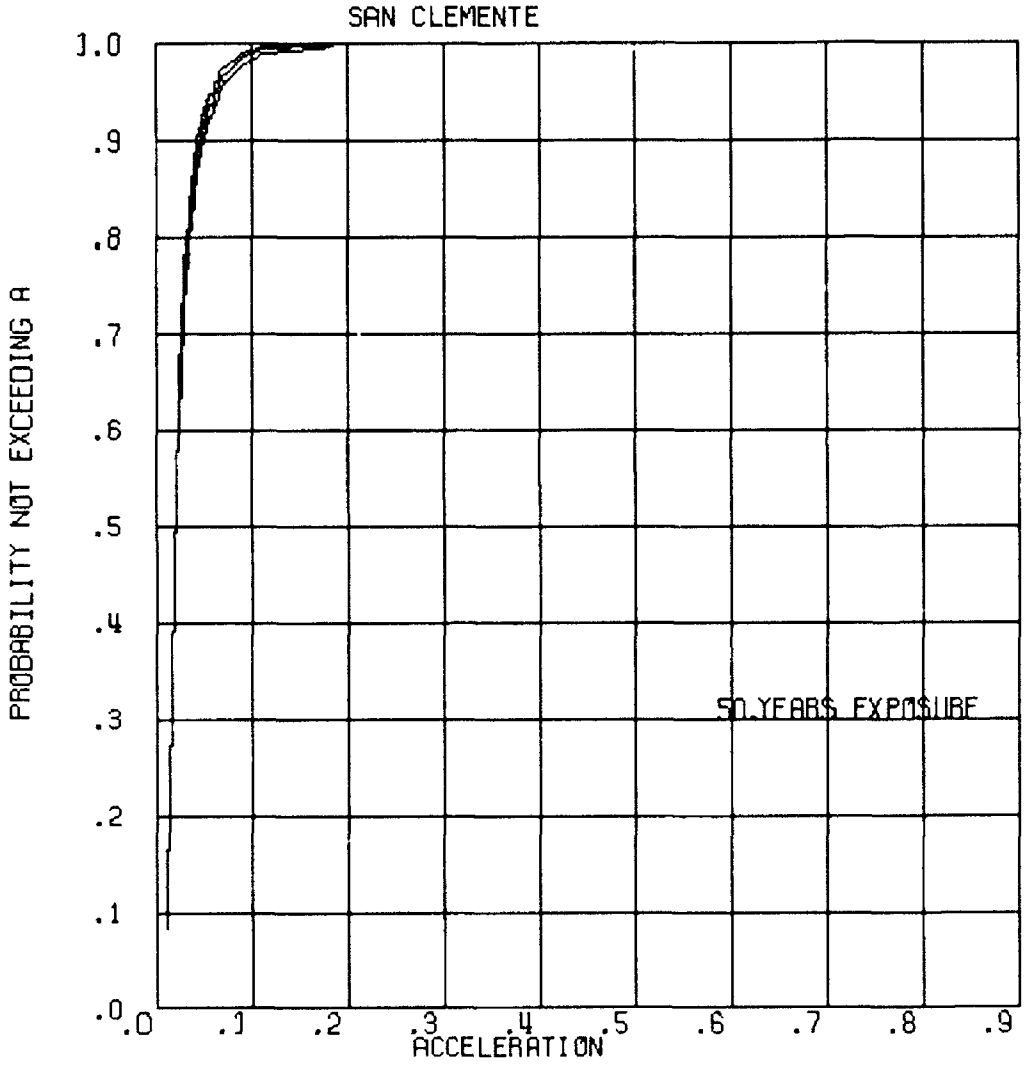

Figure 8-4a.
Fault probability plot.

Figure 8-4b.
Fault probability plot.

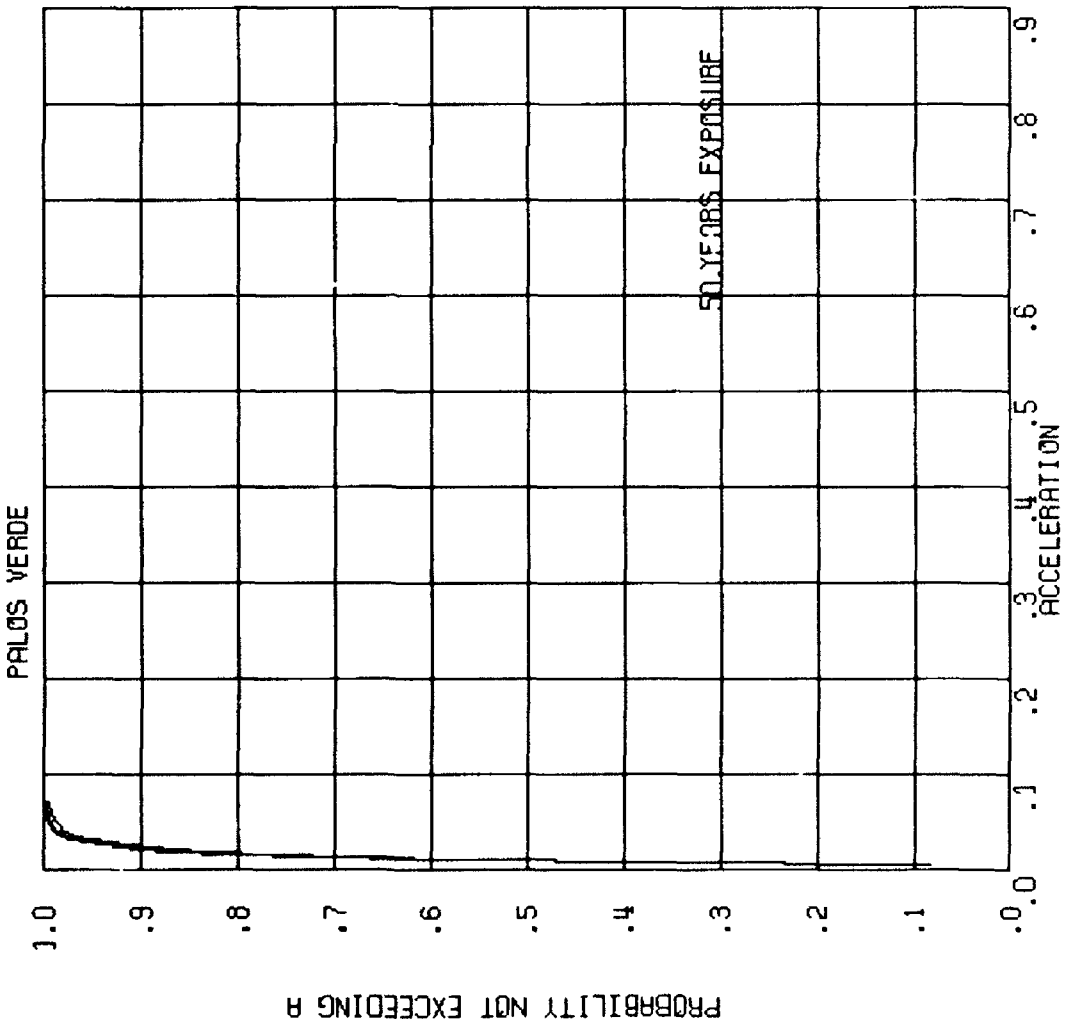

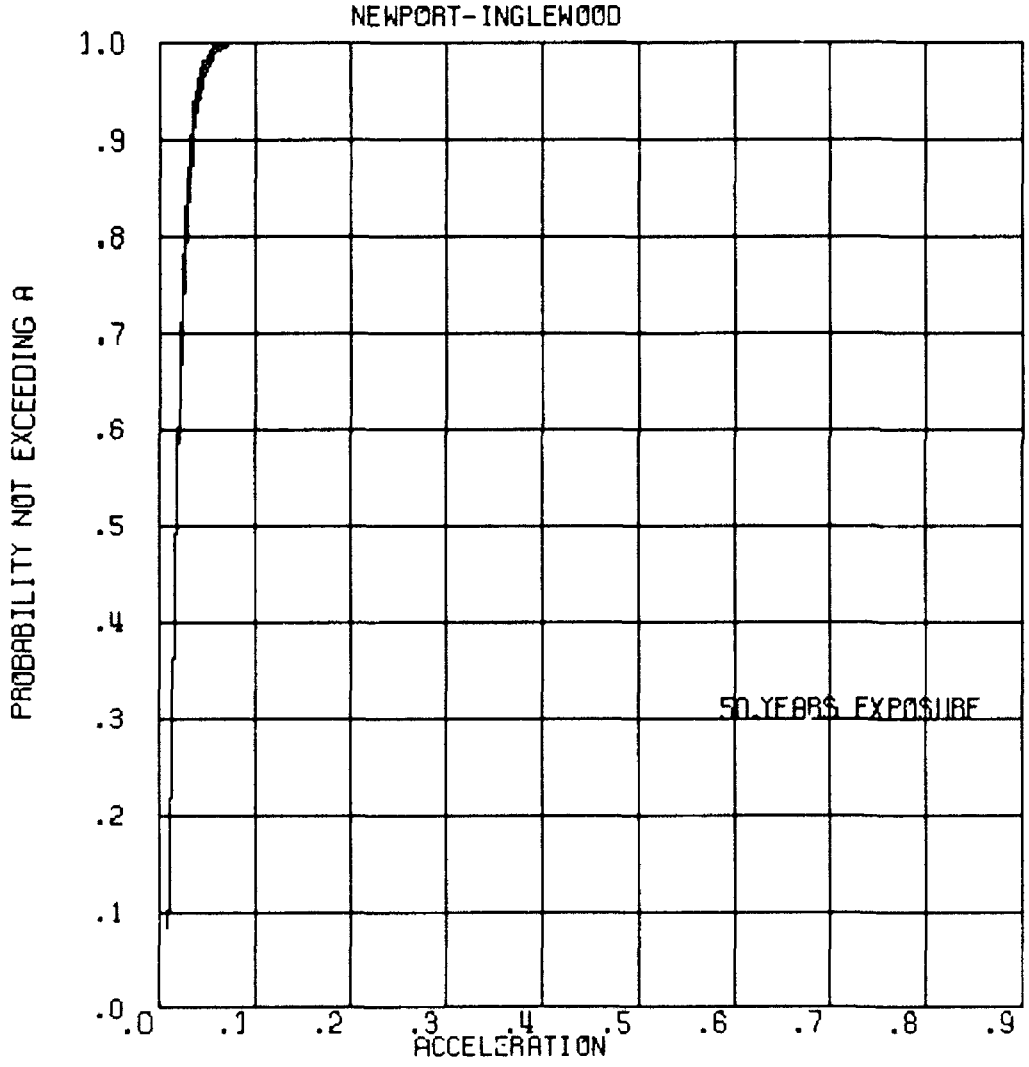

Figure 8-4c.
Fault probability plot.

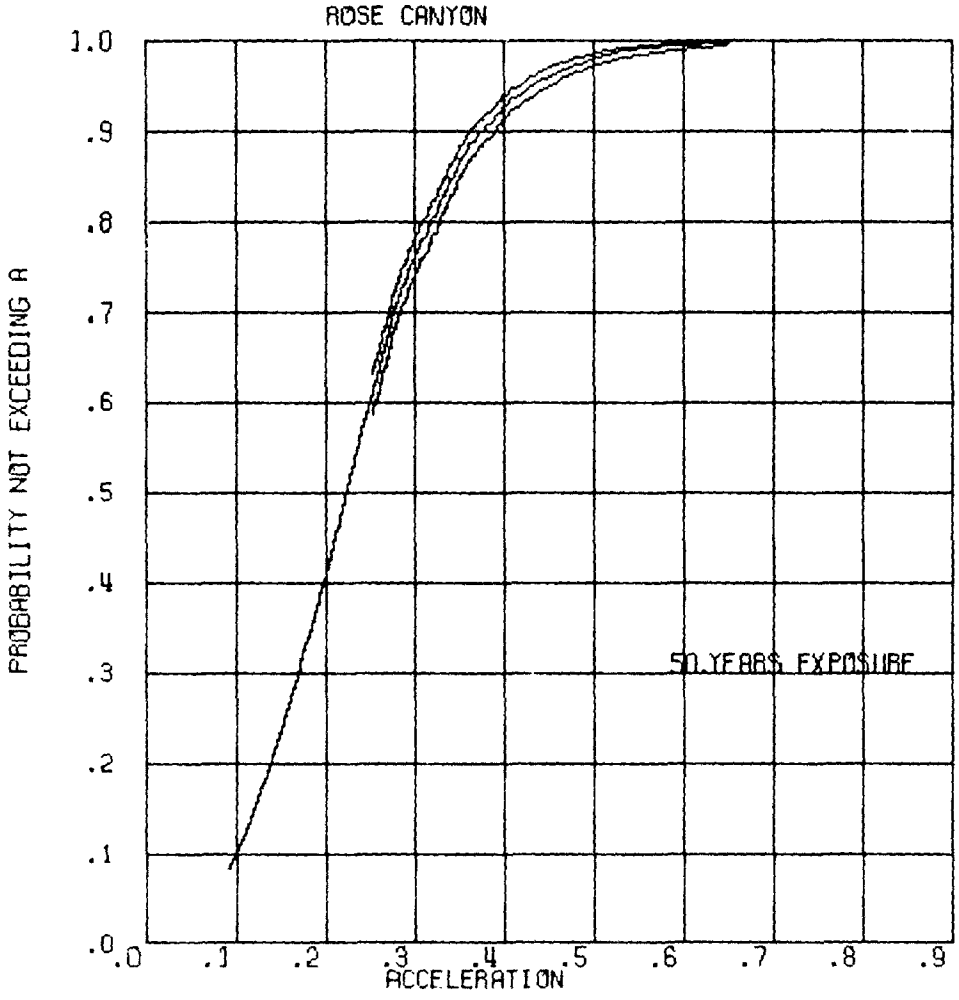

Figure 8-4d.
Fault probability plot.

Figure 8-4e.
Fault probability plot.

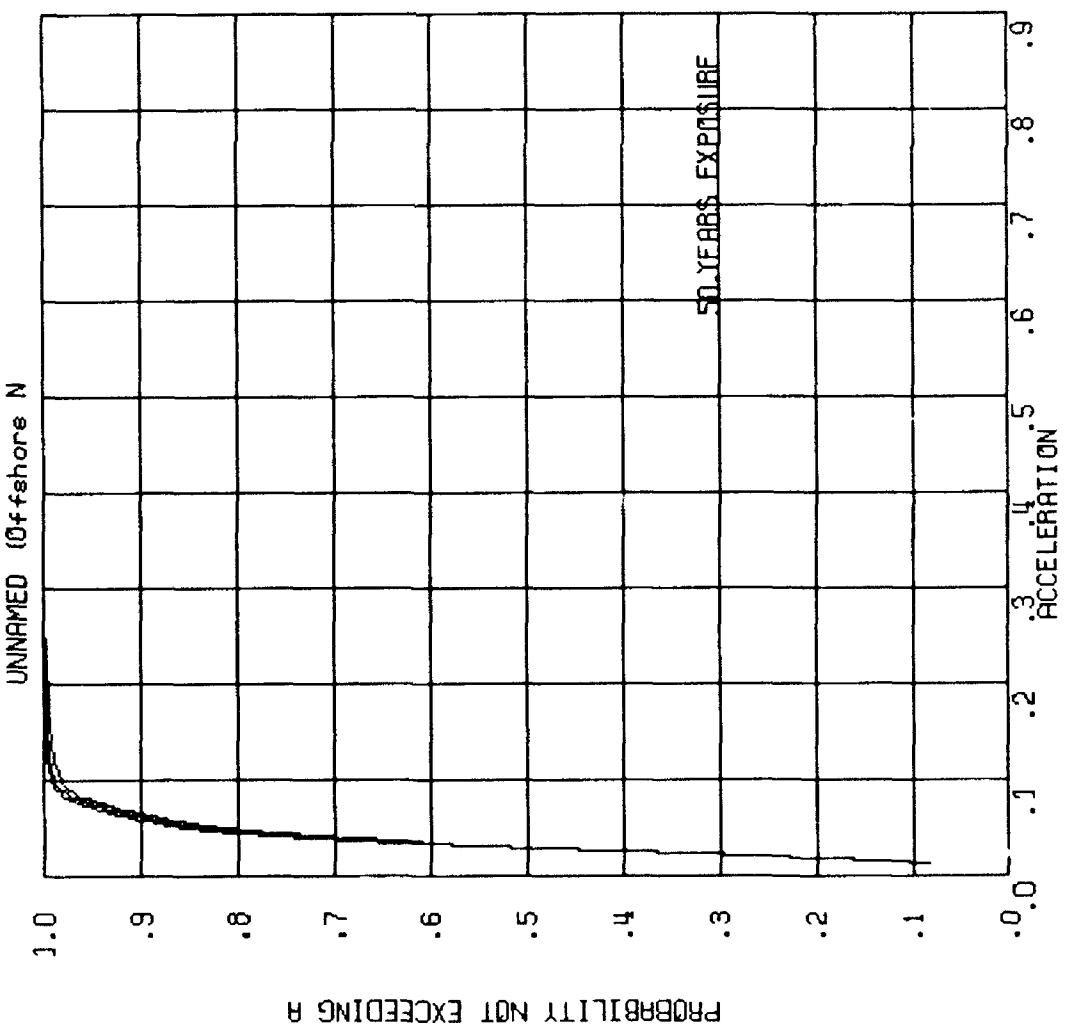

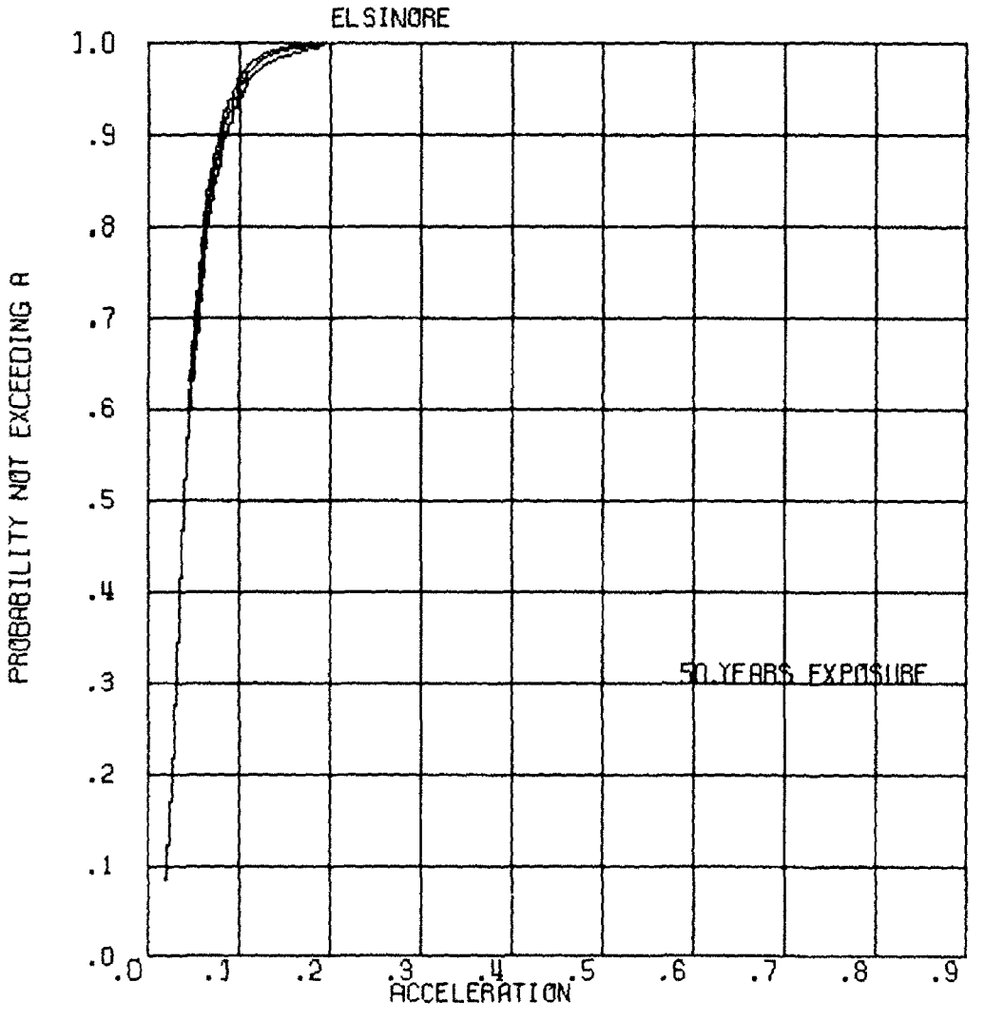

Figure 8-4f.
Fault probability plot.

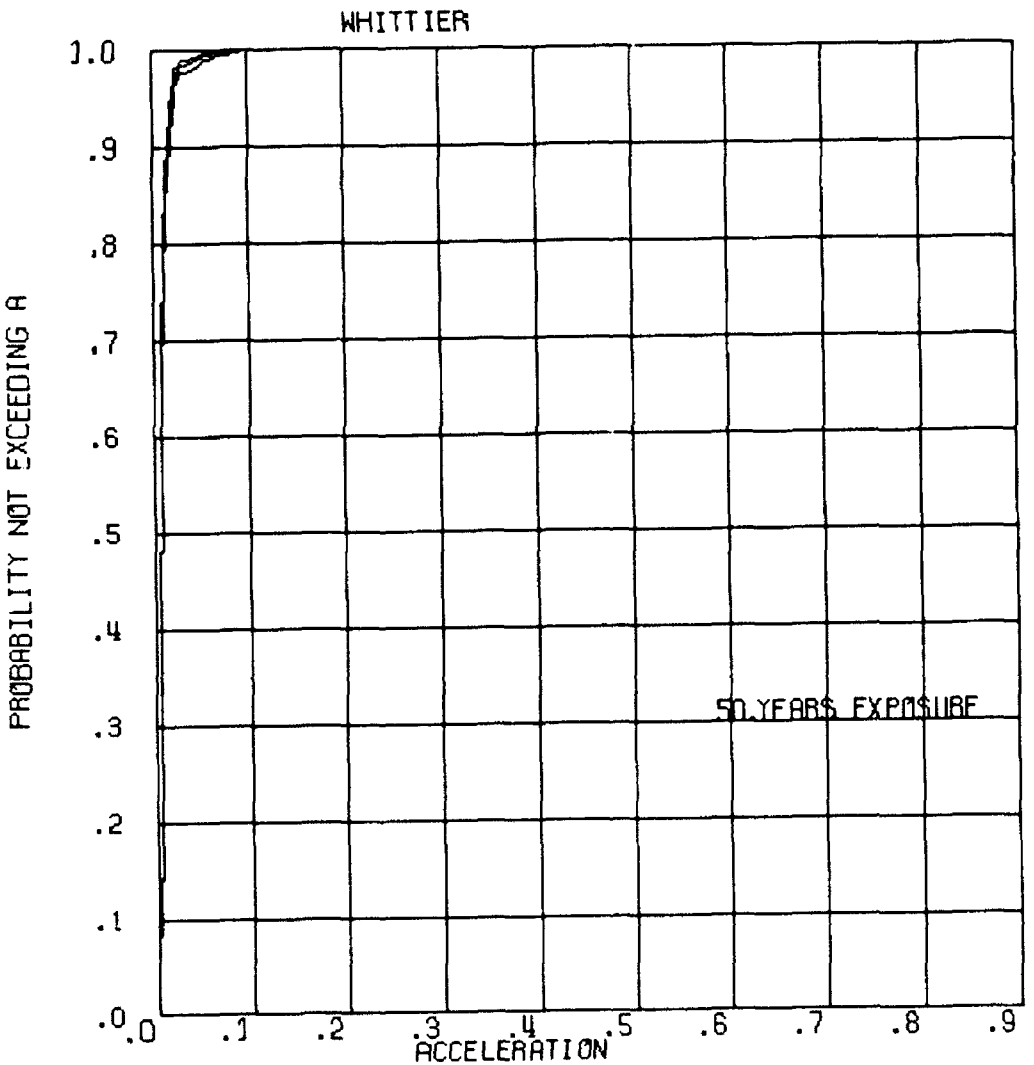

Figure 8-4g.
Fault probability plot.

Figure 8-4h.
Fault probability plot.

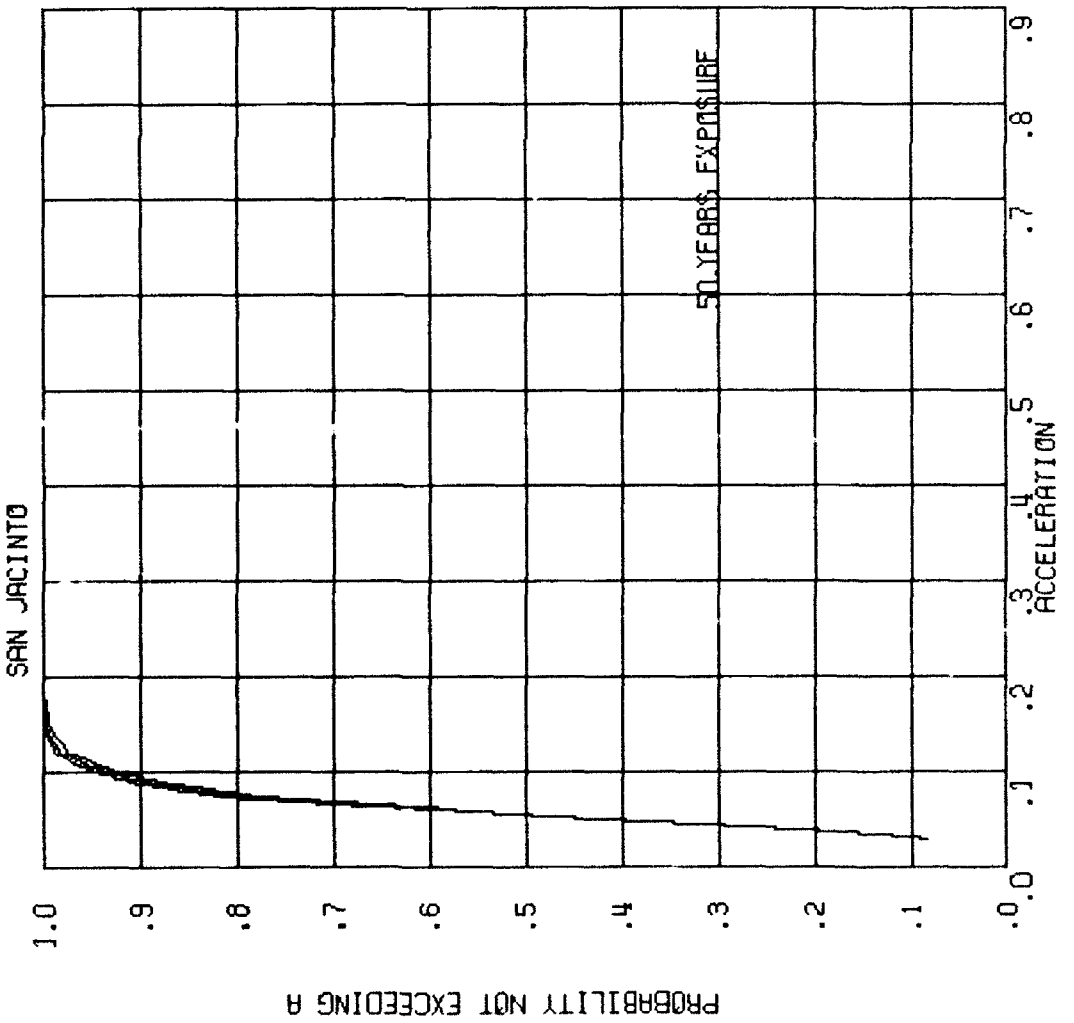

Figure 8-4i
Fault probability plot.

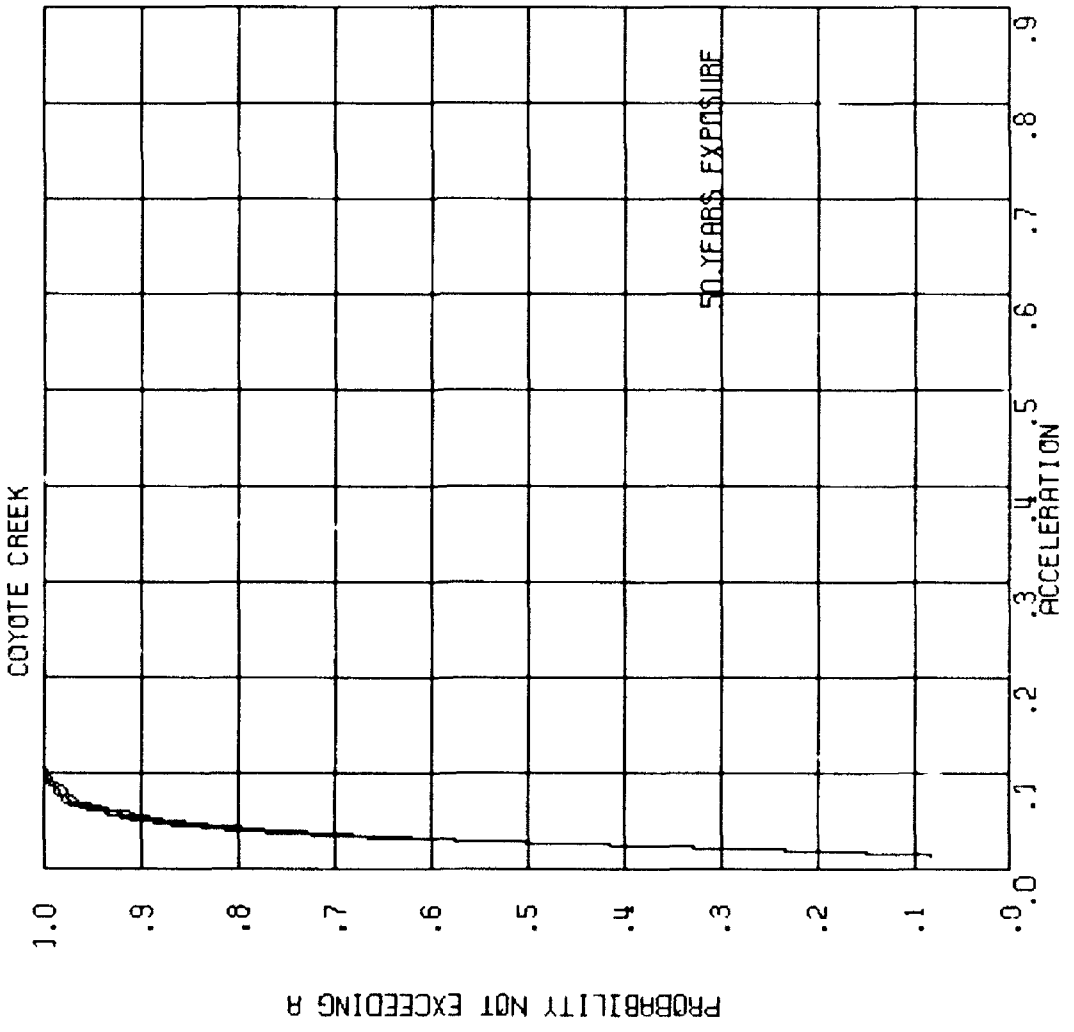

Figure 8-4j
Fault probability plot.

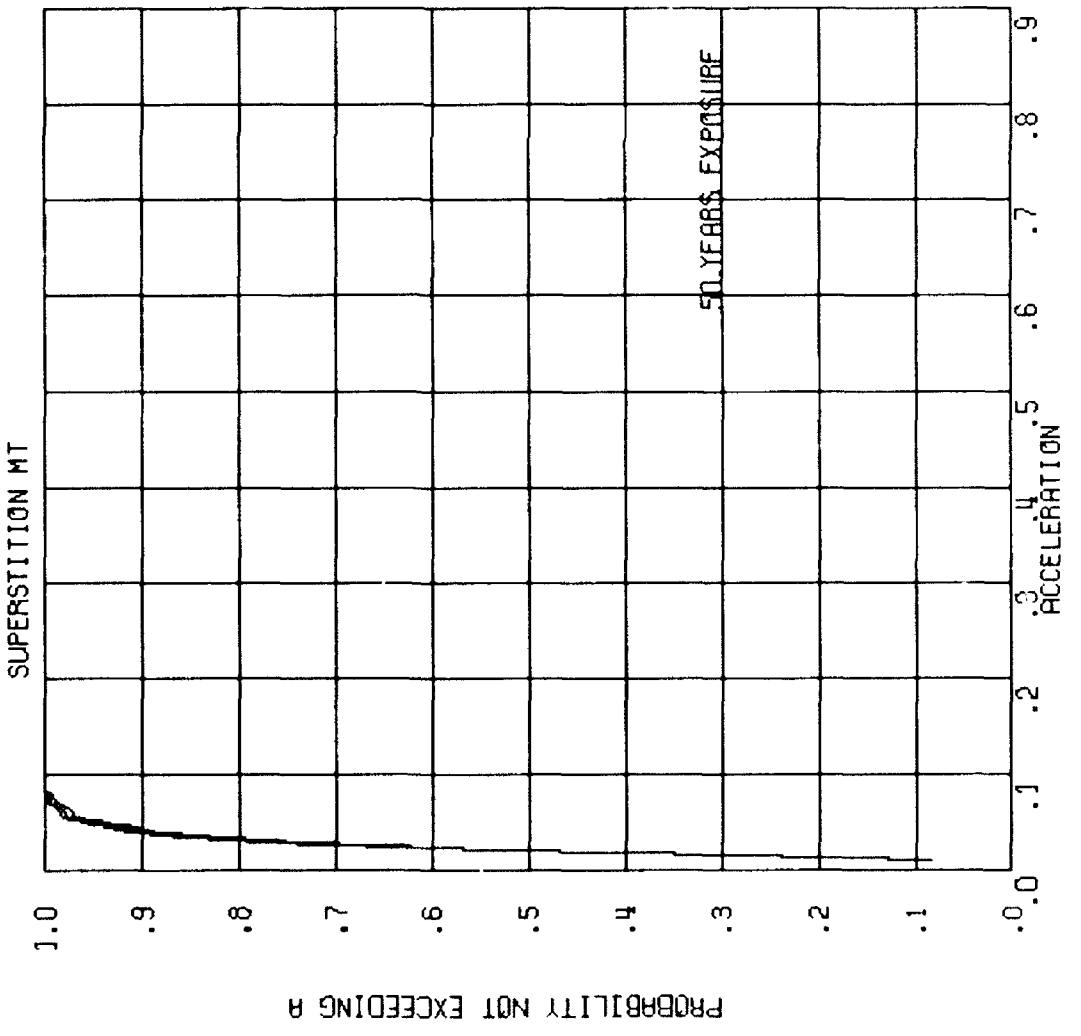

Figure 8-4k
Fault probability plot.

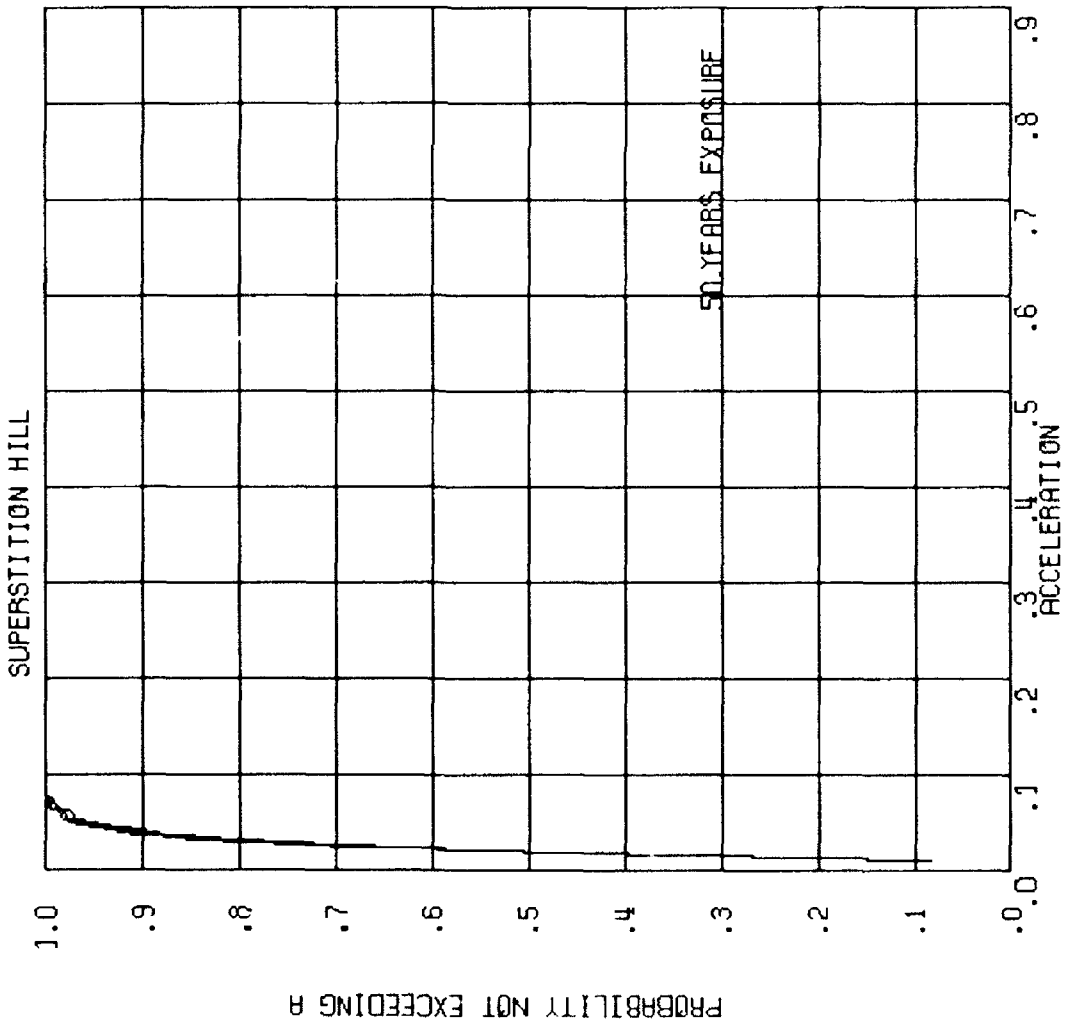

Figure 8-41
Fault probability plot.

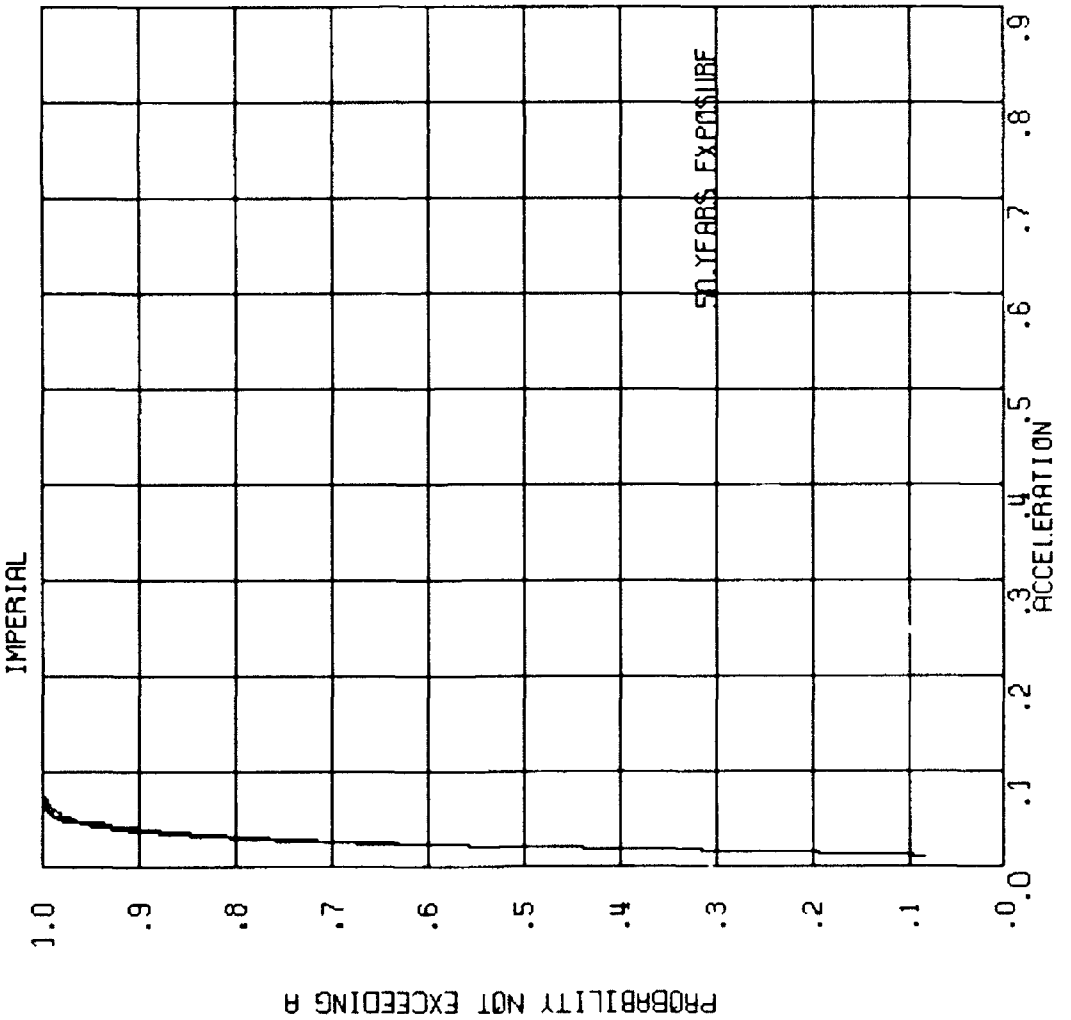

Figure 8-4m.
Fault probability plot.

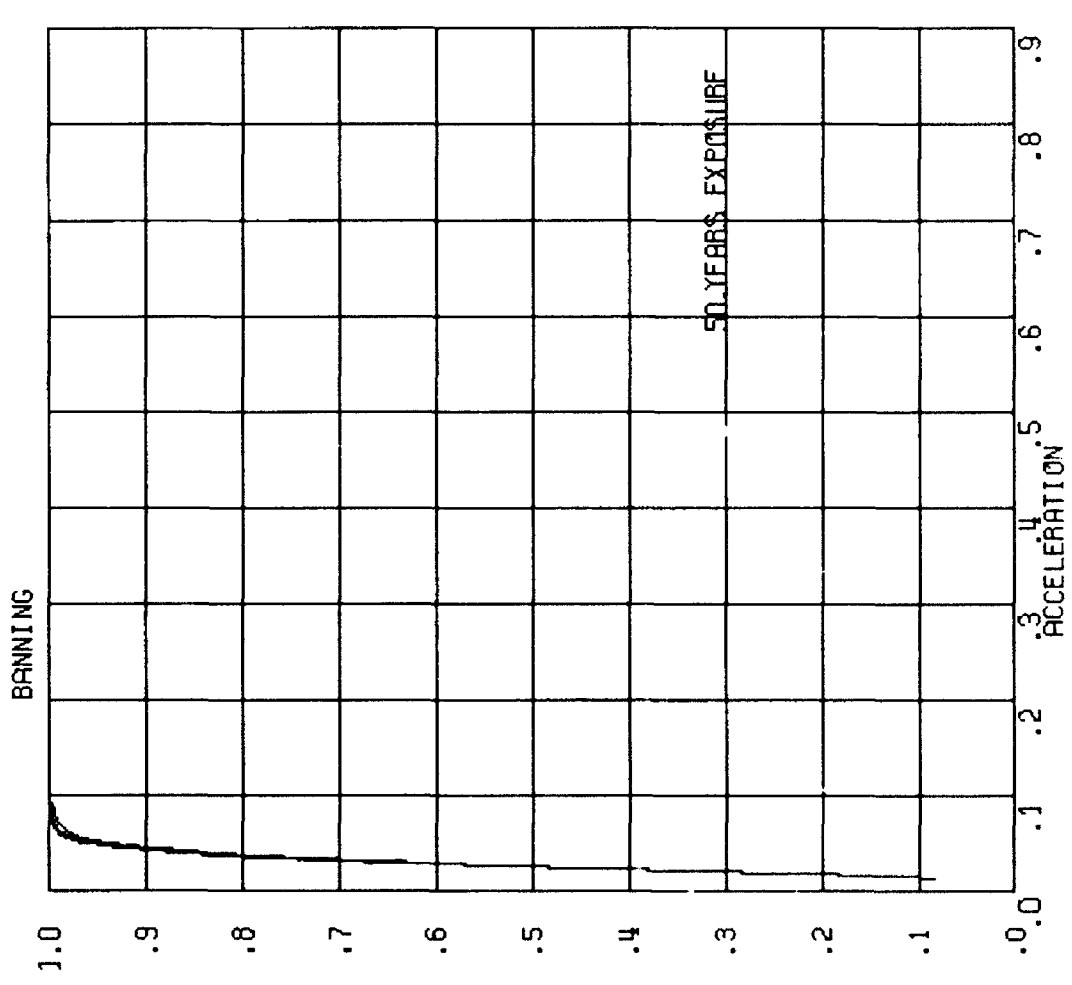

Figure 8-4n.
Fault probability plot.

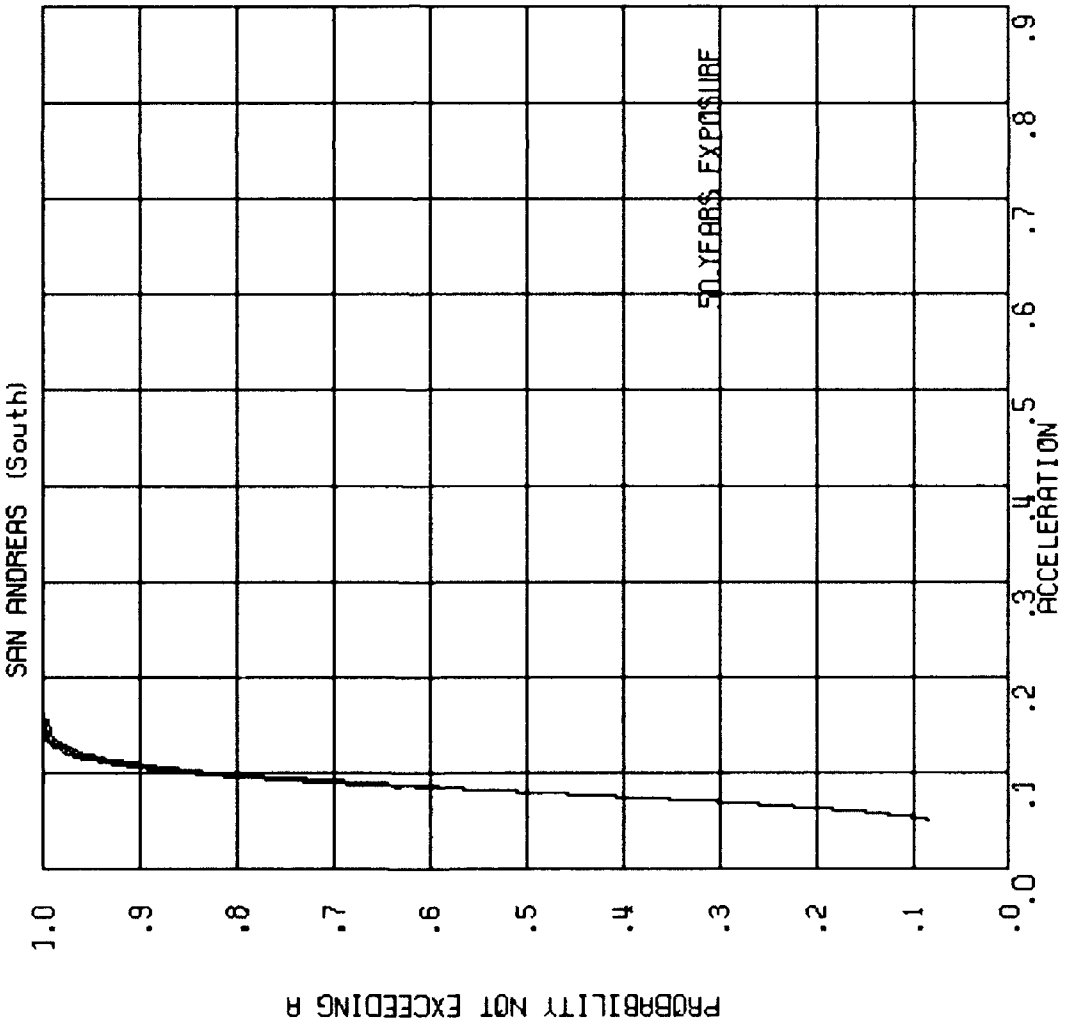

Figure 8-4o.
Fault probability plot.

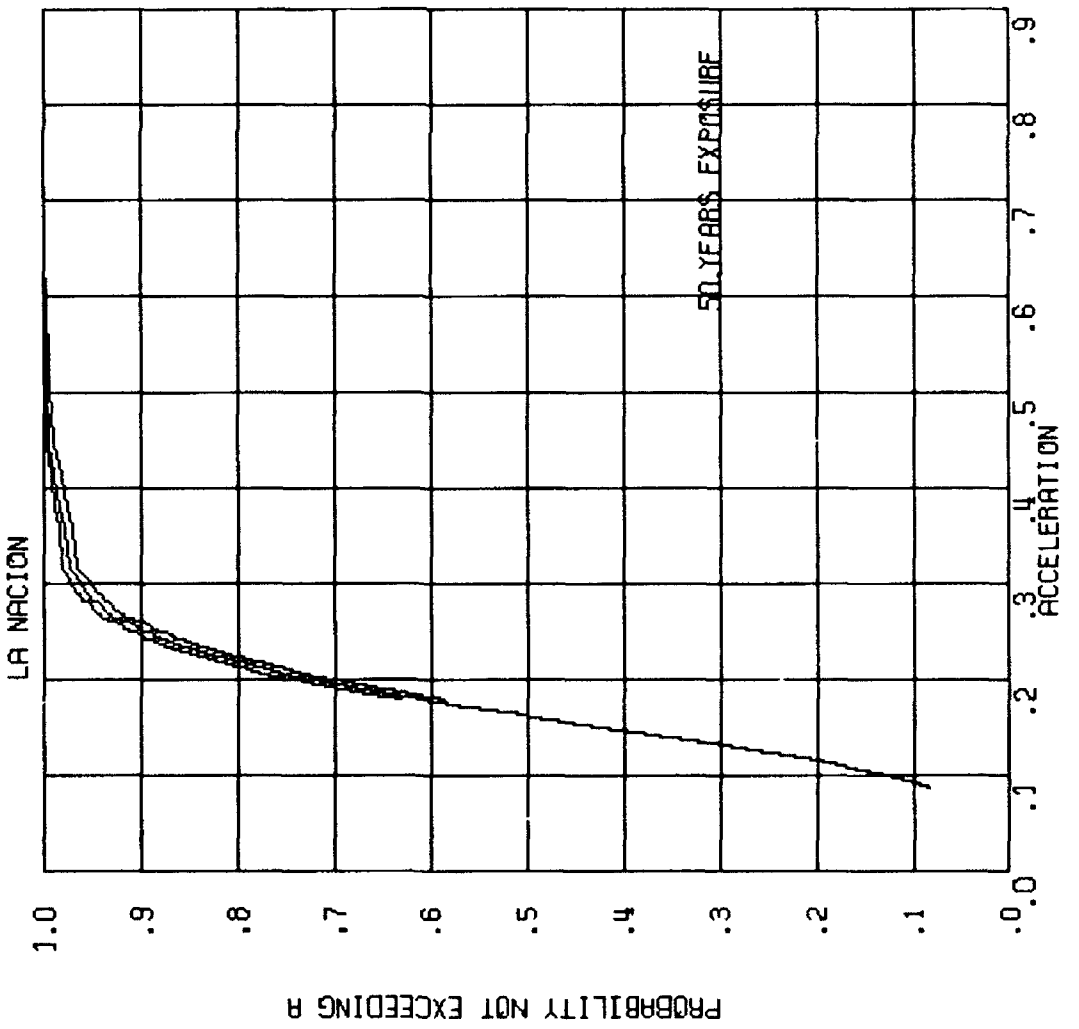

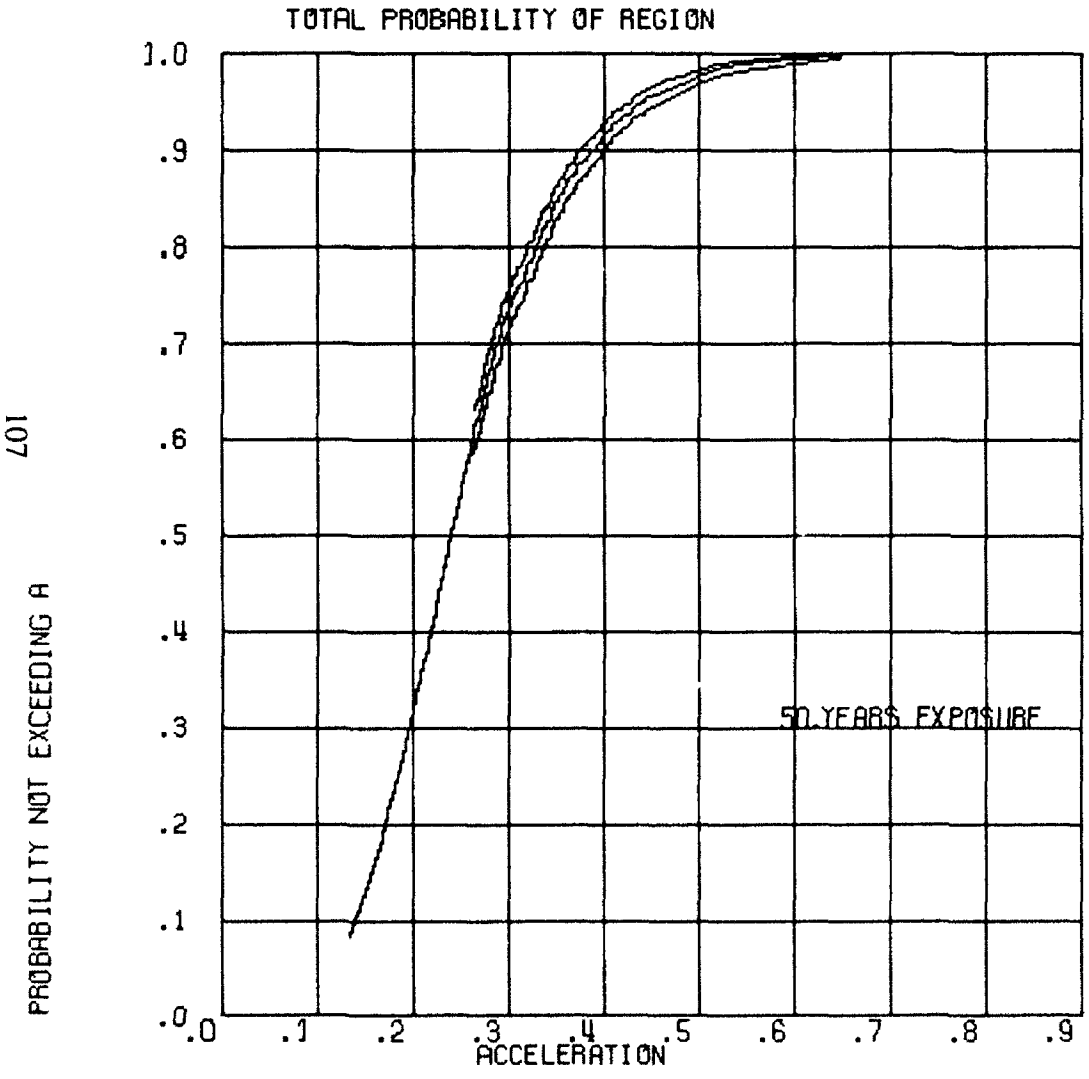

Figure 8-5.
Total Site probability.

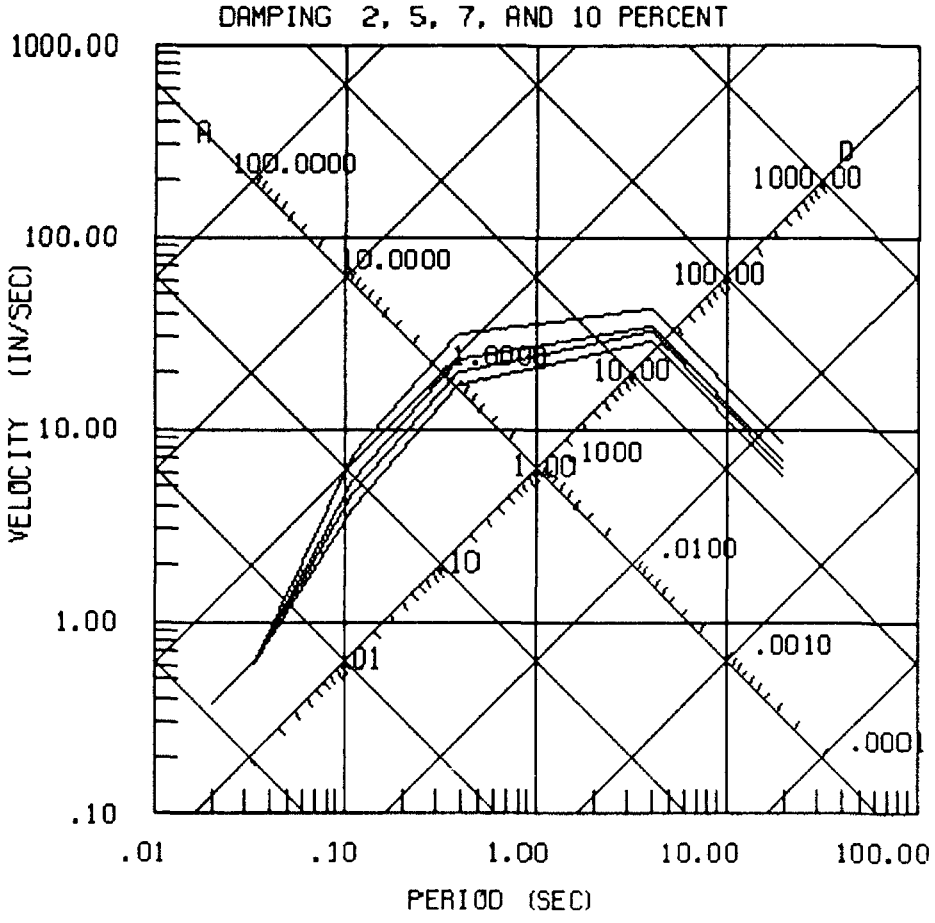

Figure 8-6.
Site independent spectra.

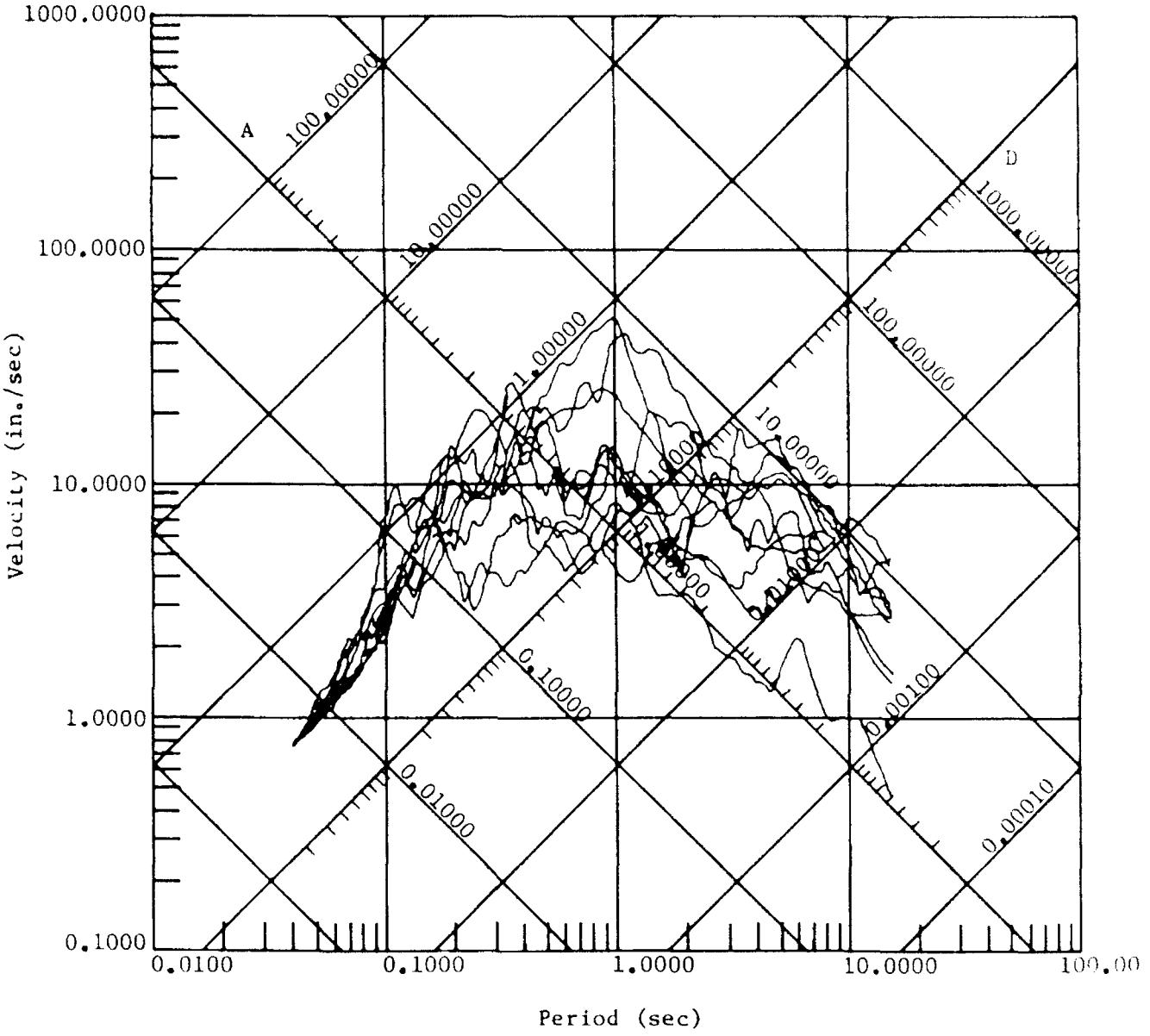

Figure 8-7. Site dependent spectra, 10 closest matching records.

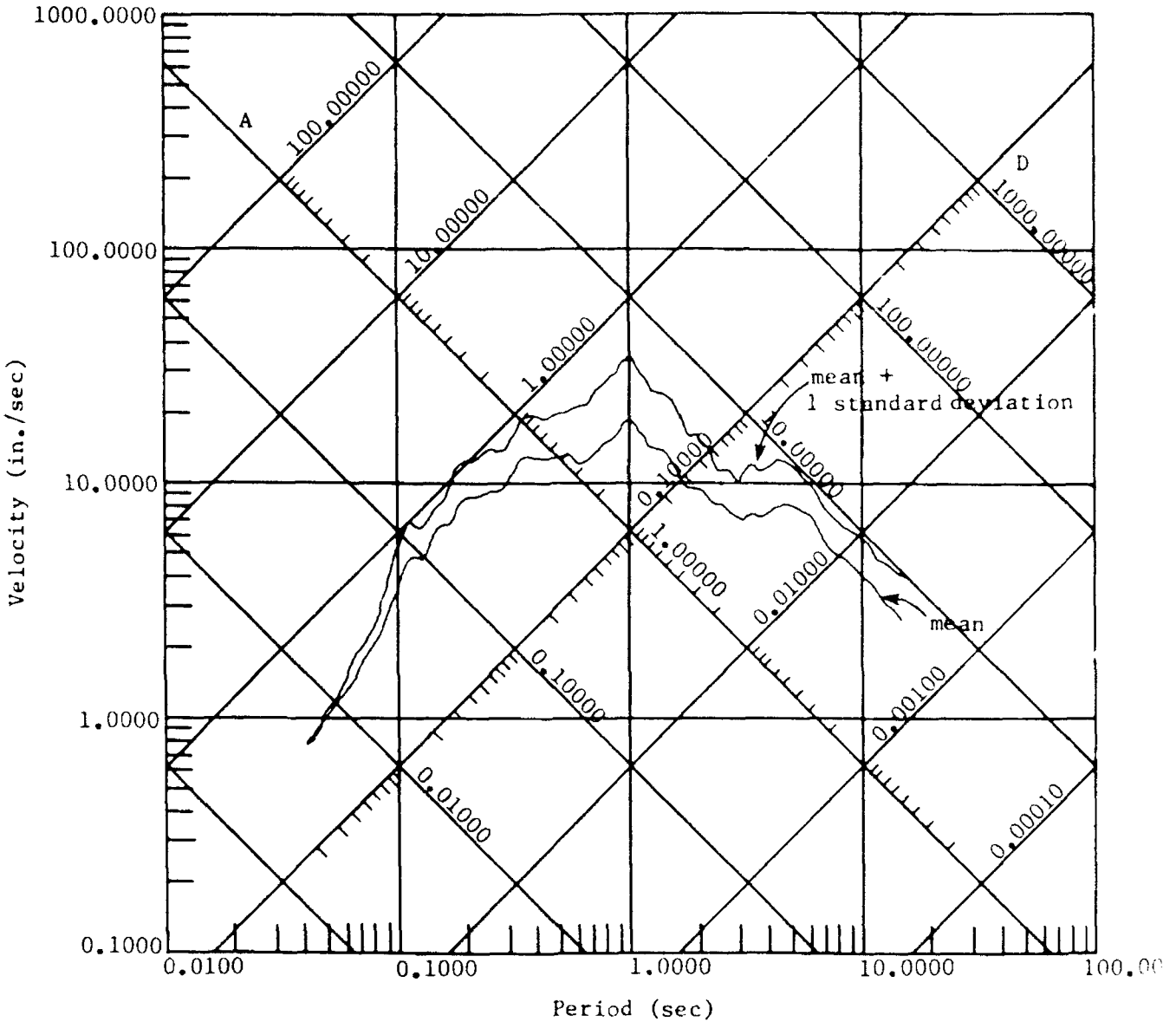

Figure 8-8. Site dependent spectra, mean and mean + 1 std deviation.

CHAPTER 9
SUMMARY

NAVFAC instructions suggest that, in conducting site seismicity studies for key facilities, ground motion and response spectra be defined on a probabilistic basis. However, no procedure was specified by NAVFAC to accomplish this. This project was initiated to provide a procedure and the required software.

An automated procedure has been developed to perform a seismic analysis using available historic data and geologic data. The objective of the seismicity study is to determine the probability of occurrence of acceleration at the site. To do this, site coordinates and the study bounds are specified in terms of latitude and longitude. A regional study is first performed in which all of the historic epicenters are used with an attenuation relationship to compute site acceleration for all historic earthquakes. A regression analysis is performed to obtain regional recurrence coefficients, and a map of epicenters is plotted. The regional recurrence can be used to compute the probability of site acceleration for randomly located events in the study area. Such a condition is used when individual faults are not known well enough to be specified.

Where individual fault areas can be specified, individual subsets of the historic data are used in conjunction with geologic data to determine fault recurrence coefficients; these are used to compute the probability of site acceleration from individual fault sources. The total risk is determined for all faults specified. Confidence bounds are given on the site acceleration as a function of probability of not being exceeded.

The structural design engineer may use either reponse spectra or time history techniques in the analysis of a structure. The data base of recorded accelerograms has been obtained and a program was prepared to search the record of accelerograms, given a desired magnitude event, epicenter-site distance, acceleration level, and soil condition, to determine the closest matching records. The program takes selected response spectra, and scales them, and then computes the mean and standard deviation spectra and the maximum envelope spectrum. The spectra are plotted either in tripartite form or in semilog form. The program also is able to scale, plot, and create files of time history accelerograms for use as input to dynamic finite element programs.

Case studies were conducted to evaluate the procedure. Results compare favorably with results by others.

DISTRIBUTION LIST

1SG/CEEE / LT MARSH, LANGLEY AFB, VA
AF / 438 ABG/DEE (WILSON), MCGUIRE AFB, NJ
AFB / HQ TAC/DEMM (POLLARD), LANGLEY AFB, VA
AFESC / TECH LIB, TYNDALL AFB, FL
AMERICAN CONCRETE / LIB, DETROIT, MI
ARMY / CEHSC-FU-N (KRAJEWSKI), FORT BELVOIR, VA; R&D LAB, STRNC-UE, NATICK, MA
ARMY CECOM R&D TECH LIBRARY / ASNC-ELC-I-T, FORT MONMOUTH, NJ
ARMY CERL / CECER-FME (HAYES), CHAMPAIGN, IL; LIB, CHAMPAIGN, IL
ARMY DEPOT / LETTERKENNY, SDSLE-EN, CHAMBERSBURG, PA
ARMY ENGRG DIST / CENPS-ED-SD, SEATTLE, WA; LIB, PHILADELPHIA, PA; LIB, SEATTLE, WA
ARMY ENGRG DIV / CEEUD-ED-TA (MCVAY), FRANKFURT, GE, APO AE; CEHND-ED-CS, HUNTSVILLE, AL; ED-SY (LOYD), HUNTSVILLE, AL
ARMY EWES / CEWES-CD-P, VICKSBURG, MS; LIB, VICKSBURG, MS; WESCD-P (MELBY), VICKSBURG, MS
ARMY MISSILE R&D CMD / CH, DOCS, SCI INFO CTR, REDSTONE ARSENAL, AL
ARVID GRANT & ASSOC / OLYMPIA, WA
ASO / PWO, PHILADELPHIA, PA; PWP-A, PHILADELPHIA, PA
ATLANTIC RICHFIELD CO / RE SMITH, DALLAS, TX
BATTELLE / D. FRINK, COLUMBUS, OH
BECHTEL CIVIL, INC / K. MARK, SAN FRANCISCO, CA
BEN C GERWICK INC / FOTINOS, SAN FRANCISCO, CA
BETHLEHEM STEEL CO / ENGRG DEPT, BETHLEHEM, PA
BLAYLOCK ENGINEERING GROUP / T SPENCER, SAN DIEGO, CA
BRITISH EMBASSY / SCI & TECH DEPT (WILKINS), WASHINGTON, DC
BROWN, ROBERT / TUSCALOOSA, AL
BULLOCK, TE / LA CANADA, CA
BUREAU OF RECLAMATION / D-1512 (GS DEPUY), DENVER, CO
CAL STATE UNIV / C.V. CHELAPATI, LONG BEACH, CA
CASE WESTERN RESERVE UNIV / CE DEPT (PERDIKARIS), CLEVELAND, OH
CBC / CODE 430, GULFPORT, MS; PWO (CODE 400), GULFPORT, MS
CESO / CODE 155, PORT HUENEME, CA
CHAO, JC / HOUSTON, TX
CHEE, WINSTON / GRETNA, LA
CHESNAVFACENGCOM / CODE 112.1, WASHINGTON, DC; CODE 402 (FRANCIS), WASHINGTON, DC; CODE 407, WASHINGTON, DC; YACHNIS, WASHINGTON, DC
CHEVRON OIL FLD RSCH CO / ALLENDER, LA HABRA, CA
CHILDS ENGRG CORP / K.M. CHILDS, JR., MEDFIELD, MA
CITY OF SACRAMENTO / GEN SVCS DEPT, SACRAMENTO, CA
CITY OF WINSTON-SALEM / RJ ROGERS, PWD, WINSTON SALEM, NC
CLARK, T. / SAN MATEO, CA
CLARKSON UNIV / CEE DEPT, POTSDAM, NY
COGUARD / SUPERINTENDENT, NEW LONDON, CT
COLLEGE OF ENGINEERING / CE DEPT (GRACE), SOUTHFIELD, MI
COLLINS ENGRG, INC / M GARLICH, CHICAGO, IL
COLORADO STATE UNIV / CE DEPT (CRISWELL), FORT COLLINS, CO
COMCBLANT / CODE S3T, NORFOLK, VA
COMFLEACT / PWO, FPO AP

COMNAVSURF / CODE N42A, NORFOLK, VA
CONRAD ASSOC / LUISONI, VAN NUYS, CA
CONSOER TOWNSEND & ASSOC / DEBIAK, CHICAGO, IL
CONSTRUCTION TECH LABS, INC / G. CORLEY, SKOKIE, IL
CORNELL UNIV / CIVIL & ENVIRON ENGRG, ITHACA, NY; LIB, ITHACA, NY
DAMES & MOORE / LIB, LOS ANGELES, CA
DAVY DRAVO / WRIGHT, PITTSBURG, PA
DELAWARE / EMERGENCY MGMT, DELAWARE CITY, DE
DEPT OF BOATING / ARMSTRONG, SACRAMENTO, CA
DEPT OF STATE / FOREIGN BLDGS OPS, BDE-ESB, ARLINGTON, VA
DFSC-F / ALEXANDRIA, VA
DOBROWOLSKI, JA / ALTADENA, CA
DOD / EXPLOS SAFETY BRD, ALEXANDRIA, VA
DTRCEN / CODE 172, BETHESDA, MD
EDWARD K NODA & ASSOC / HONOLULU, HI
ENGINEERING DATA MANAGEMENT / RONALD W. ANTHONY, FORT COLLINS, CO
ESCO SCIENTIFIC PRODUCTS (ASIA) / PTE LTD, CHAI
FAA / ARD 200, WASHINGTON, DC
FACILITIES DEPT / FACILITIES OFFICER, FPO AP
FLORIDA ATLANTIC UNIV / OCEAN ENGRG DEPT (MARTIN), BOCA RATON, FL; OCEAN ENGRG DEPT (SU), BOCA RATON, FL
GEI CONSULTANTS, INC. / T.C. DUNN, WINCHESTER, MA
GEIGER ENGINEERS / FUNSTON, BELLINGHAM, WA
GEOCON INC / CORLEY, SAN DIEGO, CA
GEORGE WASHINGTON UNIV / ENGRG & APP SCI SCHL (FOX), WASHINGTON, DC
GEORGIA INST OF TECH / CE SCHL (KAHN), ATLANTA, GA; CE SCHL (SWANGER), ATLANTA, GA; CE SCHL (ZURUCK), ATLANTA, GA
GERWICK, BEN / SAN FRANCISCO, CA
GIORDANO, A.J. / SEWELL, NJ
GRUMMAN AEROSPACE CORP / TECH INFO CENTER, BETHPAGE, NY
GSA / HALL, WASHINGTON, DC
HAN-PADRON ASSOCIATES / DENNIS PADRON, NEW YORK, NY
HARDY, S.P. / SAN RAMON, CA
HARTFORD STEAM BOILER INSP & INS CO / SPINELLI, HARTFORD, CT
HAYNES & ASSOC / H. HAYNES, PE, OAKLAND, CA
HAYNES, B / LYNDEN, WA
HEUZE, F / ALAMO, CA
HJ DEGENKOLB ASSOC / W. MURDOUGH, SAN FRANCISCO, CA
HOIDRA / NEW YORK, NY
HOPE ARCHTS & ENGRS / SAN DIEGO, CA
HQ AFLC / CAPT SCHMIDT, WRIGHT PATTERSON AFB, OH
HUGHES AIRCRAFT CO / TECH DOC CEN, EL SEGUNDO, CA
INFOTEAM INC / M. ALLEN, PLANTATION, FL
INST OF MARINE SCIENCES / LIB, PORT ARANSAS, TX
INTL MARITIME, INC / D. WALSH, SAN PEDRO, CA
JOHN HOPKINS UNIV / CE DEPT, JONES, BALTIMORE, MD
JOHN J MC MULLEN ASSOC / LIB, NEW YORK, NY
KAISER PERMANENTE MEDCIAL CARE PROGRAM / OAKLAND, CA
LAWRENCE LIVERMORE NATL LAB / FJ TOKARZ, LIVERMORE, CA; PLANT ENGRG LIB (L-654), LIVERMORE, CA
LEO A DALY CO / HONOLULU, HI
LIN OFFSHORE ENGRG / P. CHOW, SAN FRANCISCO, CA

LONG BEACH PORT / ENGRG DIR (ALLEN), LONG BEACH, CA; ENGRG DIR (LUZZI), LONG BEACH, CA
MARATHON OIL CO / GAMBLE, HOUSTON, TX
MARCORBASE / CODE 4.01, CAMP PENDLETON, CA; CODE 406, CAMP LEJEUNE, NC; FACILITIES COORDINATOR, CAMP PENDLETON, CA; PAC, PWO, FPO AP
MARITECH ENGRG / DONOGHUE, AUSTIN, TX
MCAS / CODE 1JE.50 (ISAACS), SANTA ANA, CA; CODE LE, CHERRY POINT, NC
MCRD / PWO, SAN DIEGO, CA
MICHIGAN TECH UNIV / CO DEPT (HAAS), HOUGHTON, MI
MOBIL R&D CORP / OFFSHORE ENGRG LIB, DALLAS, TX
MT DAVISSON / CE, SAVOY, IL
NAF / ENGRG DIV, PWD, FPO AP; PWO, FPO AP
NAS / CHASE FLD, PWO, BEEVILLE, TX; CODE 18300, LEMOORE, CA; CODE 421, SAN DIEGO, CA; CODE 8, PATUXENT RIVER, MD; CODE 85GC, GLENVIEW, IL; DIR, ENGRG DIV, PWD, KEFLAVIK, ICELAND, FPO AE; FAC MGMT OFFC, ALAMEDA, CA; MIRAMAR, SAN DIEGO, CA; MIRAMAR, PWO, SAN DIEGO, CA; PWO, KEY WEST, FL; PWO, CECIL FIELD, FL; PWO, SIGONELLA, ITALY, FPO AE; SCE, FPO AP; SCE, BARBERS POINT, HI; WHITING FLD, PWO, MILTON, FL
NAS OCEANA / ADAMETZ, VIRGINIA BEACH, VA
NAVAIRDEVCEN / CODE 832, WARMINSTER, PA
NAVAVNDEPOT / CODE 640, PENSACOLA, FL
NAVCOASTSYSCEN / PWO (CODE 740), PANAMA CITY, FL
NAVCOMMSTA / PWO, FPO AP
NAVEODTECHCEN / TECH LIB, INDIAN HEAD, MD
NAVFAC / PWO (CODE 50), BRAWDY WALES, UK, FPO AE; PWO, OAK HARBOR, WA
NAVFACENGCOM / CODE 04A3, ALEXANDRIA, VA; CODE 07, ALEXANDRIA, VA; CODE 07M (BENDER), ALEXANDRIA, VA
NAVMAG / SCE, FPO AP
NAVMEDCOM / NWREG, FAC ENGR, PWD, OAKLAND, CA
NAVOCEANO / CODE 6200 (M PAIGE), NSTL, MS
NAVPGSCOL / PWO, MONTEREY, CA
NAVPHIBASE / PWO, NORFOLK, VA; SCE, SAN DIEGO, CA
NAVSCOLCECOFF / CODE C35, PORT HUENEME, CA
NAVSCSCOL / PWO, ATHENS, GA
NAVSECGRUACT / CODE 31 PWO, FPO AA
NAVSHIPREFAC / LIB, FPO AP
NAVSHIPREPFAC / SCE, FPO AP
NAVSHIPYD / CODE 244.13, LONG BEACH, CA; CODE 440, PORTSMOUTH, VA; MARE IS, PWO, VALLEJO, CA; TECH LIB, PORTSMOUTH, NH
NAVSTA / CODE N4214, MAYPORT, FL; ENGR DIV, PWD, FPO AA; ENGRG DIR, PWD, ROTA, SPAIN, FPO AE
NAVSTA PANAMA CANAL / CODE 54, FPO AA
NAVSUPACT / CODE 430, NEW ORLEANS, LA
NAVSUPPACT / PWO, NAPLES, ITALY, FPO AE
NAVSUPSYSCOM / CODE 0622, WASHINGTON, DC
NAVSWC / CODE W41C1, DAHLGREN, VA
NAVWPNCEN / PWO (CODE 266), CHINA LAKE, CA
NAVWPNSTA / CODE 092B (HUNT), YORKTOWN, VA; CODE 104, CHARLESTON, SC; PWO, YORKTOWN, VA
NCCOSC / CODE 9642, SAN DIEGO, CA
NEESA / CODE 111E (MCCLAINE), PORT HUENEME, CA
NEW MEXICO SOLAR ENERGY INST / LAS CRUCES, NM

NEW ZEALAND CONCRETE RSCH ASSN / LIB, PORIRUA
NIEDORODA, AW / GAINESVILLE, FL
NOAA / JOSEPH VADUS, ROCKVILLE, MD
NORTHNAVFACENGCOM / CO, PHILADELPHIA, PA
NRL / CODE 4670, WASHINGTON, DC
NSY / CODE 214.3 (WEBER), PORTSMOUTH, VA
NUHN & ASSOC / A.C. NUHN, WAYZATA, NM
NUSC DET / CODE 2143 (VARLEY), NEW LONDON, CT; CODE 44 (MUNN), NEW LONDON, CT; CODE TA131, NEW LONDON, CT; LIB, NEWPORT, RI; PWO, NEW LONDON, CT
OICC / ENGR AND CONST DEPT, APO AE
OMEGA MARINE, INC. / SCHULZE, LIBRARIAN, HOUSTON, TX
OREGON STATE UNIV / CE DEPT (HICKS), CORVALLIS, OR
PACIFIC MARINE TECH / M. WAGNER, DUVALL, WA
PACNAVFACENGCOM / CODE 102, PEARL HARBOR, HI
PENNSYLVANIA STATE UNIV / GOTOLSKI, UNIVERSITY PARK, PA; RSCH LAB, STATE COLLEGE, PA
PERKOWSKI, MICHAEL T. / TIPPECANOE, OH
PILE BUCK, INC / SMOOT, JUPITER, FL
PMB ENGRG / LUNDBERG, SAN FRANCISCO, CA
PMTC / CODE 1018, POINT MUGU, CA; CODE 5041, POINT MUGU, CA; CODE P4234 (G. NUSSEAR), POINT MUGU, CA
PORTLAND CEMENT ASSOC / AE FIORATO, SKOKIE, IL
PORTLAND STATE UNIV / ENGRG DEPT (MIGLIORI), PORTLAND, OR
PURDUE UNIV / CE SCOL (CHEN), WEST LAFAYETTE, IN; CE SCOL (LEONARDS), WEST LAFAYETTE, IN
PWC / CODE 101.5, FPO AP; CODE 102, OAKLAND, CA; CODE 123C, SAN DIEGO, CA; CODE 400, OAKLAND, CA; CODE 400A.3, FPO AP; CODE 420, OAKLAND, CA; CODE 421 (KAYA), PEARL HARBOR, HI; CODE 421 (REYNOLDS), SAN DIEGO, CA; CODE 421, NORFOLK, VA; CODE 422, SAN DIEGO, CA; CODE 423, SAN DIEGO, CA
SAN DIEGO PORT / PORT FAC, PROJ ENGR, SAN DIEGO, CA
SAN DIEGO STATE UNIV / CE DEPT (KRISHNAMOORTHY), SAN DIEGO, CA
SANDIA LABS / LIB, LIVERMORE, CA
SARGENT & HERKES, INC / JP PIERCE, JR, NEW ORLEANS, LA
SEATECH CORP / PERONI, MIAMI, FL
SEATTLE PORT / DAVE VAN VLEET, SEATTLE, WA; DAVID TORSETH, SEATTLE, WA
SEATTLE UNIV / CE DEPT (SCHWAEGLER), SEATTLE, WA
SHELL OIL CO / E. DOYLE, HOUSTON, TX
SIMPSON, GUMPERTZ & HEGER, INC / HILL, ARLINGTON, MA
SMELSER, D / SEVIERVILLE, TN
SOUTHNAVFACENGCOM / CODE 04A, CHARLESTON, SC; CODE 102H, CHARLESTON, SC; CODE 1622, CHARLESTON, SC
SOUTHWEST RSCH INST / ENERGETIC SYS DEPT (ESPARZA), SAN ANTONIO, TX; KING, SAN ANTONIO, TX; M. POLCYN, SAN ANTONIO, TX; MARCHAND, SAN ANTONIO, TX; THACKER, SAN ANTONIO, TX
SOWESTNAVFACENGCOM / LANGSTRAAT, SAN DIEGO, CA
SPCC / PWO, MECHANICSBURG, PA
STATE UNIV OF NEW YORK / CE DEPT, BUFFALO, NY
SUPSHIP / TECH LIB, NEWPORT, VA
TEXAS A&M UNIV / CE DEPT (MACHEMEHL), COLLEGE STATION, TX; CE DEPT (NIEDZWECKI), COLLEGE STATION, TX; OCEAN ENGR PROJ, COLLEGE STATION, TX

THE WORLD BANK / ARMSTRONG, WASHINGTON, DC
TRW INC / ENGR LIB, CLEVELAND, OH
TRW SPACE AND TECHNOLOGY GROUP / CARPENTER, REDONDO BEACH, CA
TUDOR ENGRG CO / ELLEGOOD, PHOENIX, AZ
UNIV OF CALIFORNIA / CE DEPT (FENVES), BERKELEY, CA; CE DEPT (FOURNEY), LOS ANGELES, CA; CE DEPT (TAYLOR), DAVIS, CA; CE DEPT (WILLIAMSON), BERKELEY, CA; NAVAL ARCHT DEPT, BERKELEY, CA
UNIV OF HAWAII / CE DEPT (CHIU), HONOLULU, HI; MANOA, LIB, HONOLULU, HI; OCEAN ENGRG DEPT (ERTEKIN), HONOLULU, HI; RIGGS, HONOLULU, HI
UNIV OF ILLINOIS / METZ REF RM, URBANA, IL
UNIV OF MARYLAND / CE DEPT, COLLEGE PARK, MD
UNIV OF MICHIGAN / CE DEPT (RICHART), ANN ARBOR, MI
UNIV OF N CAROLINA / CE DEPT (AHMAD), RALEIGH, NC
UNIV OF NEW MEXICO / NMERI (BEAN), ALBUQUERQUE, NM; NMERI, HL SCHREYER, ALBUQUERQUE, NM
UNIV OF PENNSYLVANIA / DEPT OF ARCH, PHILADELPHIA, PA
UNIV OF RHODE ISLAND / CE DEPT (KARAMANLIDIS), KINGSTON, RI; CE DEPT (KOVACS), KINGSTON, RI; CE DEPT (TSIATAS), KINGSTON, RI; DR. VEYERA, KINGSTON, RI
UNIV OF TEXAS / CONSTRUCTION INDUSTRY INST, AUSTIN, TX; ECJ 4.8 (BREEN), AUSTIN, TX
UNIV OF WASHINGTON / CE DEPT (HARTZ), SEATTLE, WA; CE DEPT (MATTOCK), SEATTLE, WA
UNIV OF WISCONSIN / GREAT LAKES STUDIES CEN, MILWAUKEE, WI
UNIV OF WYOMING / SCHMIDT, LARAMIE, WY
US NUCLEAR REGULATORY COMMISSION / KIM, WASHINGTON, DC
USACOE / CESPD-CO-EQ, SAN FRANCISCO, CA
USAE / CEWES-IM-MI-R, VICKSBURG, MS
USDA / FOR SVC, REG BRIDGE ENGR, ALOHA, OR
USNA / CH, MECH ENGRG DEPT (C WU), ANNAPOLIS, MD; OCEAN ENGRG DEPT, ANNAPOLIS, MD; USNA / PWO, ANNAPOLIS, MD
USPS / BILL POWELL, WASHINGTON, DC
VALLEY FORGE CORPORATE CENTER / FRANKLIN RESEARCH CENTER, NORRISTOWN, PA
VAN ALLEN, B / KINGSTON, NY
VSE / OCEAN ENGRG GROUP (MURTON), ALEXANDRIA, VA; LOWER, ALEXANDRIA, VA
VULCAN IRON WORKS, INC / DC WARRINGTON, CLEVELAND, TN
WESTINGHOUSE ELECTRIC CORP / LIB, PITTSBURG, PA
WESTNAVFACENGCOM / VALDEMORO, SAN BRUNO, CA
WISS, JANNEY, ELSTNER, & ASSOC / DW PFEIFER, NORTHBROOK, IL
WISWELL, INC. / SOUTHPORT, CT
WOODWARD-CLYDE CONSULTANTS / WEST REG, LIB, OAKLAND, CA

DISTRIBUTION QUESTIONNAIRE

The Naval Civil Engineering Laboratory is revising its primary distribution lists.

SUBJECT CATEGORIES

1 **SHORE FACILITIES**
1A Construction methods and materials (including corrosion control, coatings)
1B Waterfront structures (maintenance/deterioration control)
1C Utilities (including power conditioning)
1D Explosives safety
1E Aviation Engineering Test Facilities
1F Fire prevention and control
1G Antenna technology
1H Structural analysis and design (including numerical and computer techniques)
1J Protective construction (including hardened shelters, shock and vibration studies)
1K Soil/rock mechanics
1L Airfields and pavements
1M Physical security
2 **ADVANCED BASE AND AMPHIBIOUS FACILITIES**
2A Base facilities (including shelters, power generation, water supplies)
2B Expedient roads/airfields/bridges
2C Over-the-beach operations (including breakwaters, wave forces)
2D POL storage, transfer, and distribution
2E Polar engineering
3 **ENERGY/POWER GENERATION**
3A Thermal conservation (thermal engineering of buildings, HVAC systems, energy loss measurement, power generation)
3B Controls and electrical conservation (electrical systems, energy monitoring and control systems)
3C Fuel flexibility (liquid fuels, coal utilization, energy from solid waste)
3D Alternate energy source (geothermal power, photovoltaic power systems, solar systems, wind systems, energy storage systems)
3E Site data and systems integration (energy resource data, integrating energy systems)
3F EMCS design
4 **ENVIRONMENTAL PROTECTION**
4A Solid waste management
4B Hazardous/toxic materials management
4C Waterwaste management and sanitary engineering
4D Oil pollution removal and recovery
4E Air pollution
4F Noise abatement
5 **OCEAN ENGINEERING**
5A Seafloor soils and foundations
5B Seafloor construction systems and operations (including diver and manipulator tools)
5C Undersea structures and materials
5D Anchors and moorings
5E Undersea power systems, electromechanical cables, and connectors
5F Pressure vessel facilities
5G Physical environment (including site surveying)
5H Ocean-based concrete structures
5J Hyperbaric chambers
5K Undersea cable dynamics

ARMY FEAP
BDG Shore Facilities
NRG Energy
ENV Environmental/Natural Responses
MGT Management
PRR Pavements/Railroads

TYPES OF DOCUMENTS

D – Techdata Sheets; **R** – Technical Reports and Technical Notes; **G** – NCEL Guides and Abstracts; **I** – Index to TDS; **U** – User Guides; ☐ None - remove my name

Old Address:

_____

_____

_____

_____

Telephone No.: _____

New Address:

_____

_____

_____

_____

Telephone No.: _____

INSTRUCTIONS

The Naval Civil Engineering Laboratory has revised its primary distribution lists. To help us verify our records and update our data base, please do the following:

- Add - circle number on list
- Remove my name from all your lists - check box on list.
- Change my address - line out incorrect line and write in correction **(DO NOT REMOVE LABEL).**
- Number of copies should be entered after the title of the subject categories you select.
- Are we sending you the correct type of document? If not, circle the type(s) of document(s) you want to receive listed on the back of this card.

Fold on line, staple, and drop in mail.

DEPARTMENT OF THE NAVY
Naval Civil Engineering Laboratory
560 Laboratory Drive
Port Hueneme CA 93043-4328

Official Business
Penalty for Private Use, $300

NO POSTAGE NECESSARY IF MAILED IN THE UNITED STATES

BUSINESS REPLY CARD
FIRST CLASS PERMIT NO. 12503 WASH D.C.

POSTAGE WILL BE PAID BY ADDRESSEE

COMMANDING OFFICER
CODE L34
560 LABORATORY DRIVE
NAVAL CIVIL ENGINEERING LABORATORY
PORT HUENEME CA 93043-4328

NCEL DOCUMENT EVALUATION

You are number one with us; how do we rate with you?

We at NCEL want to provide you our customer the best possible reports but we need your help. Therefore, I ask you to please take the time from your busy schedule to fill out this questionnaire. Your response will assist us in providing the best reports possible for our users. I wish to thank you in advance for your assistance. I assure you that the information you provide will help us to be more responsive to your future needs.

R. N. STORER, Ph.D, P.E.
Technical Director

DOCUMENT NO. _____ TITLE OF DOCUMENT: _____

_____

Date: _____ Respondent Organization : _____

Name: _____ Activity Code: _____
Phone: _____ Grade/Rank: _____

Category (*please check*):

Sponsor ____ User ____ Proponent ____ Other (*Specify*) _____

Please answer on your behalf only; not on your organization's. Please check (*use an X*) only the block that most closely describes your attitude or feeling toward that statement:

SA Strongly Agree A Agree O Neutral D Disagree SD Strongly Disagree

---

	SA	A	N	D	SD
1. The technical quality of the report is comparable to most of my other sources of technical information.	( )	( )	( )	( )	( )
2. The report will make significant improvements in the cost and or performance of my operation.	( )	( )	( )	( )	( )
3. The report acknowledges related work accomplished by others.	( )	( )	( )	( )	( )
4. The report is well formatted.	( )	( )	( )	( )	( )
5. The report is clearly written.	( )	( )	( )	( )	( )
6. The conclusions and recommendations are clear and directly supported by the contents of the report.	( )	( )	( )	( )	( )
7. The graphics, tables, and photographs are well done.	( )	( )	( )	( )	( )

Do you wish to continue getting NCEL reports? ☐ YES ☐ NO

Please add any comments (e.g., in what ways can we improve the quality of our reports?) on the back of this form.

Comments:

Fold on line, staple, and drop in mail.

DEPARTMENT OF THE NAVY
Naval Civil Engineering Laboratory
560 Laboratory Drive
Port Hueneme CA 93043-4328

Official Business
Penalty for Private Use, $300

NO POSTAGE
NECESSARY
IF MAILED
IN THE
UNITED STATES

BUSINESS REPLY CARD

FIRST CLASS PERMIT NO. 12503 WASH D.C.

POSTAGE WILL BE PAID BY ADDRESSEE

COMMANDING OFFICER
CODE L03
560 LABORATORY DRIVE
NAVAL CIVIL ENGINEERING LABORATORY
PORT HUENEME CA 93043-4328